THE SYNTHESIS AND CHARACTERIZATION OF A SERIES OF CAGED NEUROTRANSMITTERS WITH TWO-PHOTON SENSITIVITY FOR USE IN VIVO

by

Adam C. Rea

(under the direction of Timothy M. Dore)

ABSTRACT

The quinoline caging groups have potential for use in the release of bioactive molecules *in vivo*, and their two-photon sensitivity increases the potential spatial and temporal resolution of uncaging. Examining the photolyses of different 8-substituted quinolines in different solvent systems leads to a better understanding of the uncaging process of the quinoline caging groups. Additionally, described here is a series of quinoline-caged serotonins and capsaicinoids with sensitivity to 2PE for *in vivo* use in biological experiments. The reported compounds have by far the most favorable photochemical and photophysical properties for applications in cell biology and neurophysiology.

INDEX WORDS: Photoremovable protecting groups, Caged compounds, Two-photon excitation, Serotonin, Epilepsy, Zebrafish, Capsaicin, Nociception, Calcium.

THE SYNTHESIS AND CHARACTERIZATION OF A SERIES OF CAGED NEUROTRANSMITTERS WITH TWO-PHOTON SENSITIVITY FOR USE IN VIVO

by

ADAM C. REA

B.S. Chem., University of Georgia, 2009

A Thesis Submitted to the Graduate Faculty of The University of Georgia in Partial Fulfillment of the Requirements for the Degree

MASTERS OF SCIENCE

ATHENS, GEORGIA

2011

THE SYNTHESIS AND CHARACTERIZATION OF A SERIES OF CAGED NEUROTRANSMITTERS WITH TWO-PHOTON SENSITIVITY FOR USE IN VIVO

by

ADAM C. REA

Major Professor:	Timothy M. Dore
Committee:	George Majetich Vladimir Popik

Electronic Version Approved:

Maureen Grasso
Dean of the Graduate School
The University of Georgia
December 2011

ACKNOWLEDGEMENTS

I would first and foremost like to thank Dr. Dore for his support and guidance throughout my academic career at the University of Georgia, both graduate and undergraduate. His encouragement, advice, and criticism have all pushed me to be a better student, scientist, and critical thinker. I would also like to thank Dr. Majetich and Dr. Popik for serving on my advisory committee.

I would also like to thank my labmates, including but not limited to Duncan McLain, Matthew O'Connor, Adna Muliawan, Mark Bernard, Kyle Harris, Robert Kutlik, and Branson Simmons. Their support, advice and company have been very appreciated.

Lastly, I would like to thank my friends and family for making the past two years truly special.

TABLE OF CONTENTS

CHAPTER 1

Photoremovable protecting groups for use in biological systems

Using light to control biological processes through the use of 'caged' molecules is a well-known and useful process.[1-2] A caged molecule consists of a biologically active molecule that is covalently bound to a photo-removable protecting group (PPG), or caging group.

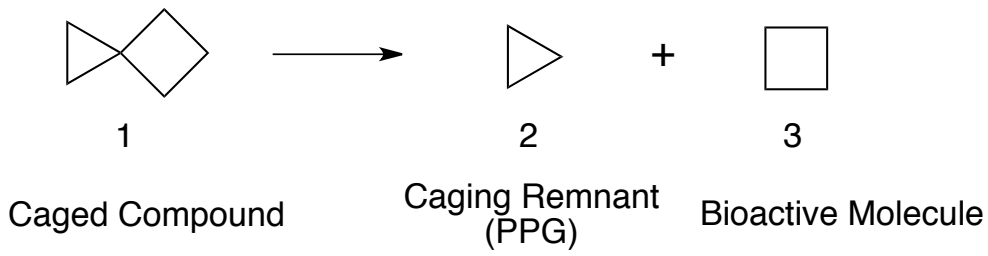

Figure 1: Caged Compounds

The caged molecule must be inert, both toward the particular receptor or process modulated by the bioactive molecule in question and toward other cellular processes as well. It also must be stable in the dark at physiological conditions, but rapidly release the bioactive molecule when exposed to light. The first biological applications of photoremovable protecting groups involved the 2-nitrobenzyl moiety, which can release phosphates, carboxylates, amines, alcohols, and phenols when exposed to UV light. The pioneering work from which the idea of a 'caged molecule' emerged was reported by Kaplan and coworkers in 1978.[3] Though 2-

nitrobenzyl photolysis was understood previously and had found applications in organic synthesis, their work, in which they report both an NB- and NPE-caged ATP, is the first example of applying a 'photoremovable protecting group' to a biological problem.

The nitrobenzyl PPG family includes the parent 2-nitrobezyl (NB), 4,5-dimethoxy-2-nitrobenzyl (DMNB), 1-(2-nitrophenyl)ethyl (NPE), 1-(4,5-dimethoxy-2-nitrophenyl)ethyl (DMNPE), and α-carboxy-2-nitrobenzyl (CNB).[4]

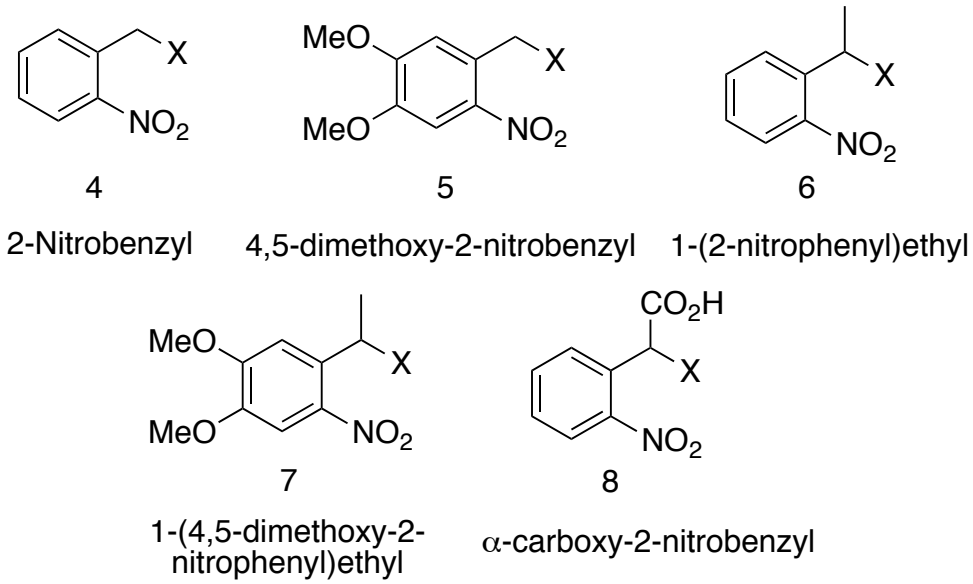

Figure 2: Nitrobenzyl PPG Family

Photorelease of compounds from the 2-nitrobenzyl PPG is well-understood mechanistically, and caged compounds using the 2-nitrobenzyl group are readily available synthetically, as the precursor reagents to protect a functional group with the various nitrobenzyl PPGs are commercially available. Indeed, in many cases, a nitrobenzyl-based PPG is the ideal choice for adding a degree of spatial and temporal control to studies involving interactions

between a biologically active effector and its target. Additionally, changes in the electronics on the benzyl ring gave the nitrobenzyl moiety a fair amount of variety in caging applications, stability, and rate of photolysis. Adding electron-donating groups, as in the case of the DMNB and NPE PPGs, in many cases increases the rate of photolysis. Work on caged nucleotides, including caged forms of the hydrolysis-resistant 8-bromo cAMP and cGMP have utilized DMNB and NPE PPGs.[5] The addition of the electron-withdrawing carboxylate in the CNB PPG adds both stability to dark hydrolysis and water-solubility,[6] and many CNB-protected neurotransmitters have been reported and used *in vivo*, often in experiments in which no 'leaking' of the bioactive molecule is tolerated.[7] Since its first use as a PPG, the NB PPG and its derivatives have been utilized in caging nucleotides, such as ATP, NAD, and NADP, neuromodulators, such as glutamate, GABA, kainate, and carbamoylcholine, and second messengers, such as cAMP, cGMP, and nitric oxide. However, despite its ubiquity, the nitrobenzyl PPG family suffers from slow release kinetics, and requires high intensities of UV light for photorelease. For a PPG to be widely useful, fast uncaging kinetics are desired, and often long irradiation periods with UV light are cytotoxic, which limit the usefulness and applications of nitrobenzyl-protected molecules *in vivo*. In the decades since nitrobenzyl-based caged compounds were first developed, improvements which seek to make uncaging a simultaneously more precise and less invasive process have been the focus of considerable effort.

Utilizing a caged form of a biological effector imparts a degree of spatial and temporal control over its activity. However, this spatial control is often of no use when tight three-dimensional control of uncaging volume is desired. Even if precisely calibrated UV lasers are utilized, the light intensity will be more than sufficient to affect uncaging at all points along the

beam path through the sample. When uncaging at single or subcellular resolution is desired, two-photon excitation-based uncaging can be a solution.[8] Two-photon excitation (2PE) is a non-linear optical process in which two photons are absorbed by a chromophore almost instantaneously, leading to an excited state identical to that of the chromophore when it absorbs one photon of light with a wavelength half that of the light involved in the two-photon process. Two-photon excitation adds the desired three-dimensional spatial resolution to the temporal resolution afforded by all caging groups, as uncaging only occurs with very high light intensities, often only in the volume of the focal point of a near-IR laser which can be focused to a single cell or subcellular structure.

Not all caging groups are sensitive to 2PE, however, and the development of caging groups that are sensitive to 2PE is an active and important area of research. Although 2PE as a photophysical process has been known since the early 20th century, it has only recently been utilized in the design of PPGs. The extent to which a caged compound can photolyze upon 2PE irradiation is given by the two-photon action cross-section (δ_u), in Goppert-Mayer (GM, 10^{-50} cm^4 s $photon^{-1}$). The first example of uncaging using 2PE was reported by Denk et al in 1994, in which a CNB-caged cabamoylcholine was used to determine the distribution of nicotinic acetylcholine receptors in cultured cells.[9]

In order to advance the field of 'caged' biomolecules, it is important to define parameters that make a PPG particularly useful in a biological setting. Though caged forms of an incredible number of bioactive molecules have been reported, very few have sensitivity to 2PE while retaining the other necessary properties for a caging group to be useful in a biological application, namely, compatibility with aqueous and cellular media. Extending aromatic and

conjugated systems, for instance, should improve the photochemical properties of chromophores, but often decreases in solubility and practicality accompany any gains in two-photo cross section. Goeldner and coworkers have reported photolabile moieties with very high two-photon action cross-sections, exceeding 1 GM and in some cases as high as 5 GM, however these are relatively large, hydrophobic extended conjugated aromatic systems which are not easily applicable to solving biological problems.[10]

Bhc was the first caging group reported to combine a high sensitivity to 2PE with desirable properties for use *in vivo*. Tsien and coworkers reported that brominated 7-hydroxycoumarin-4-ylmethyl (Bhc) esters and carbamates could release carboxylates and amines when exposed to light, and were highly sensitive to two-photon excitation.[11]

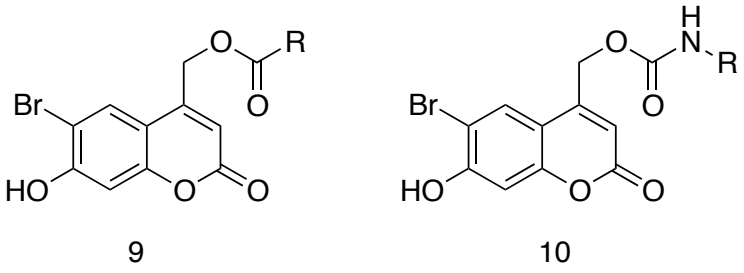

Figure 3: Bhc Ester and Carbamate

They reported a Bhc-caged glutamate with 2PE sensitivity was able to uncage it in hippocampal neurons in brain slices. They also defined the threshold of δ_u for a caged compound to be useful biologically as 0.1 GM. Bhc-caged compounds were reported to have a δ_u of 0.72 GM, the highest reported δ_u for a 2PE-sensitive PPG utilized successfully *in vivo*. As a comparison, the highest δ_u reported for a nitrobenzyl-based PPG is the DMNB, which has a δ_u of 0.03.[11] Bhc-

based caged compounds have become widely used and have been used to cage neurotransmitters and second messengers, among other applications. Bhc caged carboxylates have a high two photon action cross-section of 0.72 GM, well above the threshold for applicability of 0.1 GM.[11] However, Bhc suffers from two disadvantages: it is not highly soluble in aqueous buffers at physiological pH, and it is fluorescent, which complicates its use in biological experiments in which fluorescent imaging is used. Dore and coworkers reported the 8-bromo-7-hydroxyquinoline (BHQ) caging group that could release a variety of biologically-relevant functional groups with δ_u of 0.59 GM.[12] Though BHQ is not as sensitive to 2PE as Bhc, its 1PE quantum efficiency is an order of magnitude higher, and it possesses additional characteristics that make it extremely promising as a potential PPG for use in vivo. BHQ has a lower two photon action cross-section than Bhc, 0.59 GM versus 0.72 GM, but it is sufficiently soluble in aqueous buffers and has low fluorescence. For these reasons, quinoline-based PPGs are promising in their potential for use in vivo in biological systems.

In addition to exploring new chromophores for their relative utility as caging moieties, it is important to understand mechanistically how caged compounds photolyze, and how the photolysis reaction is affected by changes in solvent, pH, temperature, and other experimental variables. Because of the potential of BHQ as a PPG, there has been a concerted, ongoing effort to elucidate the mechanism of photolysis and to use spectroscopic methods to characterize the ground and excited states of the model compound, BHQ-OAc.

The initial mechanistic experiments that followed the report of BHQ as a PPG with 2PE sensitivity included Stern-Volmer quenching, time-resolved infrared (TRIR), and isotopic labeling.[13] Experiments with triplet quenchers suggested that the reactive excited state of BHQ-

OAc was the singlet state, as the presence of quencher did not affect rate of photolysis. The experiments involving isotopically labelled reaction solvent provided evidence that the mechanism of photolysis is solvent-assisted photoheterolysis (S_N1). The report by Dore and coworkers that various other 8-substituted-7-hydroxyquinolines were also viable candidates for use as PPGs with varying sensitivity to 2PE created another layer of complexity in understanding the photochemistry of quinoline PPGs.[14] It was already known that the addition of the bromine at the 8 position affects the chemistry of the parent 7-hydroxyquinoline.[15] Most notably, due to the inductive electron-withdrawing properties of the bromine, the pK_a of the phenolic hydroxy decreases from 9.0 for the parent compound to 6.8 for BHQ-OAc. Changing the substituent at the 8 position to a cyano (CyHQ), chloro (CHQ), or nitro (NHQ) group widely effects the photochemical properties of the caging group,[14] although BHQ-OAc had the highest reported two-photon cross section of the quinoline-caged acetates. Notably, NHQ-OAc did not photolyze

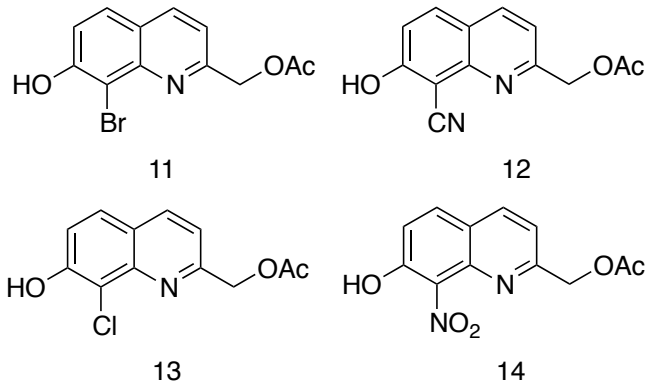

Figure 4: BHQ, CyHQ, CHQ, and NHQ-caged Acetate

in response to 1PE or 2PE irradiation. Additionally, the photohemical properties of BHQ-OAc and CHQ-OAc, which should have similar electronics due to halogenation at the 8 position, are markedly different.

BHQ-OAc and CHQ-OAc are photolabile compounds that photolyze in response to irradiation with ultraviolet or near-visible light. Not only are BHQ-, and to a lesser extent CHQ-caged compounds highly promising candidates for use in biological uncaging experiments, but the compounds BHQ-OAc and CHQ-OAc provide a good model system in which to examine the effects of changing substituents at the 8 position of the quinoline fluorophore on photolysis. The photolysis reactions of BHQ-OAc and CHQ-OAc involve both the destruction of starting material and concomitant formation of observable photolysis products and can be monitored by HPLC. The photochemical properties of BHQ-OAc and CHQ-OAc in KMOPS, pH 7.2 have been previously described.[12, 14] The most notable difference between the photolyses of the two compounds is the decrease in both one-photon quantum efficiency and two-photon cross-section of CHQ-OAc relative to BHQ-OAc. This trend is not consistent with previous studies that indicated that photolysis of BHQ-OAc proceeds through a singlet excited state.[13] The heavy atom effect promotes intersystem crossing (ISC) in fluorophores by inducing spin orbit coupling. Bromine therefore should promote intersystem crossing to the triplet excited state to a greater extent than chlorine and should therefore decrease the reactivity of the singlet state toward photolysis.

Table 1: Photochemical and Photophysical Properties of BHQ-OAc and CHQ-OAc[14]

Caged Compound	λ_{max} nm	ε $M^{-1}cm^{-1}$	Q_u	Sensitivity $Q_u \times \varepsilon$	δ_u GM	τ_{dark} h
BHQ-OAc	369	2,600	0.29	754	0.59	71
CHQ-OAc	370	2,800	0.10	280	0.12	49

To better understand the photochemistry of BHQ-OAc and CHQ-OAc, their respective photolyses were examined in multiple solvent systems, including water-rich solvent systems and dry acetonitrile. The solvent systems examined include KMOPS buffer calibrated to pH 7.2, neutral 60:40 H_2O/CH_3CN, pH 4 60:40 H_2O/CH_3CN, and dry CH_3CN. BHQ-OAc and CHQ-OAc can exist in solution as various prototropic forms, neutral, tautomeric, cationic, and anionic.

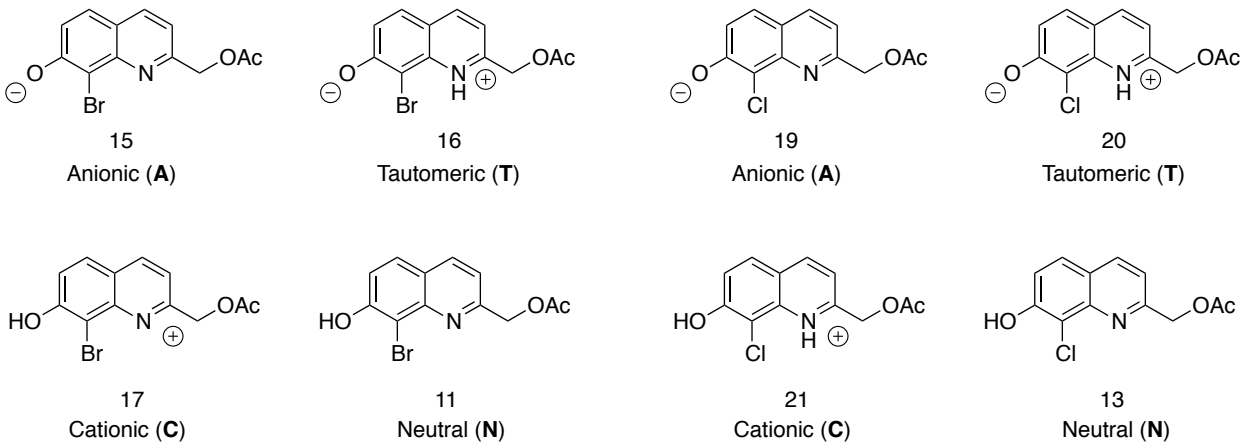

Figure 5: Prototropic Forms of BHQ-OAc and CHQ-OAc

The pH of the solution will largely determine the relative amounts of each form present, and the photochemical differences between the forms should be represented in the measured properties of each compound. Though previous characterization of quinoline-caged compounds has been performed in aqueous buffers at physiological pHs with irradiation at 365 nm, solutions of each compound were irradiated at 254 nm in a photoreactor. This shorter wavelength is not relevant to biological experiments, as near-ultraviolet light below 300 nm is cytotoxic. However, 254 nm is very close to excitation wavelengths used in previous and ongoing time-resolved spectroscopic

experiments involving BHQ-OAc and CHQ-OAc, and therefore more stringent characterization of quinoline photochemistry using irradiation wavelengths near 254 nm is of interest.

Initial qualitative trials of each photolysis reaction revealed a general trend. Solutions of BHQ-OAc and CHQ-OAc in water-rich solutions photolyzed to photoproducts observable by HPLC on fast time scales when irradiated at 254 nm. In both cases, irradiation in dry CH_3CN did not lead to observable photolysis products on any relevant short time scale. If irradiation was extended to 45 min or longer, a small amount of degradation of starting material was observed and some new peaks were observed by HPLC, but in general, these new peaks did not show the same quinoline character via UV absorbance as photolysis products in other experiments.

UV-VIS Spectra were acquired for each compound in each of the water-rich solvent systems, incorporating the relevant wavelengths examined for both BHQ-OAc and CHQ-OAc.

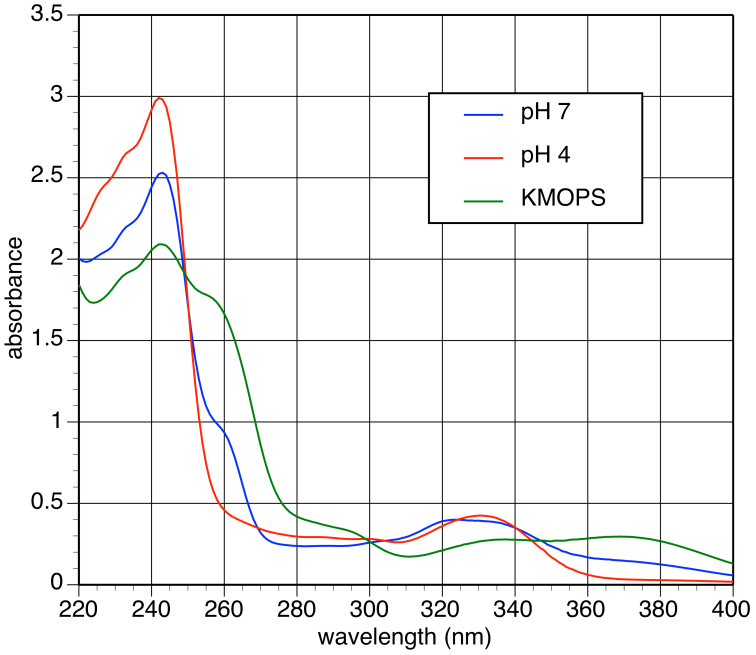

Figure 6: UV Spectra of BHQ-OAc, 60:40 H_2O/CH_3CN pH 7, 60:40 H_2O/CH_3CN pH 4, and KMOPS pH 7.2

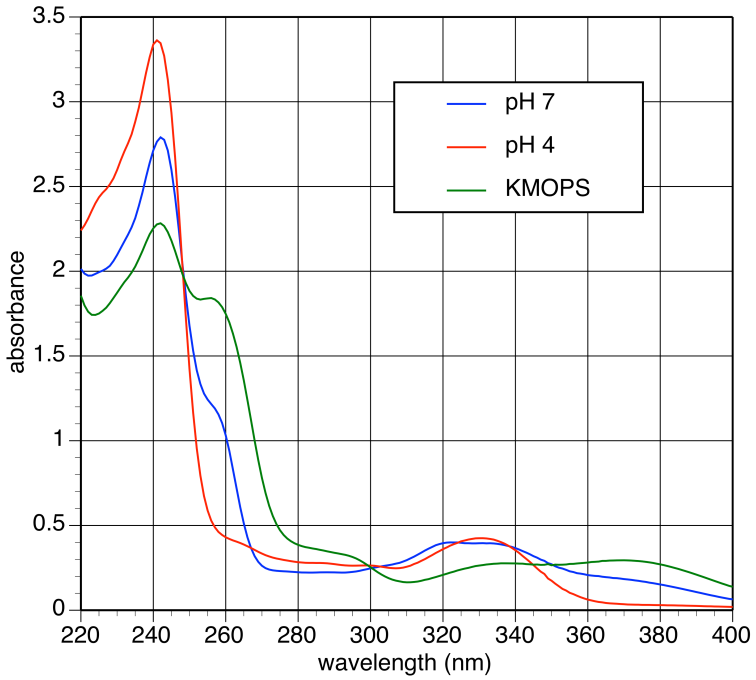

Figure 7: UV Spectra of CHQ-OAc, 60:40 H_2O/CH_3CN pH 7, 60:40 H_2O/CH_3CN pH 4, and KMOPS pH 7.2

The absorbance spectra reveal that, as expected, as pH increases, the absorbance band relating to the phenolate form, which has an absorbance max at 370 nm, is more abundant than the phenol form, which has an absorbance max at 330 nm.

Photolysis curves of BHQ-OAc and CHQ-OAc were generated by irradiating solutions of each compound in each of the water-rich solvent systems and analyzing reaction progress by HPLC. The extent of photolysis was determined by measuring starting material peak area after various lengths of irradiation.

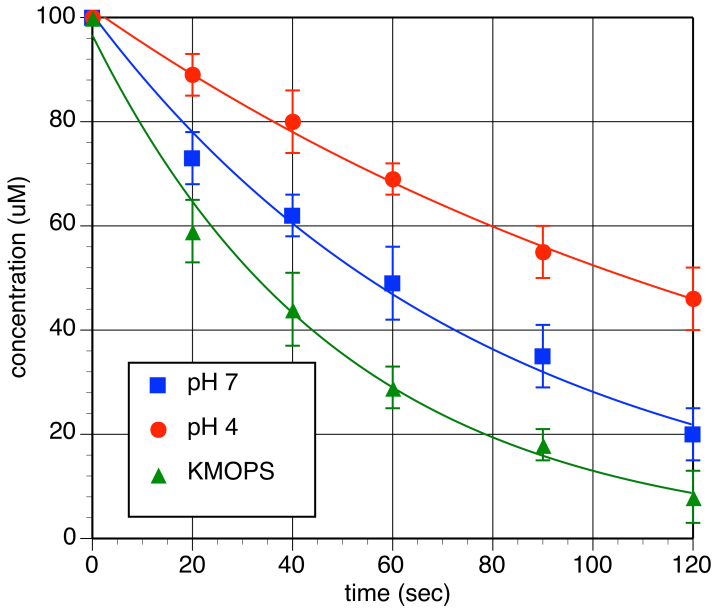

Figure 8: Photolysis of BHQ-OAc in Water-Rich Solvent Systems

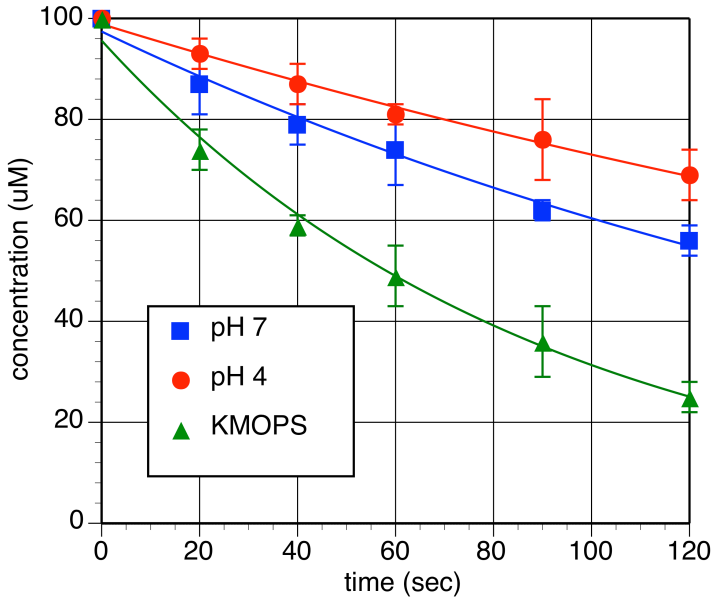

Figure 9: Photolysis of CHQ-OAc in Water-Rich Solvent Systems

Quantum efficiencies were calculated for the photolyses of BHQ-OAc and CHQ-OAc in each water-rich solvent system using the equation $Q_u = (I\sigma t_{90\%})^{-1}$, where I is the intensity of the

lamp determined by potassium ferrioxalate actinometry, σ is the decadic extinction coefficient (1000ε) measured at 254 nm, and $t_{90\%}$ is the time required for conversion of 90% of starting material to product, as measured by HPLC peak area.

As expected, the quantum efficiency of BHQ-OAc photolysis decreases with pH, as more of the less reactive cationic form of BHQ-OAc is present in solution. It is important to note that the extinction coefficient at 254 nm for both BHQ-OAc and CHQ-OAc decrease with pH, to be expected as the cationic form is less absorptive as well. Quantum efficiency is inversely proportional to extinction coefficient, so the decrease in molar absorptivity to a certain extent mitigates the slower photolysis reaction reflected by the increase in $t_{90\%}$. This is demonstrated in the fact that even though the photolysis curves of CHQ-OAc clearly show an increase in reaction rate with pH, the compound is nearly twice as absorptive at pH 7 in 60:40 H_2O/CH_3CN than at pH 4, and the resulting calculated quantum efficiencies are virtually identical.

Table 2: Quantum Efficiencies of BHQ-OAc and CHQ-OAc, 254 nm

Caged Compound	Solvent	ε at 254 nm, $M^{-1}cm^{-1}$	Q_u at 254 nm
BHQ-OAc	KMOPS, pH 7.2	17,900	0.26
	60:40 H_2O/CH_3CN, pH 7	11,700	0.25
	60:40 H_2O/CH_3CN, pH 4	8,700	0.17
CHQ-OAc	KMOPS, pH 7.2	18,400	0.14
	60:40 H_2O/CH_3CN, pH 7	12,800	0.09
	60:40 H_2O/CH_3CN, pH 4	6,700	0.10

In addition to generating photolysis curves and measuring quantum efficiencies for BHQ-OAc and CHQ-OAc in each solvent system, the products of each photolysis were identified in situ by interfacing HPLC analysis of the photolysis reaction with ESI-MS. To eliminate observation of any secondary photoproducts that may arise from extended irradiation times, irradiation length was limited to only produce enough product to be accurately identified by MS analysis. It was determined that irradiation for 15 seconds was sufficient for observing photoproducts in the photolysis of BHQ-OAc in water-rich solvent systems. For photolysis of CHQ-OAc, 30 seconds was required for observing and identifying photoproducts.

In each of the three water-rich solutions, the photolysis of CHQ-OAc led to one single observable photoproduct, determined by ESI MS to be CHQ-OH.

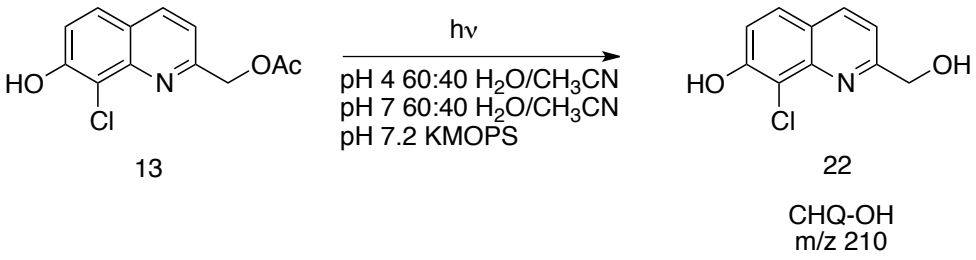

Figure 10: Photolysis of CHQ-OAc

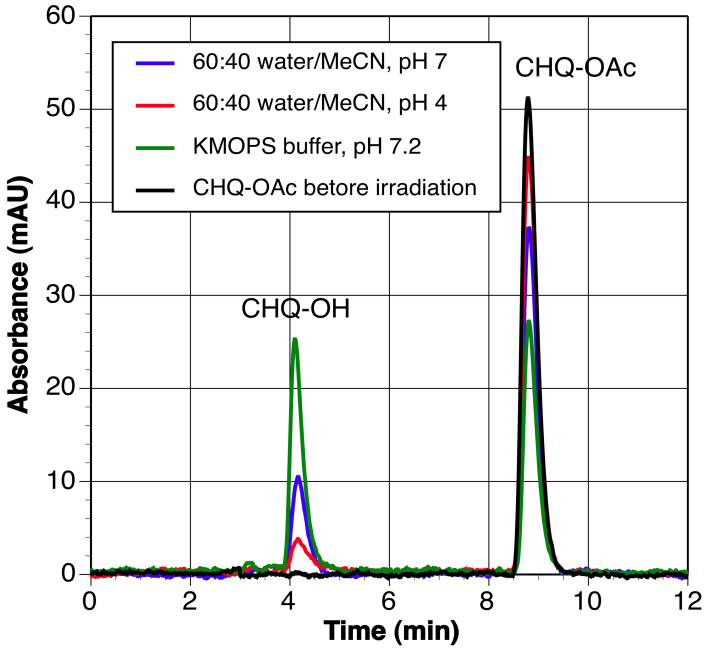

Figure 11: HPLC Traces of Photolysis of CHQ-OAc in Water-Rich Solutions

As the pH of the solution increases from pH 4 60:40 H_2O/CH_3CN to pH 7 60:40 H_2O/CH_3CN to KMOPS aqueous buffer, pH 7.2, the amount of photolysis product generated and starting material destructed increases, consistent with the expectation that the compound will exist in greater relative amounts as the anionic form as pH increases. These results confirm earlier photolysis studies of CHQ-OAc, which also showed slower photolysis reactions in acidic media than neutral or slightly basic media.

The photolysis of BHQ-OAc is more complex than that of CHQ-OAc. In contrast to the photolysis of CHQ-OAc, in the three water-rich solutions, the photolysis reaction of BHQ-OAc proceeded to two different photolysis products, determined by ESI MS to be BHQ-OH and de-brominated 7-HQ-OAc. The two products had HPLC retention times of 4.4 minutes and 4.8

minutes, respectively, and the identity of the two observed photoproducts was confirmed by analysis of pure samples of each.

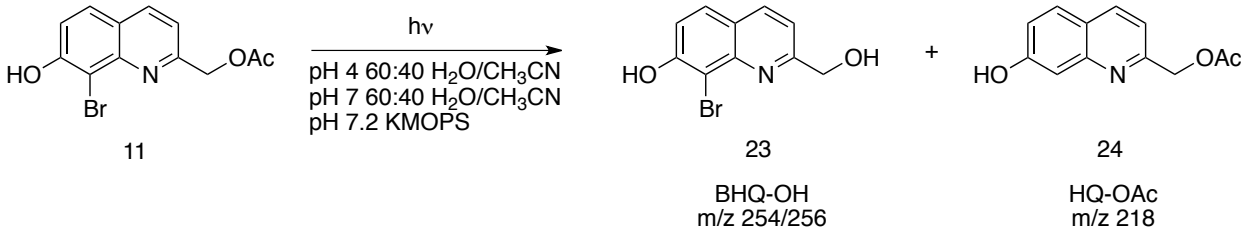

Figure 12: Photolysis of BHQ-OAc

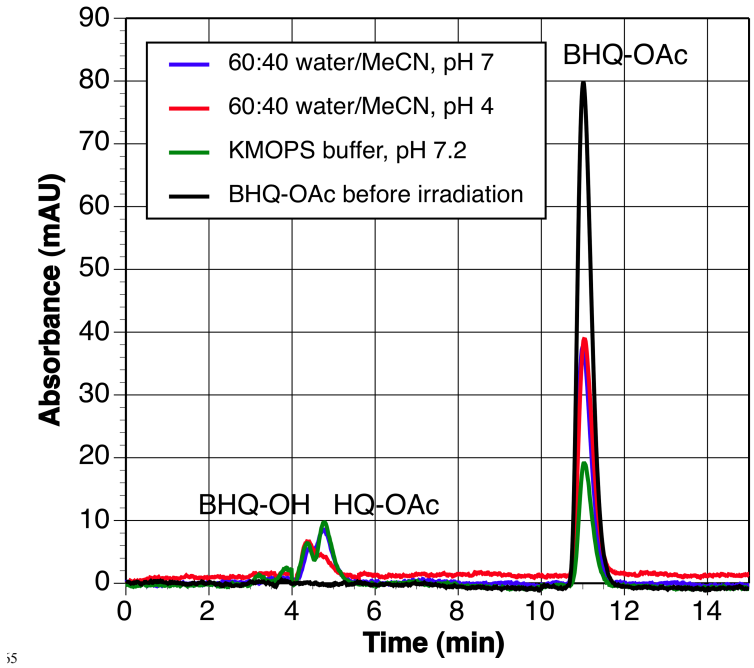

Figure 13: HPLC Traces of Photolysis of BHQ-OAc in Water-Rich Solutions

Dehalogenation appears to be a competitive process to uncaging of the acetate during photolysis of BHQ-OAc, unlike the photolysis of CHQ-OAc in which no dehalogenation is observed. This evidence alone suggests that CHQ is a better PPG for use in biological systems

than BHQ, as more discovery of more direct uncaging processes and elimination of side reactions that do not lead to the desired uncaged product is often a high priority. However, as discussed previously, the photochemical properties of BHQ-OAc are much more desirable than those of CHQ-OAc. One- and two-photon uncaging is much more efficient, and yields of compounds released from BHQ-caged compounds are often in excess of 50%. The desirable uncaging properties of BHQ-caged compounds, despite their undesirable side reactions, can be partially explained by the observation that HQ-OAc is photoreactive and can also release acetate when exposed to light. Even if a significant amount of dehalogenation initially occurs, this dehalogenated initial product can also contribute to the measured yield of photoreleased effector. The complexity of uncaging of BHQ-caged compounds, while interesting and worth exploration, does not ultimately reduce the potential for use of BHQ-caged compounds i*n vivo* due to their highly favorable one- and two-photon properties.

As important as it is to gain a better understanding of the photochemistry of the quinoline PPGs, applying their desirable photochemical properties to biological systems is of more importance. Caging groups have found biological applications in gene activation and silencing, regulation of protein activity, and excitation or inhibition of neural circuitry among many others. In particular, the development of caged forms of various neuromodulators has been an incredibly active area of research. Because of its solubility in aqueous media, low fluorescence, and high sensitivity to 2PE-induced uncaging, BHQ is an ideal candidate for use in creating a library of 2PE-sensitive photoactivatable neuromodulators. Two such neuromodulators, serotonin and capsaicin, are of interest due to the lack of variety of their respective caged forms in the literature.

CHAPTER 2

The synthesis and characterization of a caged serotonin with 2PE sensitivity

Serotonin (5-hydroxytryptamine or 5HT) is a monoamine similar in structure and function to other monoamines such as melatonin, another tryptamine, and the catecholamines noradrenaline, adrenaline, and dopamine. Serotonin is found primarily in the intestines, where it

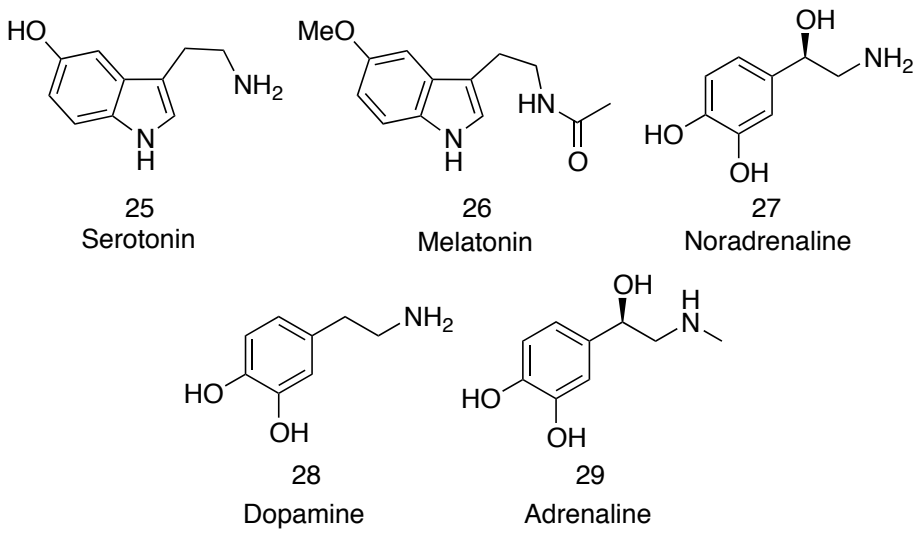

Figure 14: Monoamine Family

regulates motility and can be implicated in the pathologies of intestinal disorders such as irritable bowel syndrome, and in the central nervous system, where it acts as a neuromodulator and is involved in regulating mood, appetite, memory, learning, and other cognitive functions.[16] In the

central nervous system, serotonin originates mainly in the raphe nuclei, a cluster of neurons in the brain stem that project into other brain regions.[17] Serotonin is released from these neurons, and initiates various signal transduction pathways by activating serotonin receptors located in the cell membrane of adjacent neurons.

The serotonin receptors and their respective signaling pathways have been studied extensively. There are seven classes of 5HT receptors, designated $5HT_{1-7}$ receptors, that are further subdivided into subtypes. Overall, there are 15 different 5HT receptors that are expressed in the central nervous system, all of which are G-protein coupled receptors except for the $5HT_3$ receptor, which is a ligand-gated ion channel.[18] G-protein coupled receptors (GPCRs) are heptahelical transmembrane proteins that recognize molecules extracellularly and affect a signal transduction pathway intracellularly. Activation of a GPCR by a ligand induces a conformational change in the receptor that allows it to exchange a GTP for a GDP bound to the α subunit of the associated G-protein. The G-protein is active when it is bound to GTP, and the α subunit dissociates from the GPCR-G-protein complex and acts as a second messenger in the cell.

5HT G-protein coupled receptors are implicated in an incredibly complex network of signaling cascades, but are generally classified according to their primary signaling pathway. The $5HT_4$, $5HT_6$, and $5HT_7$ receptor classes activate adenylyl cyclase, which activates the cAMP/PKA signaling pathway.[18] The $5HT_1$ receptors inactivate adenylyl cyclase. The $5HT_5$ receptors have been shown to both activate and inactivate adenylyl cyclase. The $5HT_2$ receptors act primarily on a different signaling pathway altogether, the phospholipase C (PLC) pathway.[16]

It is important to make the distinction between the elucidation of a particular serotonergic signal transduction pathway and the integration of that pathway with others to explain large-scale

events such as mood, appetite, or other behavioral changes. However, many signaling pathways involving serotonergic neurons have been discovered, and dysfunctions in them are implicated in many pathologies, such as depression, schizophrenia, and bipolar disorder. Secondary signaling pathways involving serotonin are in many cases GABAergic in nature.[19-20] GABAergic interneurons, which are located in the cortex of the central nervous system of mammals and other higher creatures, receive large amounts of serotonergic projections from the raphe nuclei, and provide a source of inhibitory neurotransmission from the cortex through to the hippocampus.[18]

The involvement of serotonergic signaling in epilepsy has received attention in the last decade.[21-22] Epilepsy is a broad spectrum disorder characterized by synchronous, coherent activity throughout a neural network. Because the cause of seizure initiation is not immediately known, studying how epileptiform activity initiates and spreads through a neural network is of the utmost importance. Neurotransmission is often a delicate balance between excitation and inhibition with glutamatergic, or excitatory signaling, balanced by GABAergic, or inhibitory signaling. It is no wonder then, that imbalances between excitation and inhibition and dysfunction in GABAergic signaling pathways have long been implicated in the initiation and spread of seizure activity.[23]

The idea of a link between epilepsy and serotonin dates back to 1957 when Bonnycastle reported that various anticonvulsant drugs increased levels of serotonin in the brain.[21] In the recent years, a body of literature has formed that has partially characterized the link mechanistically between serotonergic signaling and seizure activity. Serotonergic neurons in the raphe nuclei project into both the cortex and hippocampus, and affect a vast network of both

excitatory and inhibitory neurotransmission, and it is the complex aggregate activation of receptors in this network that gives rise to the observed response.

The first examples of a mechanistic study of 5HT seizure modulation were reported by Salgado and coworkers in 1995.[24] They examined the effect that serotonin had on bicuculline-induced seizures in rat brain slices, and found that directly applied serotonin caused membrane hyperpolarization and inhibited seizure activity. They attributed the effect partly to activation of $5HT_{1A}$ receptors; application of a $5HT_{1A}$ receptor agonist mimicked the result of directly applied serotonin, and application of a $5HT_{1A}$ receptor antagonist reversed the inhibition of epileptic activity. Their results were further supported when Sarnyai and coworkers reported that the observed threshold to audiogenic seizures was markedly lower in transgenic $5HT_{1A}$ receptor knock-out mice.[25] In later studies, the mechanism by which $5HT_{1A}$ receptor-activation mediates spread of seizure activity was further elucidated. Both intracellular and patch-clamp recording showed that serotonin reduced both AMPA and NMDA receptor-mediated excitatory postsynaptic currents in the entorhinal cortex by as much as 40% through activation of $5HT_{1A}$ receptors.[26-27] In this case, it was argued that serotonergic signaling projecting from the raphe nuclei into the cortex disrupted the balance between excitation and inhibition by decreasing excitatory neurotransmission.

The $5HT_{1A}$ receptor is not the only 5HT receptor that has been implicated in epilepsy. It was reported that transgenic mice lacking the $5HT_{2C}$ receptor have exceedingly low thresholds to audiogenic seizures and are prone to increased lethality of seizure activity relative to normal mice expressing the $5HT_{2C}$ receptor.[28] Though the effects of $5HT_{2C}$ receptor on seizure activity is not as well understood as that of the $5HT_{1A}$ receptor, some pharmacological data does exist.

Studies have shown that application of a $5HT_{2B}$ and $5HT_{2C}$ agonist increases the seizure threshold of mice and rats treated with PTZ.[29] Various $5HT_2$ receptor antagonists have been shown to reverse the effects of the agonists. Mechanistically, the effects are different from the $5HT_{1A}$ receptors. $5HT_2$ receptors are expressed heavily in GABAergic interneurons in the cortex, projected into by serotonergic neurons in the raphe nuclei. A report by Abi-Saab and coworkers in 1999 examined the effect of $5HT_2$ receptor activation on extracellular GABA levels in the cortex.[30] They found that applied serotonin and the application of the non-specific $5HT_2$ receptor agonist 1-(2,5-dimethoxy-4-iodophenyl-2-aminopropane) (DOI) both increased extracellular GABA levels in the cortex in a dose-dependent manner. In this case, there is evidence that unlike the $5HT_{1A}$ receptor, the antiepileptic activity of the $5HT_{2C}$ receptor arises from its increase of inhibitory neurotransmission, rather than its decrease of excitatory neurotransmission.

The complexity of the serotonergic signaling pathways implicated in modulation of epileptic activity serves as an example of the difficulty in describing observed behavioral or electrical responses mechanistically. In a very general sense, serotonergic pathways have differentially expressed receptors that affect excitatory and inhibitory neurotransmission in various ways. It is when the combined signals are integrated in a neural network that behaviors arise. To a certain extent, the results of pharmacological studies on 5HT receptors are model-dependent, but at some point results are conserved and apply across organisms in which the various receptors are conserved. The body of literature surrounding serotonergic signaling indicates a crucial role of serotonin in the modulation of the balance between excitation and inhibition, and both genetic and pharmacological studies have clearly demonstrated a link

between serotonin and epilepsy. This link is not well understood, however, and more work is needed to understand how serotonin affects the generation and spread of seizure activity.

Because of its ubiquity and involvement in an incredible number of signal transduction pathways, including those involving epileptic activity, synthesizing a caged form of serotonin is of great interest, and has an enticing number of potential applications. Various forms of caged serotonin do exist in the literature, but all utilize nitrobenzyl PPGs.[31-32]

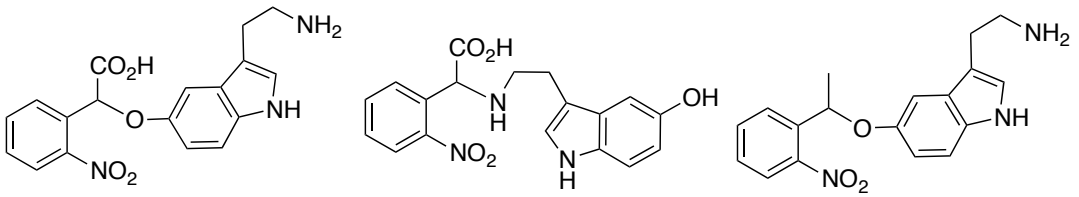

30 *O*-CNB-Serotonin

31 *N*-CNB-Serotonin

32 NPE-Serotonin

Figure 15: Caged Serotonins in the Literature

The caged serotonins reported by Hess, *O*-CNB-Serotonin and *N*-CNB-Serotonin, were used to study the kinetics of the $5HT_3$ ligand-gated ion channel. The $5HT_3$ receptor is the only known 5HT receptor that is not a GPCR, like those described above. It is a ligand-gated ion channel that is permeable to small cations. Previous studies had elucidated the mechanism of $5HT_3$ receptor activation using a cell-flow technique time-resolved to roughly 10 ms, much slower than the rate constants of channel opening and closing.[33] Caged compounds are well-suited for studying biological processes that occur on a sub-ms time scale, as uncaging with laser flash photolysis can often occur on a μs time scale. The time constants of opening and closing can be measured by saturating the receptor with the photolabile precursor, using laser flash

photolysis to release the receptor ligand, and recording the resulting current using whole-cell electrophyisiologial recording. The nitrobenzyl-caged serotonins reported uncage sufficiently fast enough to measure the time constant of $5HT_3$ receptor activation, which is measured to be around 20 ms. It was determined that at a concentration of 2.8 μM, half of the maximum activation of the receptor is obtained, demonstrating the poor yield of release of nitrobenzyl-caged compounds.

It is important to note that though Hess and coworkers were able to use their caged serotonin as they intended, and accurately determine the kinetics of the $5HT_3$ ion channel, there are serious drawbacks associated with *O*-CNB-Serotonin and *N*-CNB-Serotonin, and their utility for applications beyond ion-channel kinetic studies is questionable. *N*-CNB-Serotonin has a rate constant of uncaging of 1.2 ms, which is too slow to be useful in almost any experiment. The phenol form of caged serotonin (*O*-CNB-5HT) has faster release kinetics by a factor of 80, which is consistent with the relative rates of uncaging caged amines and phenols, and is the focus of the kinetic experiments. However, in the UV-VIS spectrum of *O*-CNB-5HT the λ_{max} is around 280 nm with absorbance dropping off precipitously above 300 nm. An irradiation wavelength of 337 nm was used, noting that irradiation below 337 nm leads to significant cytotoxicity. However, the extinction coefficient of the compound at 337 nm, while not explicitly reported by Hess, is qualitatively quite low based on the UV-VIS spectrum of the compound. Finally, the quantum yield determined via HPLC for *O*-CNB-5HT is reported to be 0.03, a poor indicator of its usefulness beyond the limited scope of the experiments performed.

In designing a caged serotonin with broader utility and in particular for applications involving the elucidation of serotonergic signaling pathways, it is important to focus on two

main aspects: increased quantum yield and higher extinction coefficient at longer and more biologically relevant irradiation wavelengths, and more importantly, sensitivity to 2PE. The quinoline-based PPGs, most notably BHQ, are ideally suited for use in creating a greatly improved series of caged serotonins. In particular, they absorb at much longer wavelengths than the nitrobenzyl PPGs, have higher quantum yields, and have adequate 2PE sensitivity for use in vivo.[12, 14] In addition, quinolines have previously been shown to release phenols (Zhu, unpublished results) and amines, caged as carbamates.[34] The two forms of caged serotonin utilizing the improvements of the quinoline PPGs versus nitrobenzyl-based PPGs are designated BHQ-*O*-Serotonin (or BHQ-*O*-5HT) and BHQ-*N*-Serotonin (or BHQ-*N*-5HT).

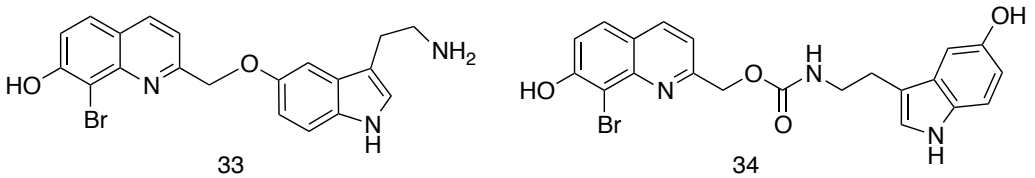

Figure 16: BHQ-*O*-Serotonin and BHQ-*N*-Serotonin

It is expected that studies of the photochemical properties of the BHQ-caged serotonins will show that they are indeed far superior to the previously reported caged serotonins.

While the potential applications of both forms of BHQ-5HT are many, and indeed include any experiments where spatial and temporal control of 5HT release is desired, the initial biological application involves suppression of seizure activity by bath applied serotonin in the zebrafish developmental seizure model. As described previously, the zebrafish seizure model is well-understood, and ideal for studying seizure activity. The effects of serotonin on seizure

activity will be studied using the zebrafish model with the chemoconvulsant PTZ. Uncaging with either form of BHQ-5HT should replicate any effect observed by bath applied serotonin, and through harnessing the sensitivity of BHQ-caged compounds to 2PE, it should be possible to examine the effects of extracellular 5HT level increases in vivo in distinct locations within the CNS.

An interesting aspect of the study of epilepsy in a general sense is the different ways in which epilepsy arises and manifests itself in developing systems relative to fully developed systems. This area of research has grown from the the clinical observations that reliable anticonvulsant drugs that work in adults have drastically different effects in children, in some cases having no effect while enhancing epileptic activity or having other harmful developmental effects.[35-36] It is important to have a good model system with which to study the differences between seizure activity in developing and adult systems. The zebrafish is one of many model organisms that have been developed to study various neurobiological disorders.[37-38] Zebrafish possess many characteristics which make them ideal model organisms. Their development is extremely well-known, and maturation is extremely precise and occurs on a relatively fast time scale. Their nervous systems mirror those of higher organisms and are also well-understood. Zebrafish have one advantage that sets them apart from other model systems - they are transparent in their early stages of development, making imaging studies using small-molecule or genetically-encoded fluorescent dyes particularly appealing, especially in developing animals. Zebrafish show seizure activity consistently and persistently when exposed to solutions of pentylenetetrazole (PTZ), a known chemoconvulsant.[39] The behavioral stages of seizure activity

in zebrafish have been defined in the literature, and the electrophysiological responses to various chemoconvulsants at varying concentrations have been characterized as well.[40-41]

Most of the studies involving transgenic animals, or 5HT receptor activation or inhibition have taken place in mice and rats. Mice and rats both offer well understood mammalian models of seizure activity, but they have disadvantages when compared to zebrafish. The serotonergic signaling network that has been so well described is conserved in zebrafish,[42] and initial studies performed on ex vivo zebrafish brain preparations have confirmed that applied serotonin indeed does have antiepileptic activity toward PTZ-induced seizures (Dore, Lauderdale, unpublished results).

The synthesis of BHQ-caged serotonin was designed with the intention of creating two forms of the caged compound, one in which serotonin is caged at the phenolic hydroxy group (BHQ-*O*-Serotonin), and one in which it is caged at the primary amine (BHQ-*N*-Serotonin). Caging both functional groups of serotonin affords even more versatility to the BHQ-caged serotonins. In particular, the differences in electronics between the amine-caged form and the phenol-caged form could potentially lead to the compounds localizing differently in biological systems.

The synthesis of BHQ-*O*-Serotonin was based partially on the synthesis of BHQ-phenol. BHQ-phenol was created to determine the extent to which BHQ can release a phenol moiety directly upon irradiation. Many molecules of interest contain phenol groups, and many forms of caged compounds exist in which the PPG is attached at a phenol. However, phenols are typically caged as carbonates and no examples exist in the literature of uncaging of phenols directly. It

was determined that BHQ-caged phenols could indeed uncage when irradiated with 1- or 2PE, with quantum efficiency (Q_u) of 0.19, and two photon uncaging cross section (δ_u) of 0.56 GM.

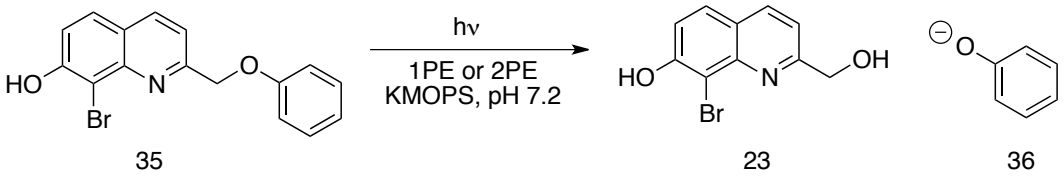

Figure 17: Uncaging of BHQ-Phenol

Therefore, BHQ affords the potential for the caging of bioactive molecules at phenolic hydroxy groups. The synthesis of BHQ-*O*-Serotonin proceeds from MOM-BHQ-OMs.

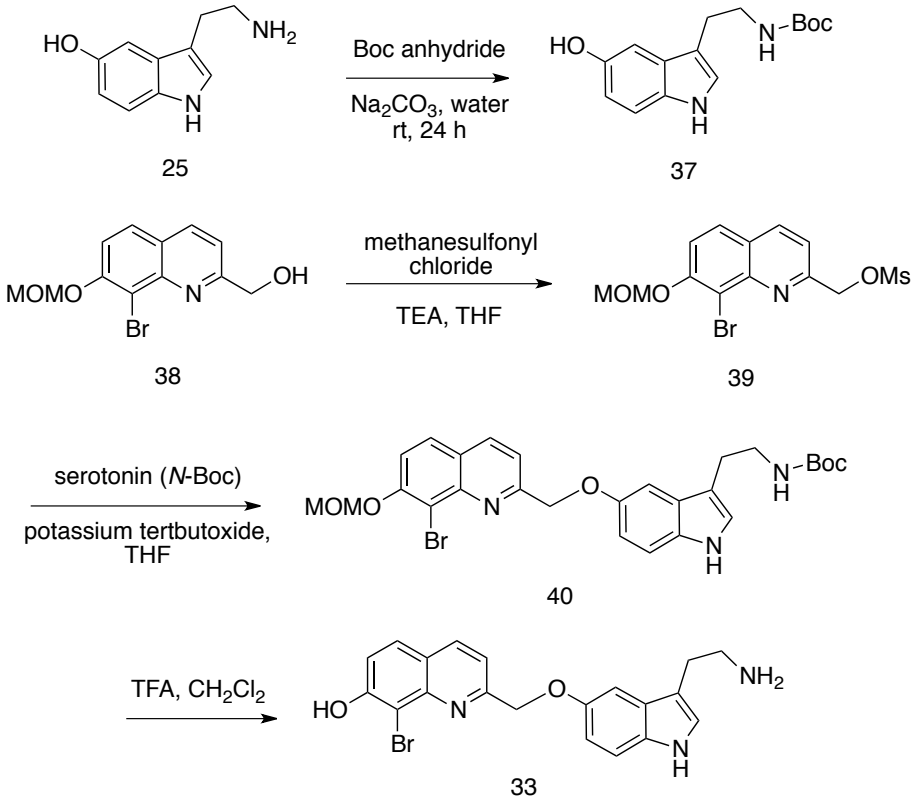

Scheme 1: Synthesis of BHQ-*O*-Serotonin (**33**)

In order for the phenol group on the indole ring of serotonin to couple to MOM-BHQ-OMs by displacing the mesylate, the amine of the hydrochloride salt of serotonin was protected with the Boc protecting group. (*N*-Boc) Serotonin was first reacted with MOM-BHQ-OMs using the procedure developed for the synthesis of MOM-BHQ-phenol. It was determined after multiple attempts that the reaction did not proceed. Ultimately, the reaction conditions were optimized by refluxing (*N*-Boc) serotonin with MOM-BHQ-OMs and potassium carbonate in acetonitrile, and afforded **40** in 78% yield. Global deprotection of the MOM and Boc protecting groups in 1:1 TFA/CH_2Cl_2 followed by purification by HPLC afforded **33** in 45% yield.

The synthesis of BHQ-*N*-Serotonin was based on previous work on BHQ and other PPGs that has demonstrated that in most cases, in order to effectively cage an amine, the amine must be caged as a carbamate. The carbamate functional group increases the rate and efficiency of uncaging versus simply covalently linking the amine at the uncaging site. The carbamic acid that is released is then decarboxylated to the active amine in a subsequent dark process. There are multiple methods for creating the carbamate functional group, and all include an intermediate with a good leaving group attached to an electrophilic carbonyl carbon.

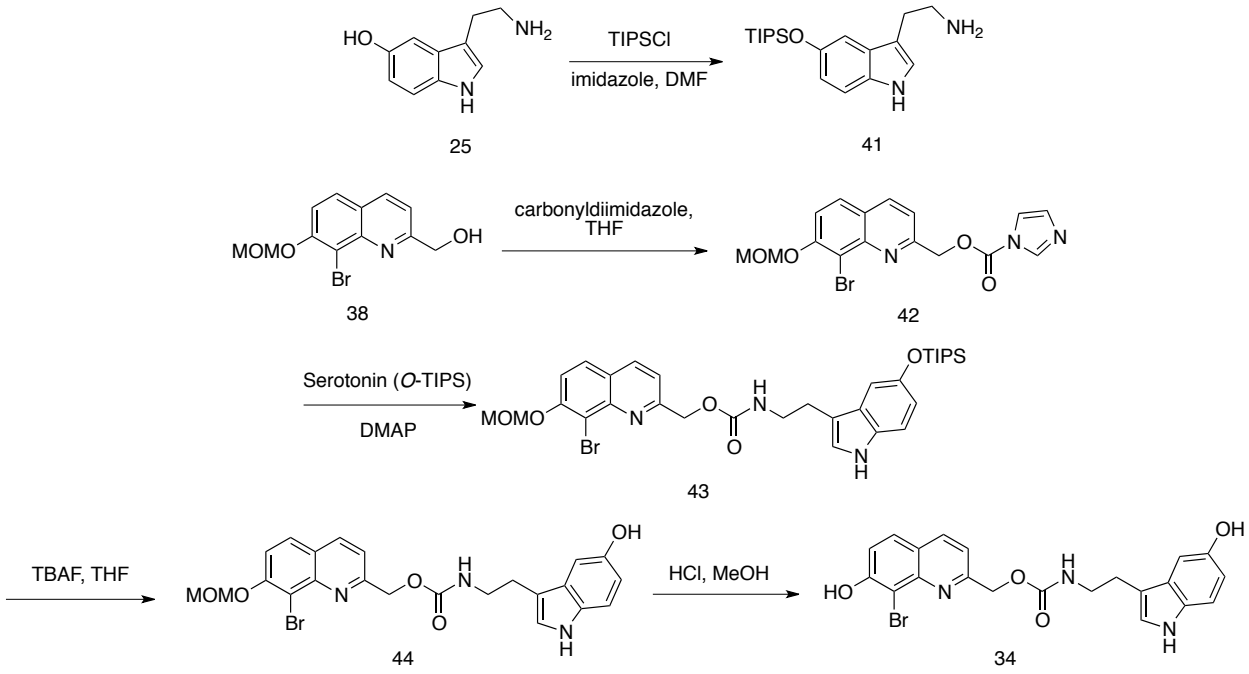

Scheme 2: Synthesis of BHQ-*N*-Serotonin (**34**)

In the case of the synthesis of BHQ-*N*-Serotonin, carbonyldiimidazole was reacted with MOM-BHQ-OH to yield **42** in 63% yield. Hoping to take advantage of the increased nucleophilicity of amines versus phenols, we tried to couple unprotected serotonin to MOM-BHQ-Carbonylimidazole. However, the reaction did not cleanly produce the desired carbamate, and significant amounts of cross or di-coupled products were observed. In hopes of increasing the yield of the desired product, serotonin was protected with a triisopropylsilyl (TIPS) protecting group. Once the known serotonin (*O*-TIPS) was isolated, the coupling reaction with MOM-BHQ-Carbonylimidazole proceeded smoothly in 65% yield to **43**. Removal of the TIPS group with TBAF followed by MOM deprotection with HCl in methanol afforded **34** in 55% yield.

Both forms of BHQ-Serotonin were examined for their photochemical properties and respective utilities for use in vivo. UV-VIS spectroscopy revealed that BHQ-*O*-Serotonin and BHQ-*N*-Serotonin had λ_{max} near 370 nm, and extinction coefficients (ε) of 2,000 and 2,100, respectively. Both forms of BHQ-Serotonin were photolyzed with both 1PE and 2PE, and the photolysis reactions were examined in order to determine the parameters that determine how well a caged compound releases its effector, namely the one-photon quantum efficiency (Q_u) and two-photon action cross-section (δ_u), respectively. As expected, both BHQ-*O*-Serotonin and BHQ-*N*-Serotonin release serotonin when exposed to both 1PE and 2PE.

Standard protocols were followed when examining both the 1PE and 2PE photolyses of both forms of BHQ-Serotonin. For 1PE photolysis, solutions of each respective compound were prepared in KMOPS buffer and photolyzed with a UV lamp with filters restricting the wavelength to 365 $\pm$ 15 nm. The reactions were analyzed periodically by HPLC, and peak areas were used to determine the extent of photolysis. For 2PE photolysis, solutions of each respective compound were prepared in KMOPS, and 20 uL aliquots were placed into a microcuvette and irradiated for various times with a Ti:S laser tuned to 740 nm. Each aliquot was subsequently analyzed by HPLC to determine the extent of photolysis. In both cases, a standard curve for serotonin was used to quantify the amount of serotonin produced in the reaction. Because it is necessary for a caged compound to be resistant to any significant amount of hydrolysis prior to uncaging, the dark stability of both forms of BHQ-Serotonin were examined. Solutions of each compound were prepared in KMOPS and left in the dark at room temperature. The solutions were analyzed periodically by HPLC and peak areas were used to determine the extent of hydrolysis.

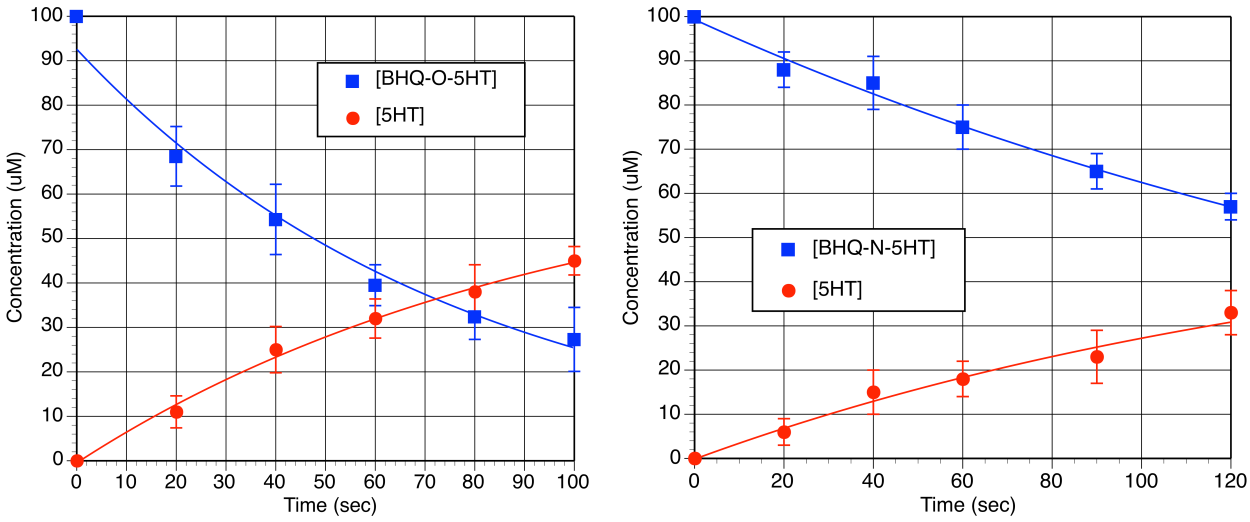

Figure 18: 1PE Photolysis of BHQ-*O*-Serotonin and BHQ-*N*-Serotonin

The photolysis curves of both BHQ-*O*-Serotonin and BHQ-*N*-Serotonin demonstrate that BHQ is ideally suited for release of serotonin in physiological conditions.

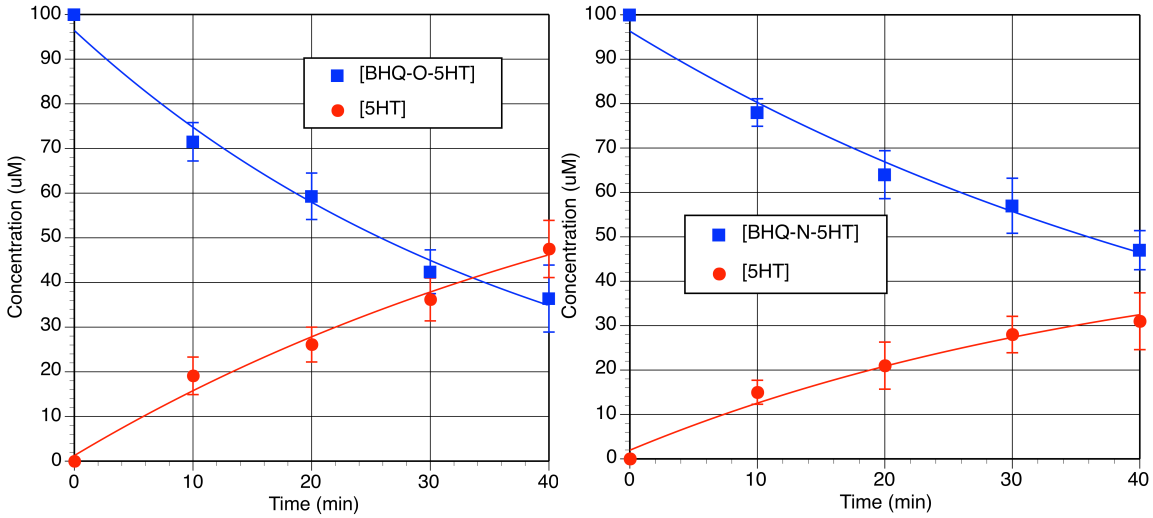

Figure 19: 2PE Photolysis of BHQ-*O*-Serotonin and BHQ-*N*-Serotonin

As evidenced by the 1PE and 2PE photolysis curves, both forms of BHQ-Serotonin uncage and release serotonin when irradiated. The photolysis curves were used to calculate the quantum efficiencies and two-photon action cross sections for both of the compounds.

Table 3: Summary of Photochemical and Photophysical Properties of BHQ-Serotonin

Caged Compound	λ_{max} nm	ε $M^{-1}cm^{-1}$	Q_u	Sensitivity $Q_u \times \varepsilon$	δ_u GM	τ_{dark} h
BHQ-*O*-Serotonin	368	2,000	0.30	600	0.50	260
BHQ-*N*-Serotonin	370	2,100	0.10	210	0.42	300
O-CNB-5HT	280	not reported	0.03	N/A	not reported	not reported

The photochemical and photophysical properties of both forms of BHQ-Serotonin are very similar to those of other BHQ-caged compounds, and are a vast improvement over the caged serotonins that exist in the literature. For comparison, reported photochemical data for *O*-CNB-5HT, the best of the previously reported caged serotonins, is included in Table 3. As nitrobenzyl-based caged compounds have very little two-photon sensitivity, no two-photon data is reported for *O*-CNB-5HT. The reported one-photon quantum yield, 0.03, is very low, however, and the UV spectra of the caged compound in HEPES buffer, pH 7.2, reveals that it absorbs strongly below 300 nm, but its absorbance decreases precipitously above 300 nm. On the other hand, the two forms of BHQ-Serotonin both have λ_{max} near 370 nm, a wavelength tolerated by biological systems. They also are highly sensitive to 2PE-induced uncaging. The two-photon action cross-sections (δ_u) reported for both forms of BHQ-Serotonin are both well above the established threshold of 0.1 GM,[11] above which a particular caged compound has

relevance for use *in vivo*. Additionally, both forms of BHQ-Serotonin are remarkably stable in the dark prior to irradiation, a definite advantage, as within reason there is no limit to the time scale for completing experiments involving BHQ-Serotonin before leakage occurs.

BHQ-*O*-Serotonin and BHQ-*N*-Serotonin are both highly valuable tools for probing serotonergic networks *in vivo*. The previously reported CNB-Serotonin proved invaluable in determining the kinetics of the $5HT_3$ ligand-gated ion channel, but its limitations have been demonstrated and the possible applications of a caged serotonin with 2PE sensitivity are nearly unlimited. It is expected that, because of their favorable 1PE and 2PE photochemical properties as well as dark stability, the dual forms of BHQ-Serotonin will be highly useful *in vivo* far beyond the initial biological experiments already conceived.

CHAPTER 3

The synthesis and characterization of a caged capsaicin with 2PE sensitivity

Capsaicin is a naturally occurring compound that is the active ingredient in chili peppers and imparts a burning sensation when it comes in contact with animal tissues. Capsaicin is also administered therapeutically in topical creams to treat mild aches and pains, and additionally is the active component in most self-defense 'pepper' sprays. Capsaicin is a member of a family of naturally-occurring and synthetically-derived compounds called capsaicinoids, all of which contain the aromatic vanilloid moiety, but differ in their hydrophobic alkyl chains.

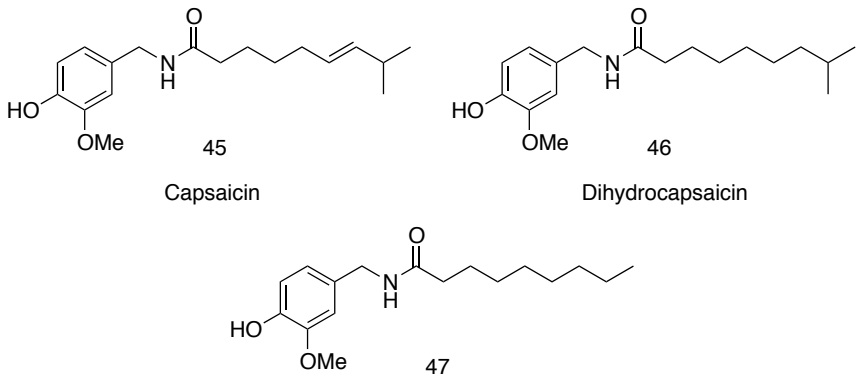

Figure 20: Capsaicin, Dihydrocapsaicin, and *N*-(vanillyl)nonanamide

Neurons that respond to noxious stimuli, called nociceptors, are found in the peripheral nervous system. When activated, they relay a signal to the central nervous system that is

interpreted generally as pain. The stimuli can be mechanical, thermal, or chemical in nature, and many pain signaling pathways have been elucidated.[43] Understanding how nociceptive neurons transmit signal is ultimately very important in imagining new ways to mediate pain through modulation of neuronal signaling. Small molecule stimuli such as capsaicin can be quite useful in studying these signaling pathways, as stimuli can be administered in a controlled and repetitive manner.

The receptor responsible for the nociceptive response to capsaicin was not known until 1997, when a report published in Nature by Julius and coworkers elucidated the structural and pharmacological characteristics of the capsaicin-receptor ion channel that subsequently became known as the TRPV1 channel.[44] The transient receptor potential (TRP) channel family is united by similarities in sequence homology and signaling transduction pathways.[45] TRP channels have six transmembrane domains and are permeable to most cations in a mostly non-specific manner; their activation is linked to both the phosphatidylinositol/PLC and Ca^{2+} signaling pathways. TRP channels are classified by sequence homology into TRPC, TRPV, and TRPM subtypes. Of the TRPV subtype, the vanilloid receptors TRPV1 and TRPV2 are most well-known. The TRPV1 is activated by both noxious heat and capsaicin, and is expressed throughout the peripheral nervous system. Experiments with TRPV1 knock-out mice have shown that it is necessary for the observation of nociceptive effects in response to capsaicin.

One observable physiological response to TRPV1 receptor activation is large Ca^{2+} signal spikes that propagate through neuronal pathways.[46] Calcium imaging using small-molecule fluorescent calcium chelators or genetically-encoded fluorescence resonance energy transfer (FRET) based calcium reporters is a very facile way of mapping neuronal circuits, as calcium

transients often accompany action potential spikes or other neuronal activity.[47-49] Calcium imaging is indeed a massive area of research that has greatly advanced knowledge of neural networks. The structural elucidation of the TRPV1 receptor allowed cloning of cells expressing the TRPV1 channel that do not endogenously express it. In order to compare the responses of TRPV1 cloned cells to those of nociceptive neurons that endogenously express the TRPV1 receptor to capsaicin and heat, Rang and coworkers transfected a chinese hamster ovary cell line with a rat TRPV1 cDNA insert and used rat dorsal root ganglion neurons (DRGs) as a comparison.[50] The cells were loaded with a small molecule fluorescent calcium chelator. They found that both capsaicin and noxious heat, with an activation threshold of 42 °C, elicited significant increases in intracellular calcium levels.

The role of calcium as a second messenger in the cell has led to increased interest in calcium signaling, and indeed having calcium wave spikes that accompany neural activity under the control of light is an incredibly powerful tool. The initiation of calcium signaling cascades subsequent to activation of the TRPV1 ion channel and the essentially equal potency of capsaicin, dihydrocapsaicin, and *N*-(vanillyl)nonanamide (VNA) toward the TRPV1 channel make a photolabile analog of the capsaicinoids a desirable synthetic target. The synthesis of photolabile TRPV1 ligands has been approached using a variety of caging methods. Capsaicinoids essentially contain two functional groups suitable for attachment of a PPG, the phenol hydroxy group and the amide nitrogen that links the vanilloid aromatic ring to the long alkyl chain. The first form of a caged TRPV1 receptor agonist, reported by Miesenbock, was a DMNB-caged capsaicin with the caging group attached at the phenol through a carbonate linkage.[51] Subsequently, a variety of caged TRPV1 ligands utilizing nitrobenzyl- or phenacyl-

based photoremovable protecting groups have been reported.[52-54] One notable exception is a BCMACOC-caged capsaicin reported by Hagen, in which the coumarin caging group is attached to the phenol through a carbonate.[55] Nitrobenzyl- and phenacyl-caged compounds suffer from slow release kinetics and low sensitivity to 2PE. Though the coumarins have increased kinetics and 2PE sensitivity relative to nitrobenzyls, because they cannot release phenols directly and a carbamate linkage must be used, the coumarin-caged compound suffers from the same problems affecting the nitrobenzyl-caged TRPV1 ligands. Because the nitrobenzyl-based PPGs cannot release phenols directly, the phenol of VNA is caged as a carbonate. Not surprisingly, the release kinetics are very slow, and the form of caged VNA with the best characteristics is reported to be the form of NB-VNA in which VNA is caged at the amide nitrogen. Though the nitrobenzyl PPG's poor sensitivity to 2PE is well-documented, due to the incredible potency of capsaicinoids toward activation of TRPV1 channels, a physiological response is observed subsequent to irradiation of NB-VNA with 740 nm light. Kao and coworkers were able to uncage NB-caged capsaicin, activate the TRPV1 channel, and observe calcium transients through fluorescent imaging methods subsequent to uncaging.[53] They even were able to uncage NB-capsaicin in small amounts in response to 2PE irradiation. However, for a caged capsaicin to be truly useful in calcium imaging studies, it needs to be highly susceptible to 2PE. As discussed previously, the two-photon uncaging cross-section for BHQ-caged compounds is an order of magnitude higher than that of nitrobenzyl-caged compounds.

The BHQ PPG is an ideal candidate for the synthesis of a caged VNA or other capsaicinoid with sensitivity to 2PE. In BHQ-caged capsaicin, as in BHQ-*O*-Serotonin, the

capsaicin will be covalently linked to the PPG at the phenolic hydroxy group. As mentioned previously, capsaicinoids contain two functional groups capable of linking to a PPG, the phenol as well as the secondary amide. In designing a caged VNA using the BHQ PPG, it is important to keep in mind that while no attempts have been made to cage an amide with BHQ, BHQ has been shown to release phenols directly with large two-photon action cross-sections. In addition, structural studies of the TRPV1 channel have revealed that the phenol of the vanilloid moiety is necessary for correct binding to the receptor.[56] Attaching the BHQ PPG to VNA at the phenol should render it inactive, while irradiation with 1PE or 2PE should release VNA from the caged compound quickly and in good yield. A BHQ-caged VNA has the same advantages that any BHQ-caged moiety has over the respective NB-caged moiety: namely vastly higher sensitivity to 2PE and increased release kinetics.

In revisiting the zebrafish model, it is important to note that the zebrafish does not endogenously express the TRPV1 channel, and is therefore not sensitive to capsaicin.[57] What initially appears to be a drawback to the zebrafish model becomes a powerful advantage when one considers the ease in which zebrafish can be manipulated genetically. Building a line of zebrafish that express the TRPV1 channel in various ways confers to a caged capsaicin with high sensitivity to 2PE the potential to be a potent tool in the control of neural activity in the zebrafish model.

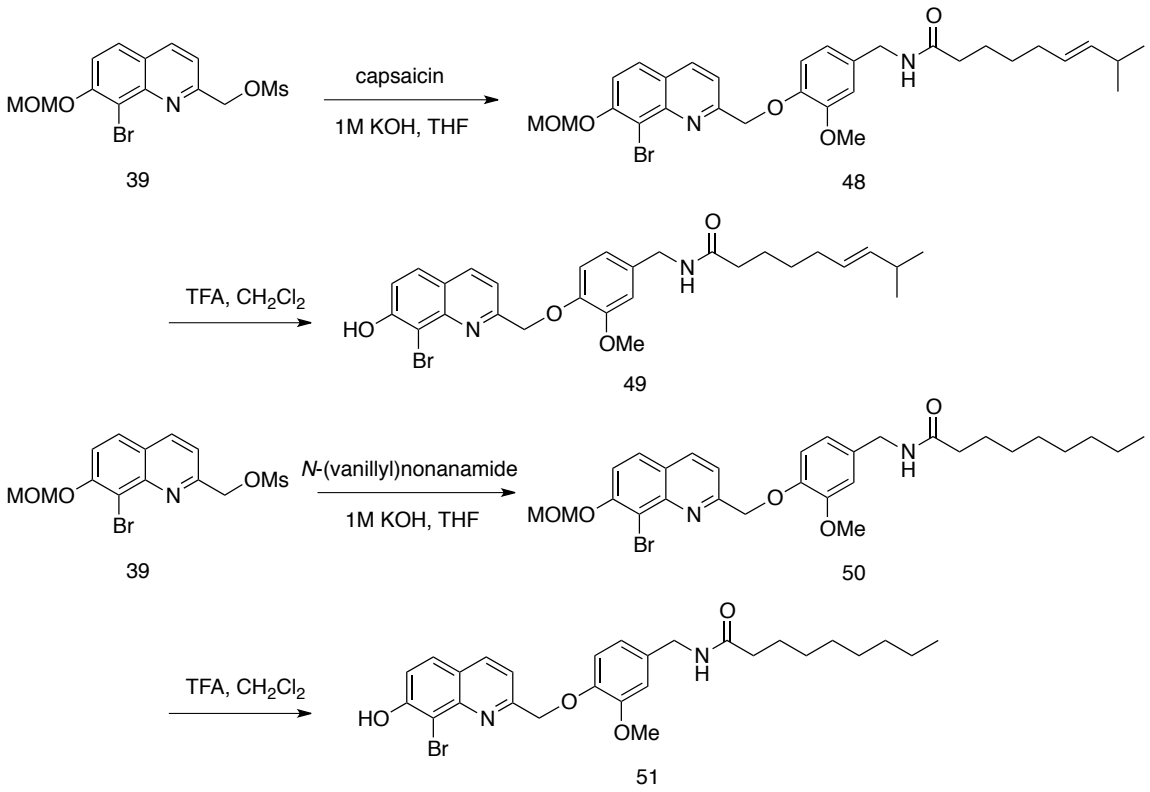

Scheme 3: Syntheses of BHQ-Capsaicin (**49**) and BHQ-VNA (**51**)

The coupling reaction between the vanilloid ligand and MOM-BHQ-OMs proceeded in 37% yield in the case of MOM-BHQ-Capsaicin and 32% in the case of MOM-BHQ-VNA. Deprotection of the MOM ether in TFA yielded the final products **49** and **51** in 30% and 57% yield, respectively.

It was determined through attempts at characterizing the photochemical properties of the caged capsaicinoids that both forms have solubility issues in aqueous buffers. Homogenous solutions of each compound in aqueous buffers were prepared, but without large amounts of organic co-solvents such as methanol or DMSO or detergents, the compound would precipitate out of the solution. Performing photochemistry using large amounts of organic co-solvents or

detergents is not ideal, and understanding the photochemistry of the caged capsaicinoids requires photolysis conditions that are the same as in previously described experiments. To resolve this issue, a soluble analogue of the BHQ-Capsaicinoids was synthesized to accurately assess their photochemistry and compare to previously characterized BHQ-caged compounds. The synthesis of BHQ-VAA, in which the long chain alkyl amide is replaced with an acetamide, was carried out in a similar fashion as that of BHQ-Capsaicin and BHQ-VNA.

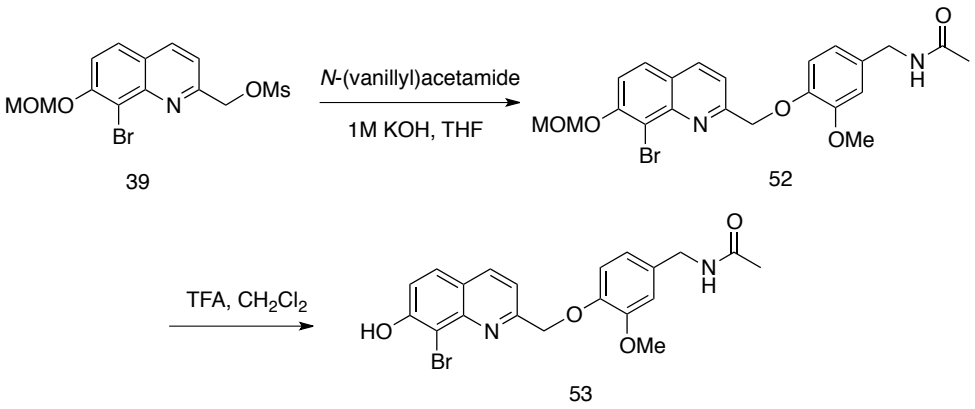

Scheme 4: Synthesis of BHQ-VAA (**53**)

BHQ-VAA should have very similar photochemistry of release as the caged capsaicinoids BHQ-Capsaicin and BHQ-VNA. By creating an analogue in which the electronics proximal to the site of uncaging are identical, but the long alkyl chain is truncated, it is possible to study the photochemistry without the use of organic co-solvents or detergents and therefore more accurately compare the photochemistry of the BHQ-capsaicinoids to previously reported BHQ-caged compounds. Indeed, BHQ-VAA was shown to be soluble in aqueous buffers, which made comparison of the photochemistry of caged capsaicinoids to previous BHQ-caged moieties

possible. UV-VIS spectroscopy was used to determine the λ_{max} and extinction coefficient (ε) of BHQ-VAA, which were determined to be 370 and 2,700, respectively.

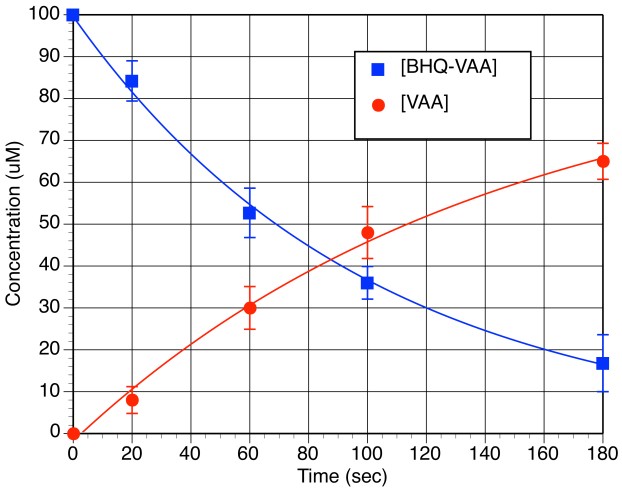

Figure 21: 1PE Photolysis of BHQ-VAA

BHQ-VAA was irradiated with a mercury lamp with filters restricting the wavelength of irradiation to 365 $\pm$ 15 nm, and photolysis was followed by HPLC. The generated photolysis curve was used to calculate the quantum efficiency. It was determined that the quantum efficiency of photolysis of BHQ-VAA was 0.18.

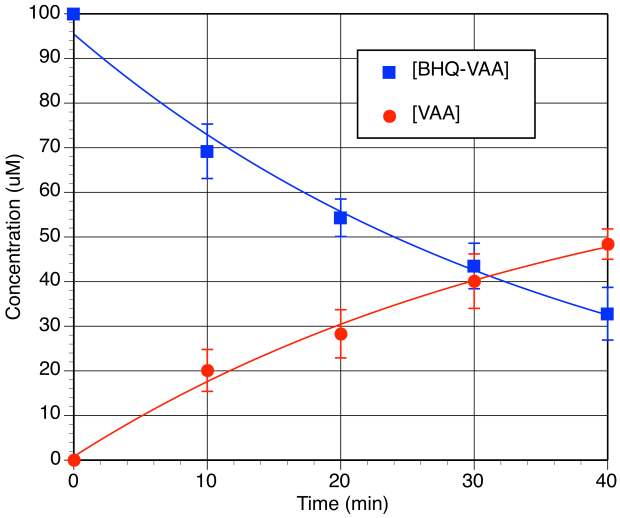

Figure 22: 2PE Photolysis of BHQ-VAA

BHQ-VAA was irradiated with a Ti:S laser with irradiation wavelength tuned to 740 nm. The course of the reaction was followed by HPLC, and it was determined that the two-photon action cross-section was 0.61 GM.

Table 4: Summary of Photochemical and Photophysical Properties of BHQ-VAA

Caged Compound	λ_{max} nm	ε $M^{-1}cm^{-1}$	Q_u	Sensitivity $Q_u \times \varepsilon$	δ_u GM	τ_{dark} h
BHQ-VAA	370	2,700	0.18	486	0.61	140

The photochemical characterization of BHQ-VAA, in particular its relative dark stability and two-photon sensitivity, provide strong evidence that BHQ-Capsaicin will release capsaicin quickly and efficiently in response to irradiation with either 1PE or 2PE. It is by far the best caged capsaicin reported thus far for studies of TRPV1 channel activation in a tightly spatiotemporally controlled manner.

CHAPTER 4

Experimental Section

Synthesis of Caged Compounds

All NMR spectra were collected either on a Varian MercuryPlus 400 MHz NMR spectrometer or a Varian Unity Inova 500 MHz NMR spectrometer. All mass spectra were collected either on a Perkin Elmer Sciex API I plus Quadrupole Mass Spectrometer or a Waters Micromass Q-TOF Micro Mass Spectrometer. HPLC was performed on a Varian ProStar system with ProStar 335 detector, binary ProStar 210 pumps, and C18 reverse phase columns interfaced with either Star Workstation or Galaxie software. All solvents and reagents were obtained reagent-grade from either Fisher Scientific, Baker, Acros, or Sigma and used without additional purification.

MOM-BHQ-*O*-Serotonin (*N*-Boc) (40)

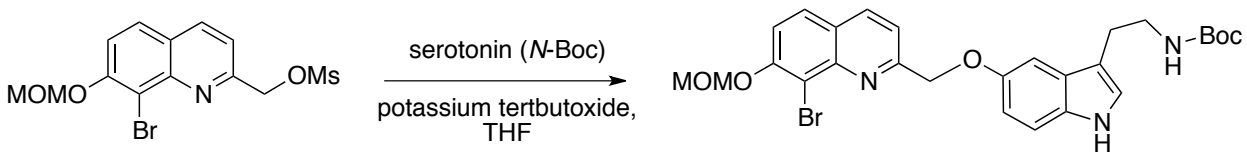

39 40

Serotonin (*N*-Boc) (97 mg, 0.35 mmol) was dissolved in acetonitrile and potassium carbonate (86 mg, 0.62 mmol) was added. MOM-BHQ-OMs (188 mg, 0.50 mmol) was added in one portion and the reaction stirred at reflux for 2 d. The reaction was allowed to cool, then filtered and concentrated. The residue was purified by column chromatography with silica gel, eluting with a gradient from 100% Hexanes to 3:1 EtOAc/hexanes, yielding a yellow oil (151 mg, 78 %).

^{1}H NMR (400 MHz, $CDCl_3$) δ 8.14 (d, J = 8.4 Hz, 1H), 7.97 (s, 1H), 7.76 (d, J = 9.0 Hz, 1H), 7.74 (d, J = 8.4 Hz, 1H), 7.50 (d, J = 9.0 Hz, 1H), 7.23 (s, 1H), 7.02 (m, 2H), 5.50 (s, 2H), 5.42 (s, 2H), 3.59 (s, 3H), 3.42 (t, J = 6.5 Hz, 2H), 2.90 (t, J = 6.5 Hz, 2H), 1.43 (s, 9H).

^{13}C NMR (101 MHz, $CDCl_3$) δ 170.7, 161.2, 161.1, 160.6, 156.1, 155.3, 153.0, 146.0, 137.2, 131.9, 128.2, 124.7, 118.5, 117.3, 112.8, 112.1, 103.5, 102.6, 95.6, 77.4, 72.2, 56.9, 40.8, 28.7, 26.0.

HRMS (ESI) calcd for $[M+H]^+$ 556.1447, 558.1427; found 556.1432, 558.1420.

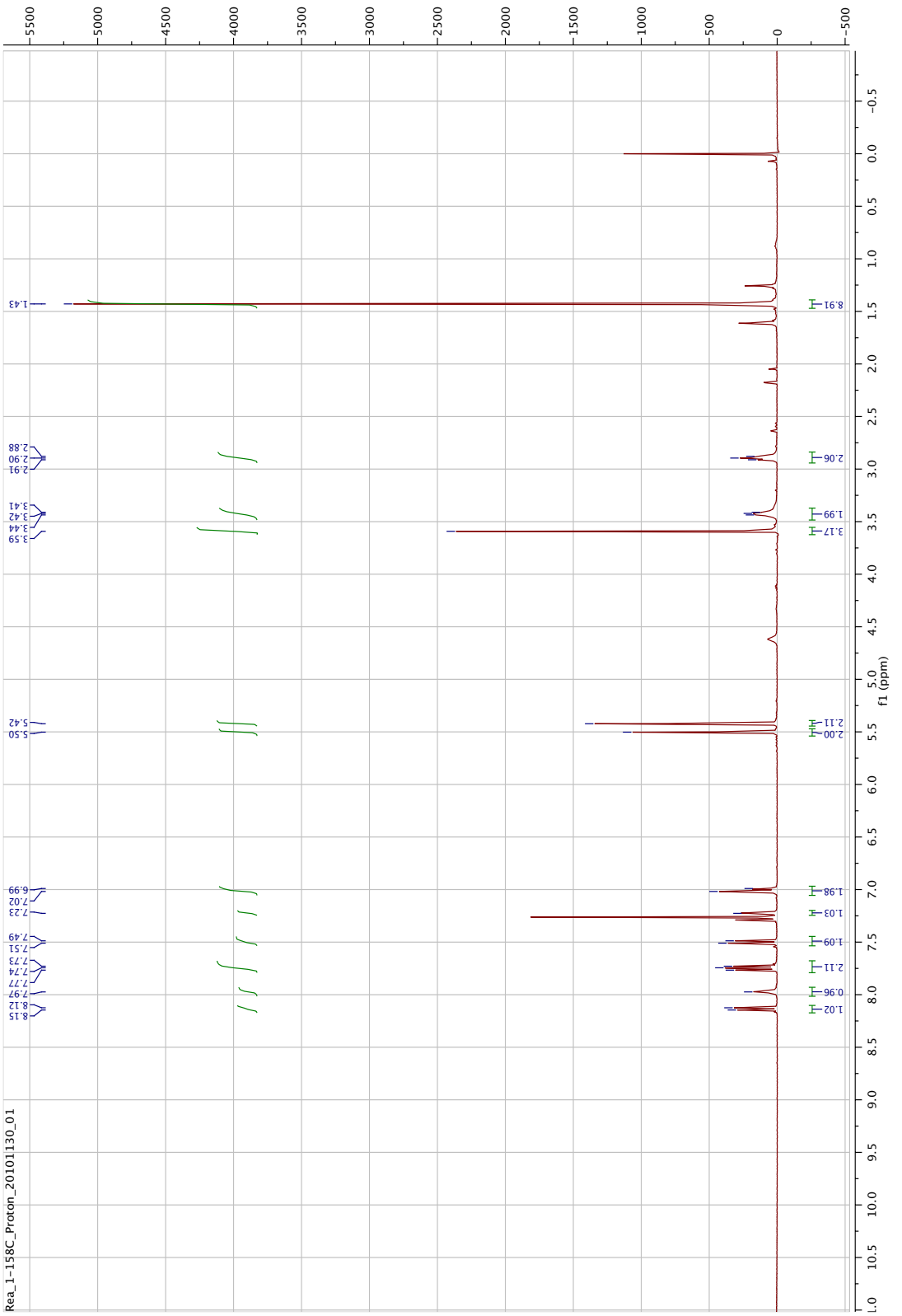
Rea_1-158C_Proton_20101130_01
f1 (ppm)
1.43
8.91
2.91
2.90
2.88
2.06
3.41
3.42
3.59
3.44
1.99
3.17
5.50
5.42
2.11
2.00
6.99
7.02
7.23
7.49
7.51
7.73
7.74
7.77
7.97
8.12
8.15
1.98
1.03
1.09
2.11
0.96
1.02

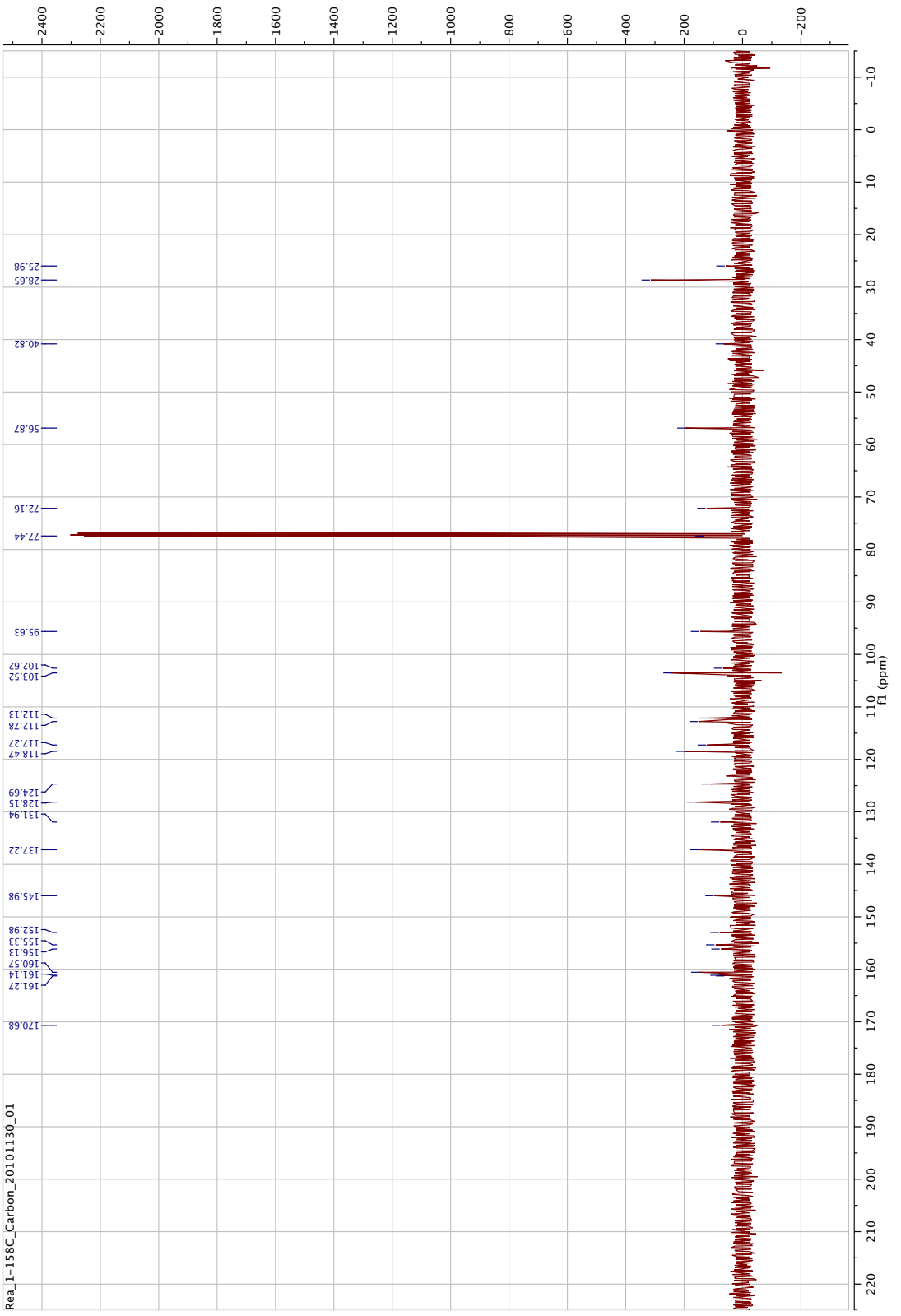
Rea_1-158C_Carbon_20101130_01
f1 (ppm)
25.98
28.65
40.82
56.87
72.16
77.44
95.63
102.62
103.52
112.13
112.78
117.27
118.47
124.69
128.15
131.94
137.22
145.98
152.98
155.33
156.13
160.57
161.14
161.27
170.68

BHQ-*O*-Serotonin (33)

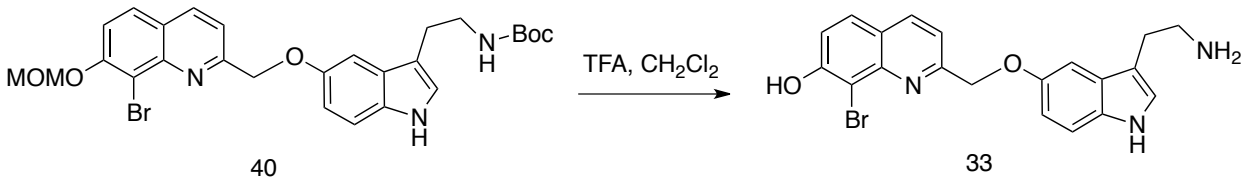

MOM-BHQ-*O*-Serotonin (*N*-Boc) (47 mg, 0.085 mmol) was dissolved in methylene chloride. Trifluoroacetic acid was added and the reaction stirred at rt for 1 h. The solvent was removed in vacuo and the residue purified by HPLC with 50% CH_3CN/50% H_2O (w/ 0.1 % TFA). Fractions containing only one peak were combined and concentrated (20 mg, 57 %).

^{1}H NMR (500 MHz, $(CD_3)_2CO$) δ 8.32 (d, J = 8.4 Hz, 1H), 7.87 (d, J = 8.9 Hz, 1H), 7.70 (d, J = 8.4 Hz, 1H), 7.45 (s, 1H), 7.44 (s, 1H), 7.38 (d, J = 8.9 Hz, 1H), 7.30 (d, J = 10.8 Hz, 1H), 7.00 (d, J = 10.8 Hz, 1H), 5.44 (s, 2H), 4.06 (t, J = 7.0 Hz, 2H), 3.30 (t, J = 7.0 Hz, 2H).

^{13}C NMR (101 MHz, $(CD_3)_2CO$) δ 161.9, 160.2, 160.7, 156.3, 155.8, 153.4, 146.1, 138.5, 131.0, 127.4, 123.2, 119.7, 118.4, 112.2, 113.0, 102.8, 102.1, 77.6, 73.1, 40.6, 25.2.

HRMS (ESI) calcd for $[M+H]^+$ 412.0661, 414.0640; found 412.0651, 414.0626.

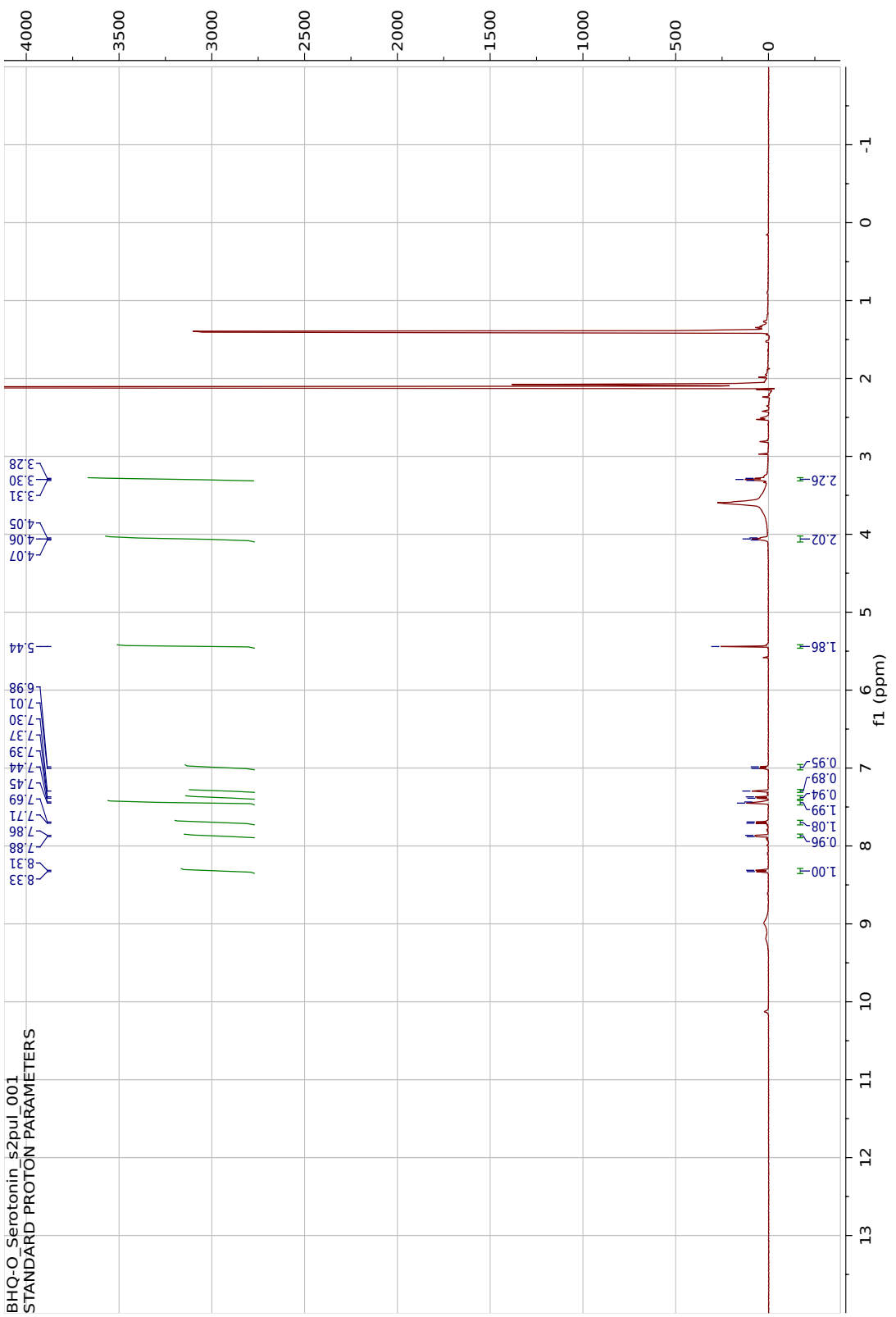
BHQ-O_Serotonin_s2pul_001
STANDARD PROTON PARAMETERS
f1 (ppm)
8.33
8.31
7.88
7.86
7.71
7.69
7.45
7.44
7.39
7.37
7.30
7.01
6.98
5.44
4.07
4.06
4.05
3.31
3.30
3.28
2.26
2.02
1.86
1.00
0.96
1.08
1.99
0.94
0.89
0.95

MOM-BHQ-Carbonylimidazole (42)

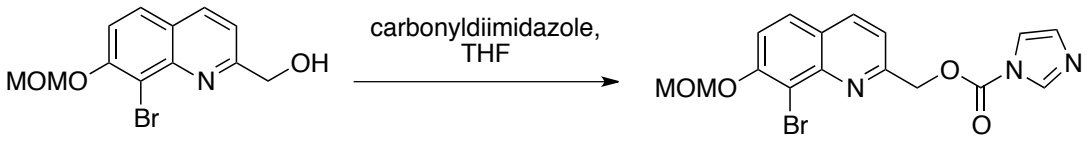

38 42

MOM-BHQ-OH (100 mg, 0.34 mmol) was dissolved in THF. Carbonyldiimidazole (82 mg, 0.50 mmol) was added, and the reaction stirred at rt for 2 h. The reaction was concentrated and the residue dissolved in EtOAc, washed with water and brine, dried over anhydrous $MgSO_4$, filtered, and concentrated *in vacuo*. The crude product was purified by column chromatography with silica gel, eluting with a gradient from 1:1 EtOAc/hexanes to 100% EtOAc, yielding a white solid (84 mg, 63 %).

^{1}H NMR (400 MHz, $CDCl_3$) δ 8.28 (s, 1H), 8.14 (d, J = 8.4 Hz, 1H), 7.74 (d, J = 9.0 Hz, 1H), 7.55 (s, 1H), 7.50 (d, J = 9.0 Hz, 1H), 7.39 (d, J = 8.4 Hz, 1H), 5.75 (s, 2H), 5.39 (s, 2H), 3.56 (s, 3H).

^{13}C NMR (101 MHz, $CDCl_3$) δ 155.8, 155.4, 148.9, 146.1, 137.6, 137.6, 131.0, 128.0, 124.7, 118.0, 117.7, 117.6, 112.6, 95.6, 69.9, 56.8.

HRMS (ESI) calcd for $[M+H]^+$ 392.0246, 394.0225; found 392.0262, 394.0244.

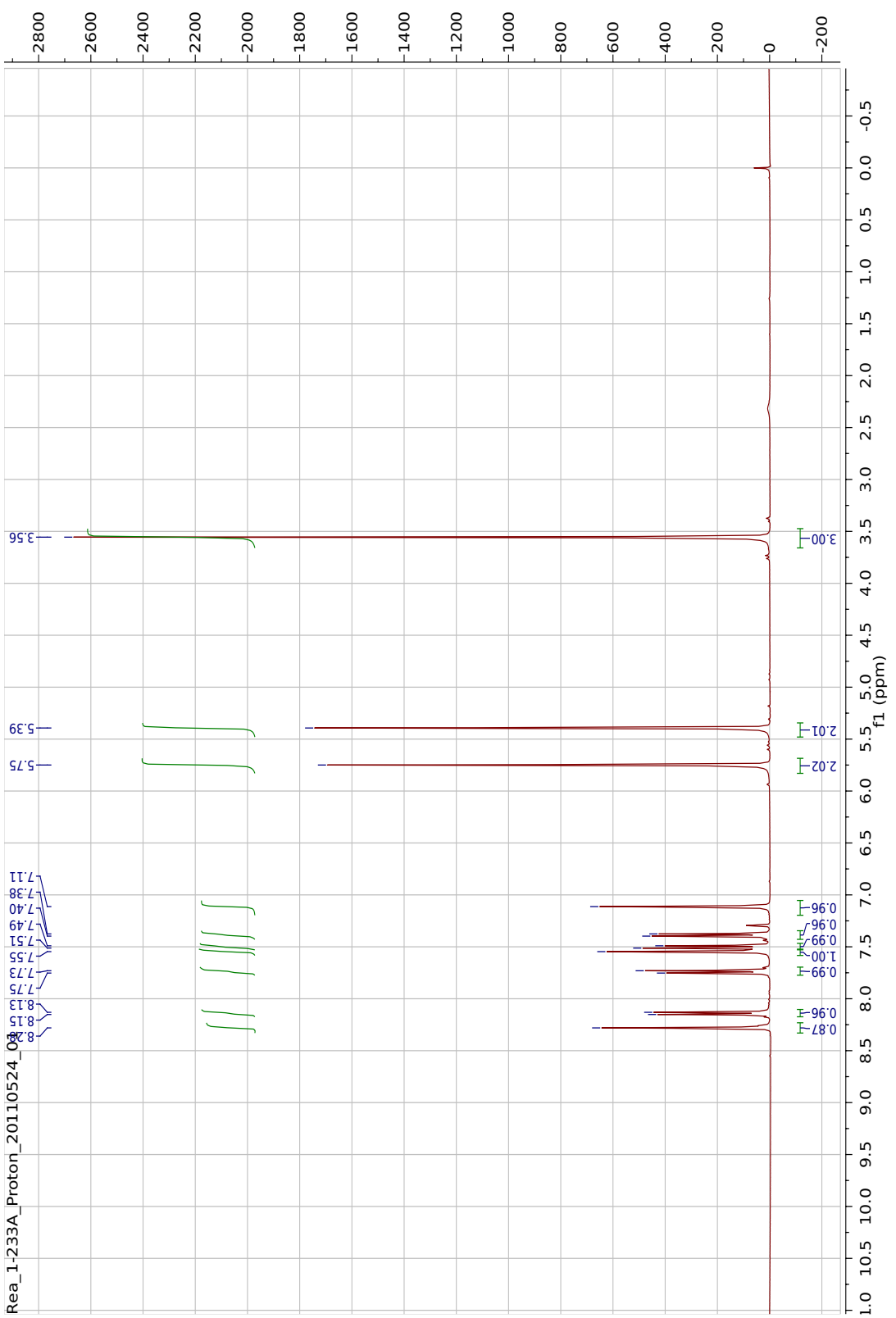
Rea_1-233A_Proton_20110524_01
f1 (ppm)
3.56
5.39
5.75
7.11
7.38
7.40
7.49
7.51
7.55
7.73
7.75
8.13
8.15
8.28
3.00
2.01
2.02
0.96
0.96
0.99
1.00
0.99
0.96
0.87

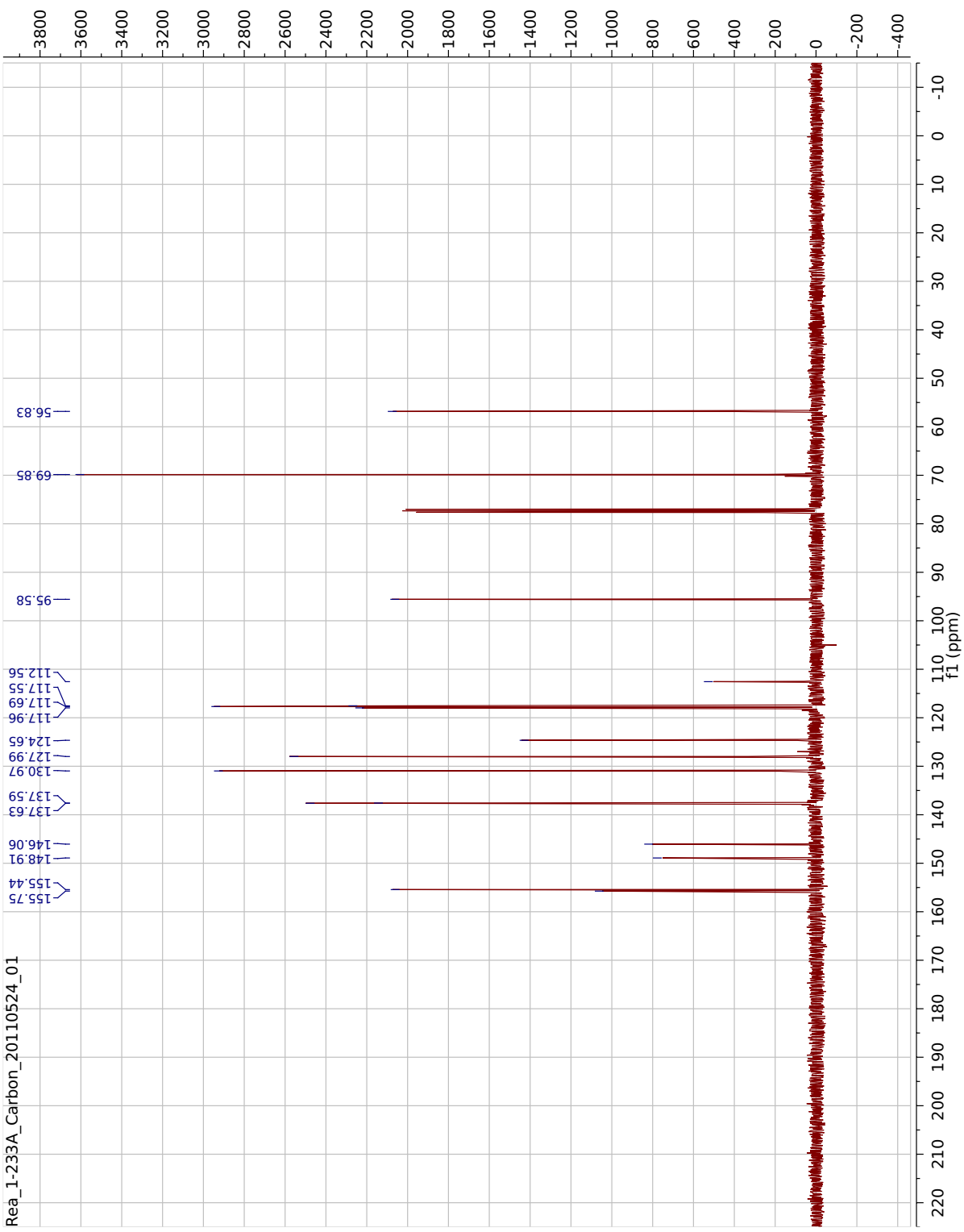
Rea_1-233A_Carbon_20110524_01
155.75
155.44
148.91
146.06
137.63
137.59
130.97
127.99
124.65
117.96
117.69
117.55
112.56
95.58
69.85
56.83
f1 (ppm)

MOM-BHQ-*N*-Serotonin (*O*-TIPS) (43)

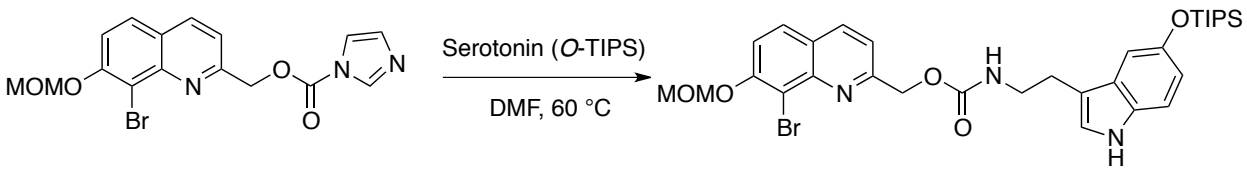

42 43

Serotonin (*O*-TIPS) (67 mg, 0.20 mmol) was dissolved in a small amount of DMF. MOM-BHQ-Carbonylimidazole (100 mg, 0.25 mmol) was added and the reaction heated to 60 °C and stirred overnight. The solvent was removed *in vacuo* and the residue partitioned between EtOAc and water. The combined organic extracts were dried over anhydrous $MgSO_4$, filtered, and concentrated *in vacuo*. The crude product was purified by column chromatography with silica gel, eluting with a gradient from 100 % hexanes to 1:1 EtOAc/hexanes, yielding the product as a solid (85.9 mg, 65 %).

^{1}H NMR (400 MHz, $CDCl_3$) δ 8.07 (d, J = 8.4 Hz, 1H), 7.95 (s, 1H), 7.72 (d, J = 9.0 Hz, 1H), 7.48 (d, J = 9.0 Hz, 1H), 7.36 (d, J = 8.4 Hz, 1H), 7.18 (d, J = 8.7 Hz, 1H), 7.04 (s, 1H), 7.00 (s, 1H), 6.81 (d, J = 8.7 Hz, 1H), 5.44 (s, 2H), 5.40 (s, 2H), 3.58 (t, J = 6.6 Hz, 2H), 3.57 (s, 3H), 2.95 (t, J = 6.6 Hz, 2H), 1.26 (m, J = 7.3 Hz, 3H), 1.11 (d, J = 7.3 Hz, 18H).

^{13}C NMR (126 MHz, $CDCl_3$) δ 158.8, 156.2, 155.2, 149.7, 145.8, 137.0, 131.8, 127.9, 127.8, 124.4, 122.9, 118.1, 117.2, 116.3, 112.3, 111.4, 107.8, 95.4, 77.2, 67.5, 56.6, 41.2, 25.7, 18.1, 12.7.

HRMS (ESI) calcd for $[M+H]^+$ 656.2155, 658.2135; found 656.2171, 658.2154.

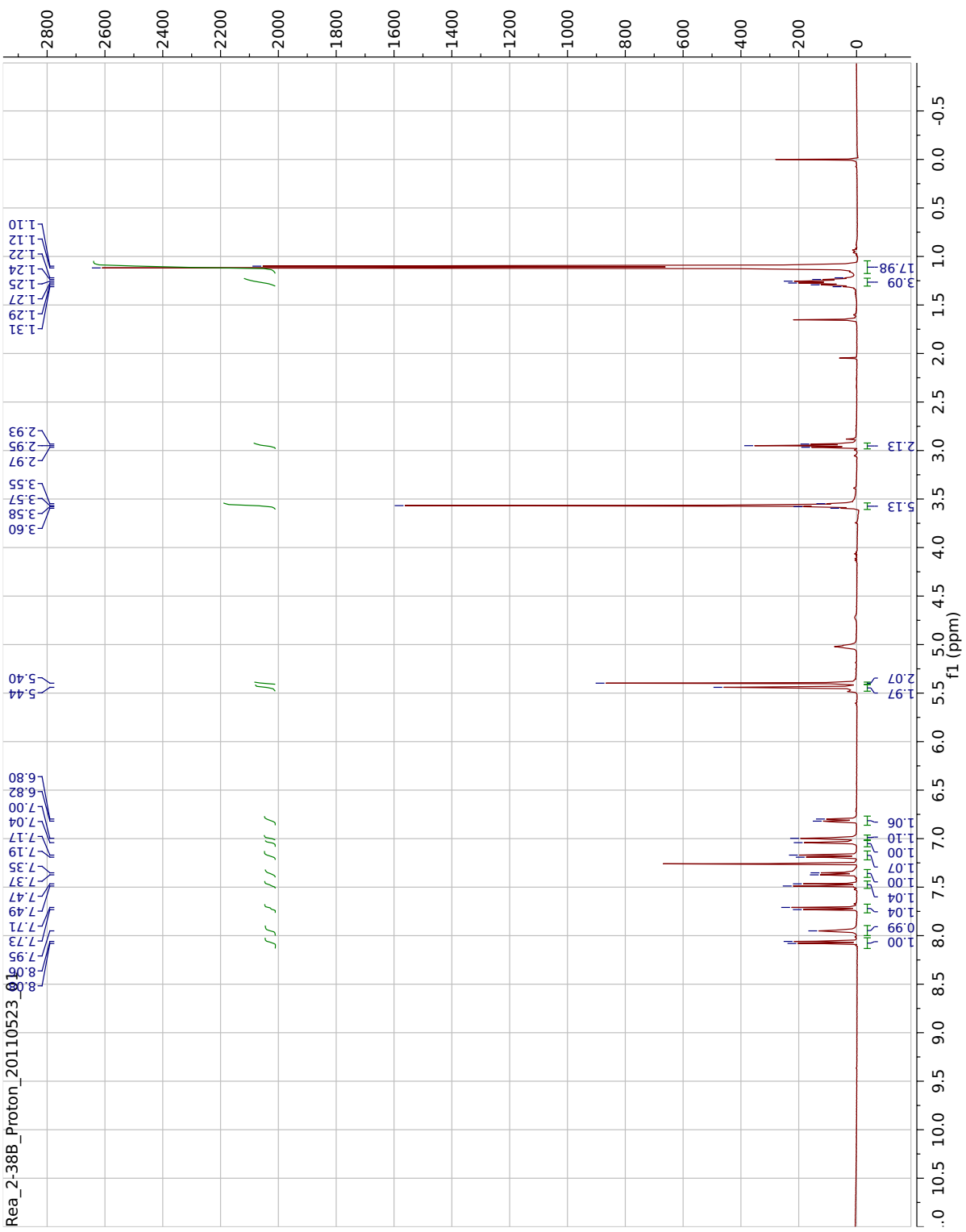
Rea_2-38B_Proton_20110523_01
f1 (ppm)

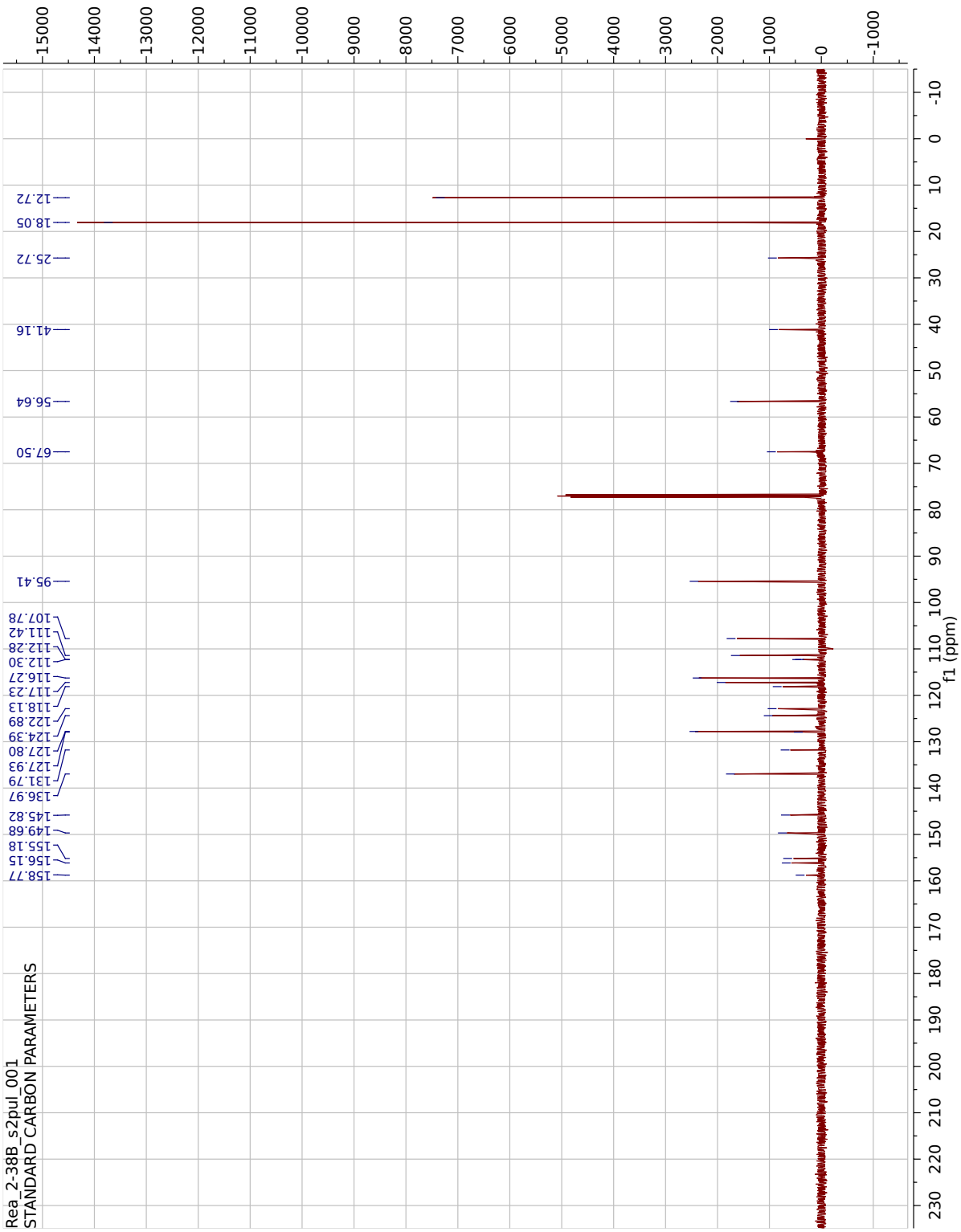
Rea_2-38B_s2pul_001
STANDARD CARBON PARAMETERS
158.77
156.15
155.18
149.68
145.82
136.97
131.79
127.93
127.80
124.39
122.89
118.13
117.23
116.27
112.30
112.28
111.42
107.78
95.41
67.50
56.64
41.16
25.72
18.05
12.72
f1 (ppm)

MOM-BHQ-*N*-Serotonin (44)

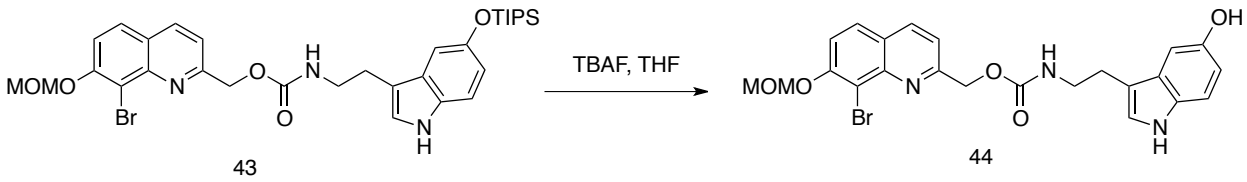

43 44

MOM-BHQ-*N*-Serotonin (*O*-TIPS) (85.9 mg, 0.13 mmol) was dissolved in a small amount of THF. TBAF (0.2 mL, 1.0 M in THF) was added slowly and the reaction stirred at rt for 15 min. The reaction was concentrated and the residue partitioned between EtOAc and water. The organic layer was washed with water and brine, dried over anhydrous $MgSO_4$, filtered, and concentrated *in vacuo*. The crude product was purified by column chromatography with silica gel, eluting with a gradient from 100 % hexanes to 1:1 EtOAc/hexanes, yielding the product as a solid (55 mg, 85 %).

^{1}H NMR (400 MHz, $CDCl_3$) δ 8.05 (d, 1H), 8.00 (s, 1H), 7.68 (d, 1H), 7.35 (d, 1H), 7.18 (d, 1H), 6.95 (m, 2H), 6.77 (d, 1H), 5.42 (s, 2H), 5.38 (s, 2H), 5.18 (broad, 1H), 3.57 (s, 3H), 3.48 (q, 2H), 2.84 (t, 2H).

^{13}C NMR (101 MHz, $CDCl_3$) δ 158.78, 156.69, 155.45, 149.81, 145.93, 137.39, 131.77, 128.10, 126.24, 124.62, 123.44, 118.30, 117.48, 115.82, 112.32, 112.12, 103.52, 103.25, 95.63, 67.70, 56.89, 41.60, 25.96.

HRMS (ESI) calcd for $[M+H]^+$ 500.0821, 502.0801; found 500.0823, 502.0810.

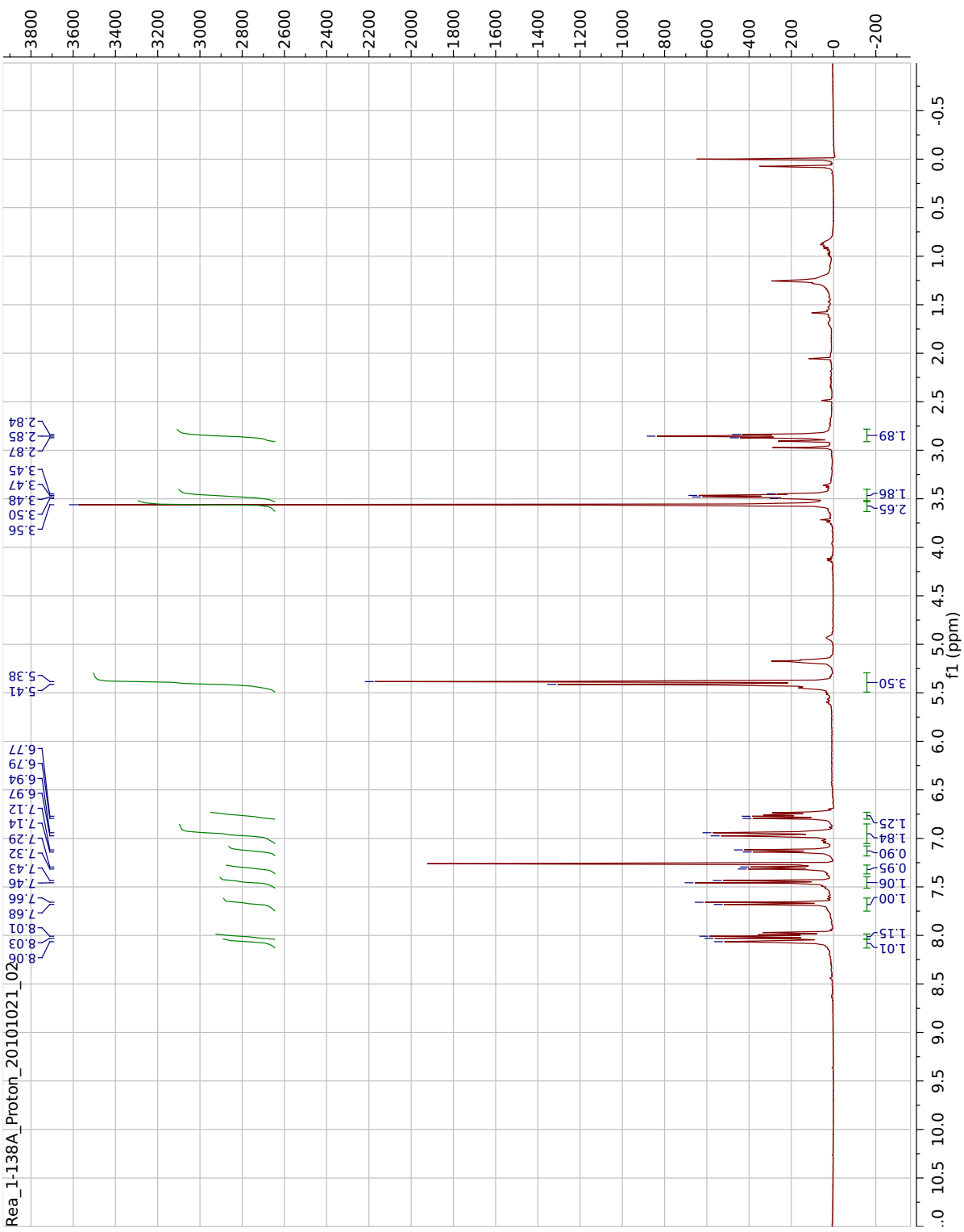
Rea_1-138A_Proton_20101021_02
f1 (ppm)
8.06
8.03
8.01
7.68
7.66
7.46
7.43
7.32
7.29
7.14
7.12
6.97
6.94
6.79
6.77
5.41
5.38
3.56
3.50
3.48
3.47
3.45
2.87
2.85
2.84
1.89
1.86
2.65
3.50
1.01
1.15
1.00
1.06
0.95
0.90
1.84
1.25

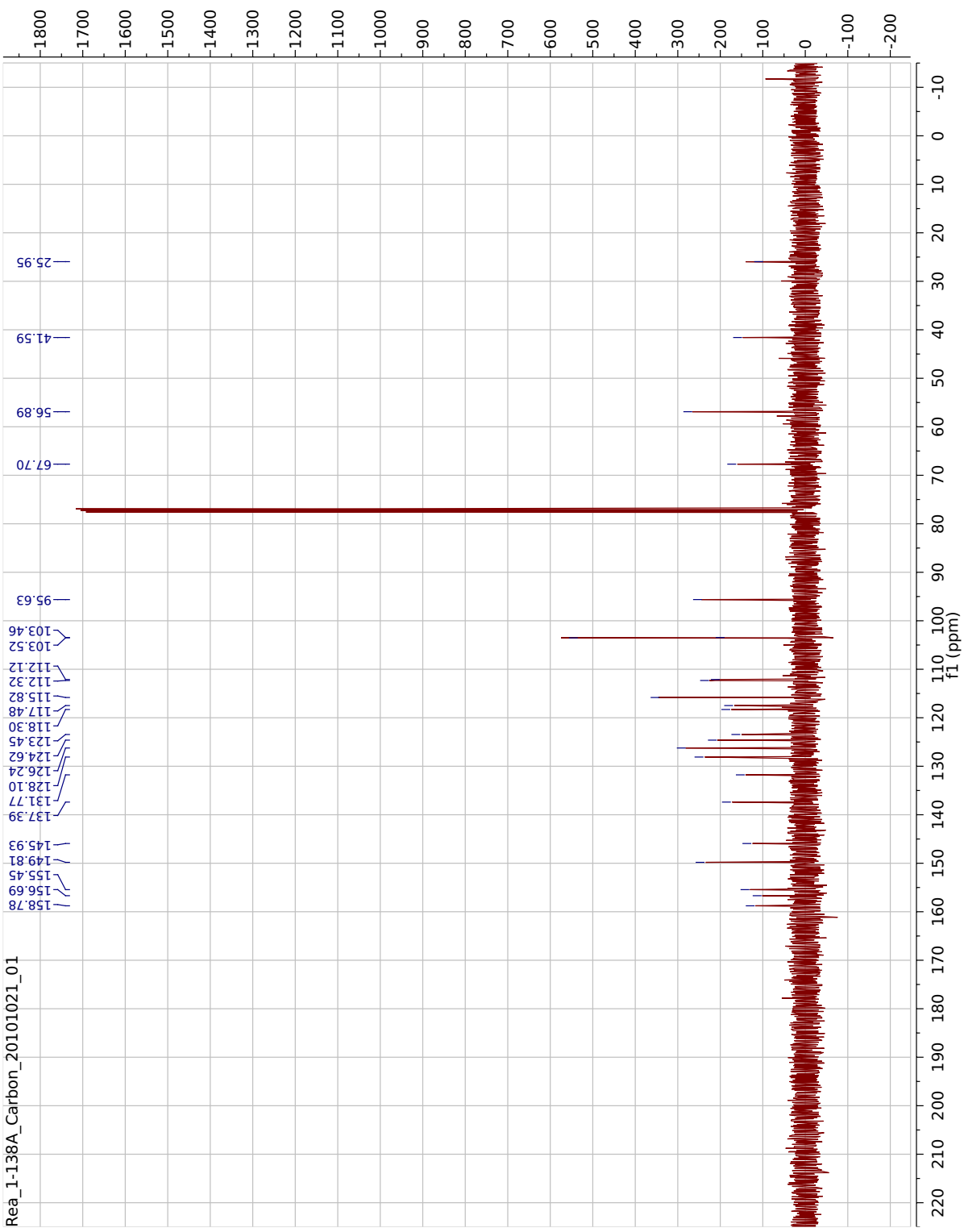
Rea_1-138A_Carbon_20101021_01
f1 (ppm)
158.78
156.69
155.45
149.81
145.93
137.39
131.77
128.10
126.24
124.62
123.45
118.30
117.48
115.82
112.32
112.12
103.52
103.46
95.63
67.70
56.89
41.59
25.95

BHQ-*N*-Serotonin (34)

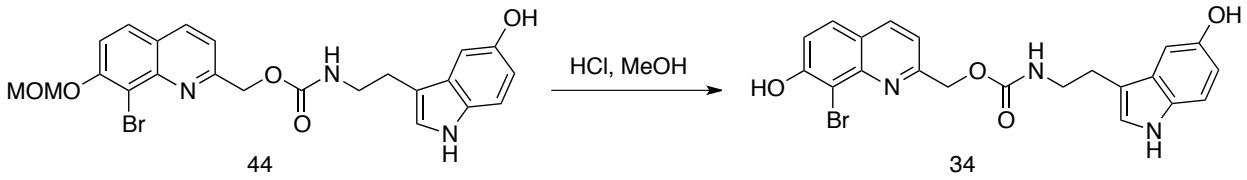

44 34

MOM-BHQ-*N*-Serotonin (45 mg, 0.090 mmol) was dissolved in methanol. A small amount of conc. HCl was added and the reaction stirred overnight. The reaction was diluted with EtOAc and washed with sat. $NaHCO_3$ and brine, dried over anhydrous $MgSO_4$, filtered, and concentrated *in vacuo*. The crude product was purified by HPLC with 50% CH_3CN/50% H_2O (w/ 0.1 % TFA) and the first peak (ret. time 4.5 min) was collected and concentrated (22.5 mg, 55 %).

^{1}H NMR (500 MHz, $(CD_3)_2CO$) δ 8.11 (d, J = 8.3 Hz, 1H), 7.68 (d, J = 8.8 Hz, 1H), 7.26 (d, J = 8.3 Hz, 2H), 7.23 (d, J = 8.8 Hz, 1H), 7.07 (d, J = 8.6 Hz, 1H), 6.98 (s, 1H), 6.88 (s, 1H), 6.57 (d, J = 8.6 Hz, 1H), 5.22 (s, 2H), 3.34 (t, J = 7.3 Hz, 2H), 2.79 (t, J = 7.3 Hz, 2H).

^{13}C NMR (101 MHz, $(CD_3)_2CO$) δ 159.08, 156.18, 155.82, 150.67, 145.90, 137.05, 131.62, 128.47, 128.14, 127.55, 123.18, 118.57, 116.77, 111.64, 111.46, 106.91, 102.57, 66.76, 41.61, 29.71, 25.90.

HRMS (ESI) calcd for $[M+H]^+$ 456.0559, 458.0538; found 456.0574, 458.0567.

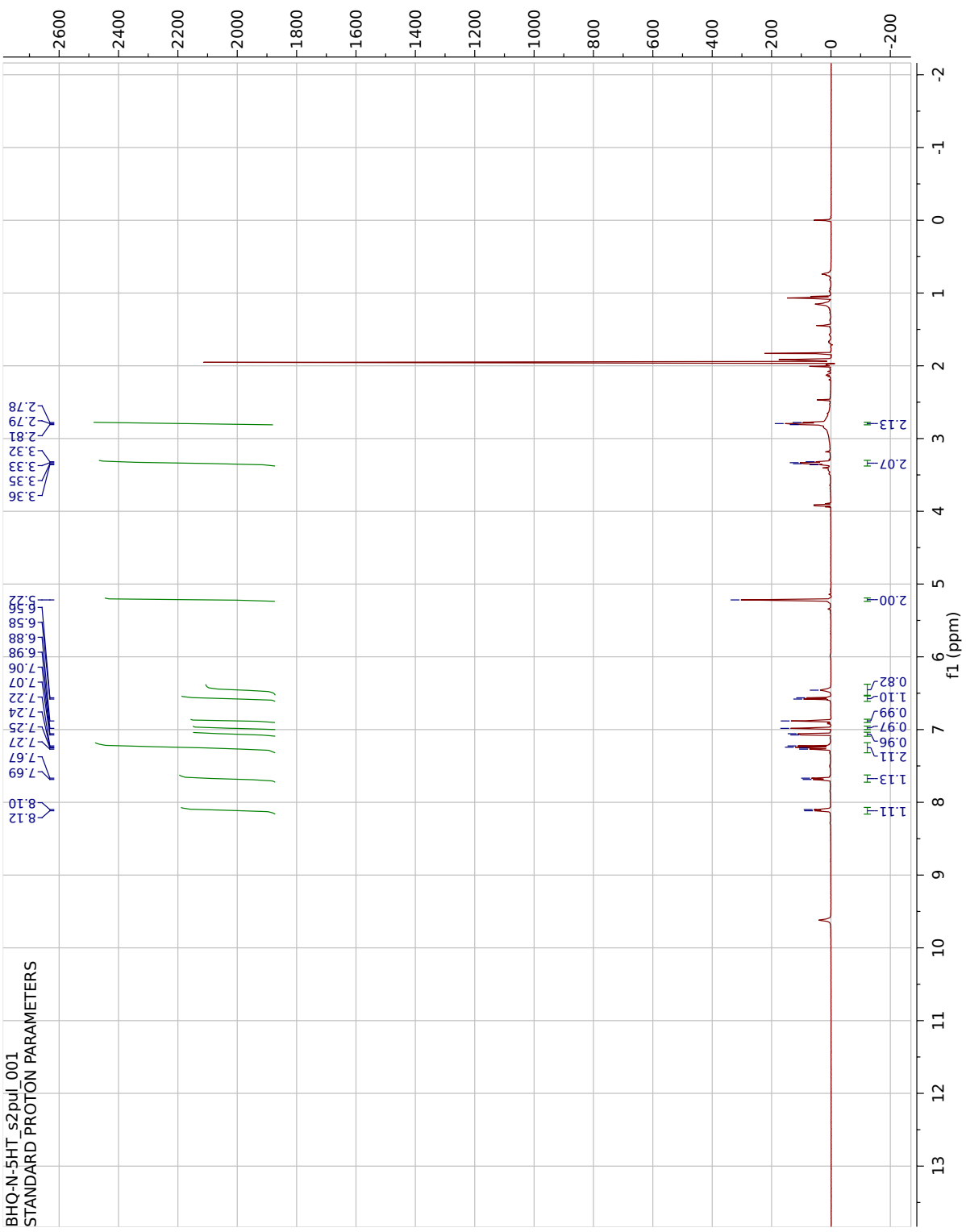
BHQ-N-5HT_s2pul_001
STANDARD PROTON PARAMETERS
f1 (ppm)
8.12
8.10
7.69
7.67
7.27
7.25
7.24
7.22
7.07
7.06
6.98
6.88
6.58
6.56
5.22
3.36
3.35
3.33
3.32
2.81
2.79
2.78
2.13
2.07
2.00
1.13
1.11
1.10
0.99
0.97
0.96
0.82

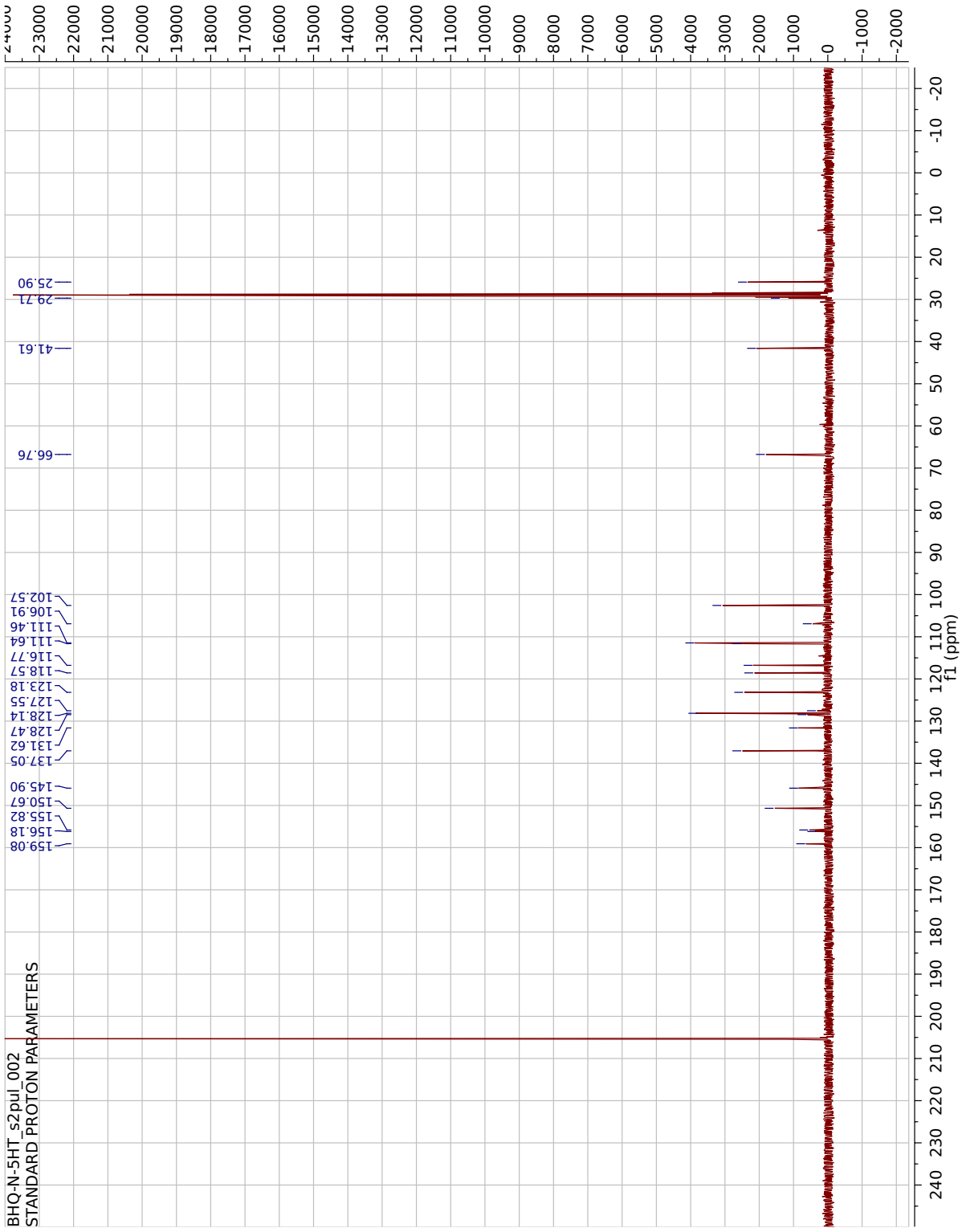
BHQ-N-5HT_s2pul_002
STANDARD PROTON PARAMETERS
159.08
156.18
155.82
150.67
145.90
137.05
131.62
128.47
128.14
127.55
123.18
118.57
116.77
111.64
111.46
106.91
102.57
66.76
41.61
29.71
25.90
f1 (ppm)

MOM-BHQ-Capsaicin (48)

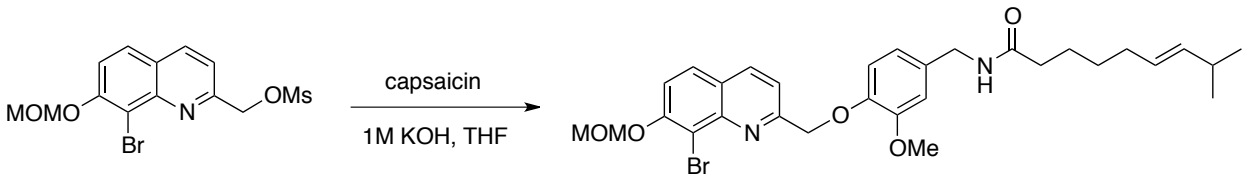

39 48

MOM-BHQ-OMs (160 mg, 0.425 mmol) was dissolved in THF. Capsaicin (95 mg, 0.31 mmol) and 1 M NaOH (0.35 mL) were added and the reaction stirred overnight. The mixture was concentrated and the residue dissolved in $CHCl_3$. The solution washed with water and brine, dried over anhydrous $MgSO_4$, filtered, and concentrated in vacuo. The crude product was purified by column chromatography with silica gel, eluting with a gradient from 10 % hexanes to 1:1 EtOAc/hexanes, yielding the product as a solid (44.6 mg, 25 %).

^{1}H NMR (400 MHz, $CDCl_3$) δ 8.10 (d, J = 8.4 Hz, 1H), 7.73 (d, J = 9.0 Hz, 1H), 7.64 (d, J = 8.4 Hz, 1H), 7.49 (d, J = 9.0 Hz, 1H), 6.88 (d, J = 8.2 Hz, 1H), 6.85 (s, 1H), 6.70 (d, J = 8.2 Hz, 1H), 5.50 (s, 2H), 5.41 (s, 2H), 5.32 (m, 2H), 4.34 (d, 2H), 3.91 (s, 3H), 3.58 (s, 3H), 2.18 (t, J = 6.8 Hz, 2H), 1.97 (q, J = 6.8 Hz, 2H), 1.87 (m, 1H), 1.64 (m, J = 7.7 Hz, 2H), 1.37 (m, J = 7.7 Hz, 2H), 0.95 (s, 3H), 0.93 (s, 3H).

^{13}C NMR (101 MHz, $CDCl_3$) δ 172.99, 159.90, 155.42, 149.85, 147.48, 146.01, 138.27, 137.31, 132.10, 128.10, 126.67, 124.70, 120.26, 118.22, 117.42, 114.11, 111.98, 95.66, 72.43, 56.83, 56.25, 43.55, 36.86, 32.40, 31.14, 29.49, 25.46, 22.85.

HRMS (ESI) calcd for $[M+H]^+$ 585.1964, 587.1944; found 585.1979, 587.1950.

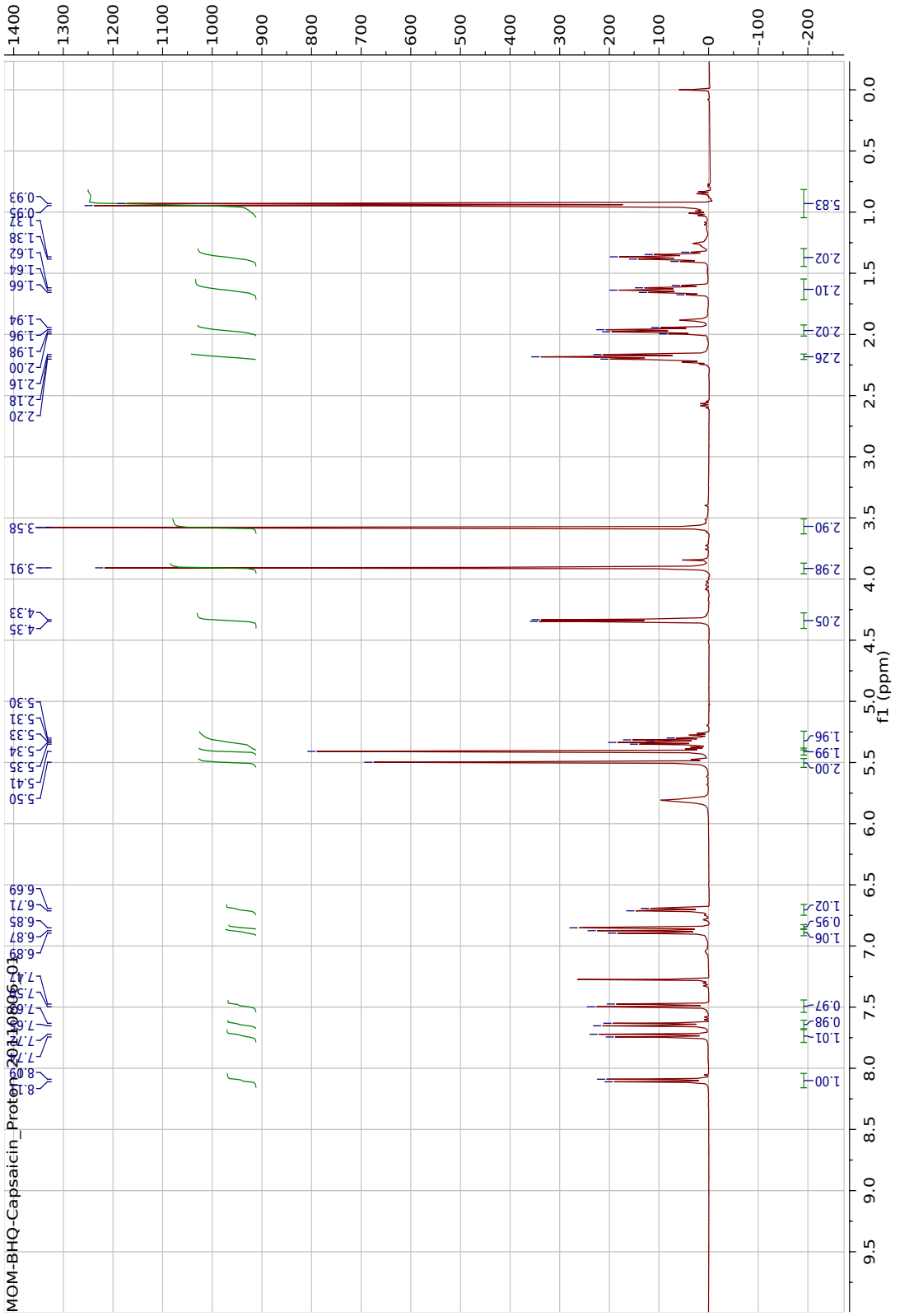
MOM-BHQ-Capsaicin_Proton_20110806_01
f1 (ppm)

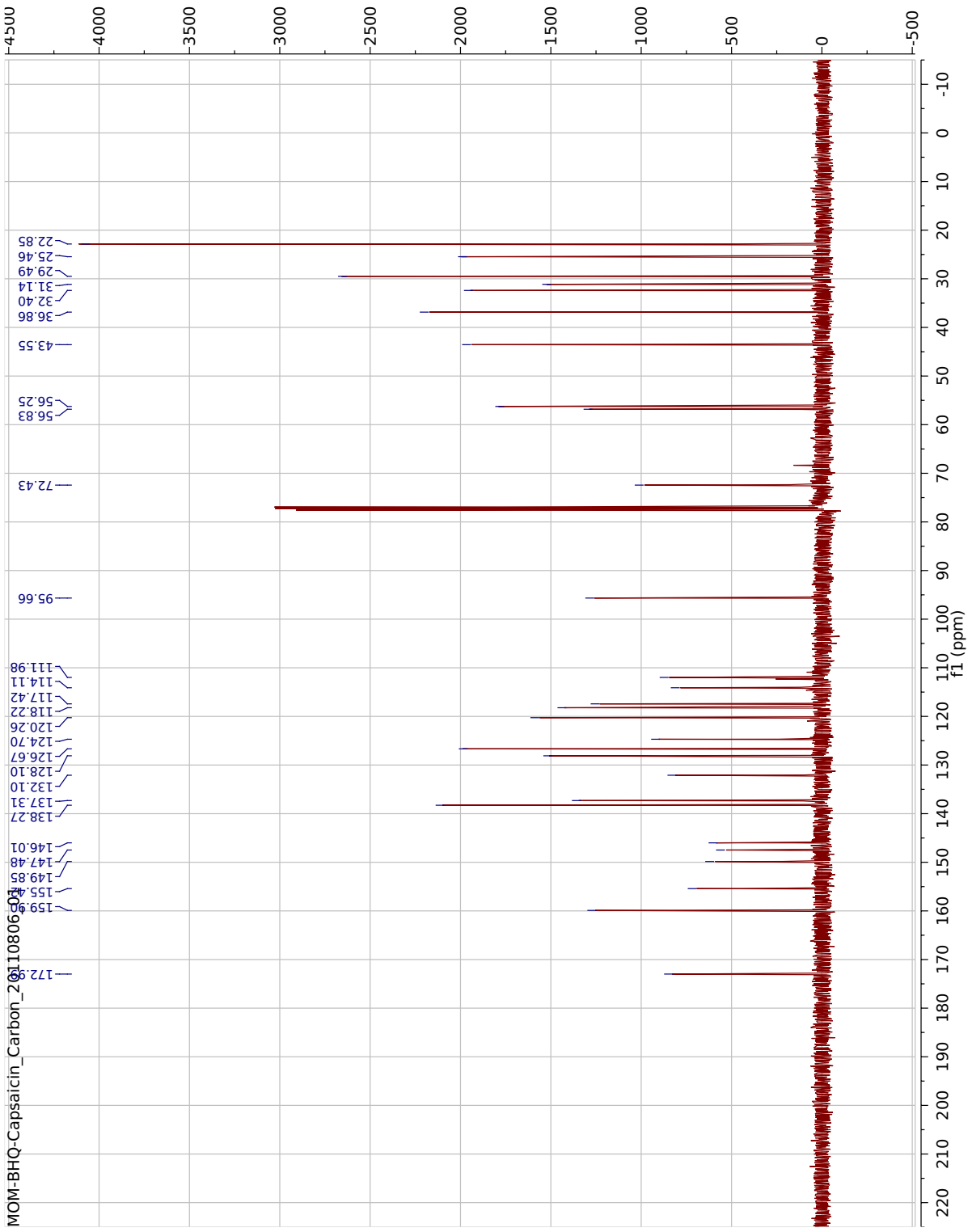
MOM-BHQ-Capsaicin_Carbon_20110806_10
f1 (ppm)
22.85
25.46
29.49
31.14
32.40
36.86
43.55
56.25
56.83
72.43
95.66
111.98
114.11
117.42
118.22
120.26
124.70
126.67
128.10
132.10
137.31
138.27
146.01
147.48
149.85
155.41
159.90
172.98

BHQ-Capsaicin (49)

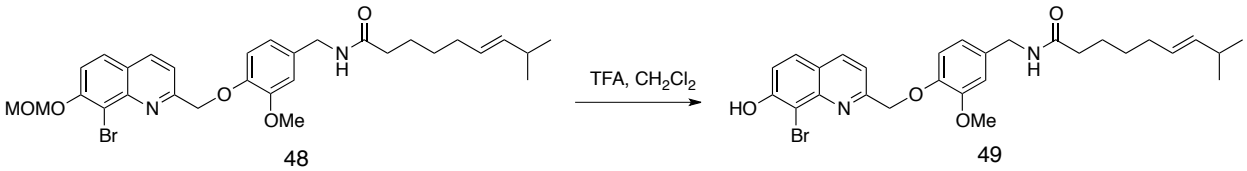

MOM-BHQ-Capsaicin (44.6 mg, 0.076 mmol) was dissolved in methylene chloride. Trifluoroacetic acid (1 mL) was added and the reaction stirred at rt for 3 h. The solvent was removed in vacuo and the residue purified by HPLC with 50% CH_3CN/50% H_2O (w/ 0.1 % TFA). Fractions containing only one peak corresponding to BHQ-Capsaicin were combined and concentrated (31.8 mg, 77%).

^{1}H NMR (400 MHz, $CDCl_3$) δ 8.07 (d, *J* = 8.4 Hz, 1H), 7.66 (d, *J* = 8.9 Hz, 1H), 7.59 (d, *J* = 8.4 Hz, 1H), 7.31 (d, *J* = 8.9 Hz, 1H), 6.88 (d, *J* = 8.2 Hz, 1H), 6.85 (s, 1H), 6.71 (d, *J* = 8.2 Hz, 1H), 5.48 (s, 2H), 5.33 (m, 2H), 4.36 (d, 2H), 3.91 (s, 3H), 2.20 (t, *J* = 7.6 Hz, 2H), 1.97 (q, *J* = 6.9 Hz, 2H), 1.63 (t, *J* = 7.6 Hz, 2H), 1.39 (t, *J* = 7.6 Hz, 2H), 1.25 (m, broad, 1H), 0.94 (d, 6H).

^{13}C NMR (101 MHz, $CDCl_3$) δ 173.20, 159.62, 154.64, 149.86, 147.52, 145.54, 138.31, 137.37, 131.99, 128.40, 126.64, 123.83, 120.27, 118.08, 117.55, 114.11, 111.99, 107.84, 72.37, 56.27, 43.62, 36.87, 32.39, 31.15, 29.47, 25.46, 22.85.

HRMS (ESI) calcd for $[M+H]^+$ 541.1702, 543.1681; found 541.1699, 543.1688.

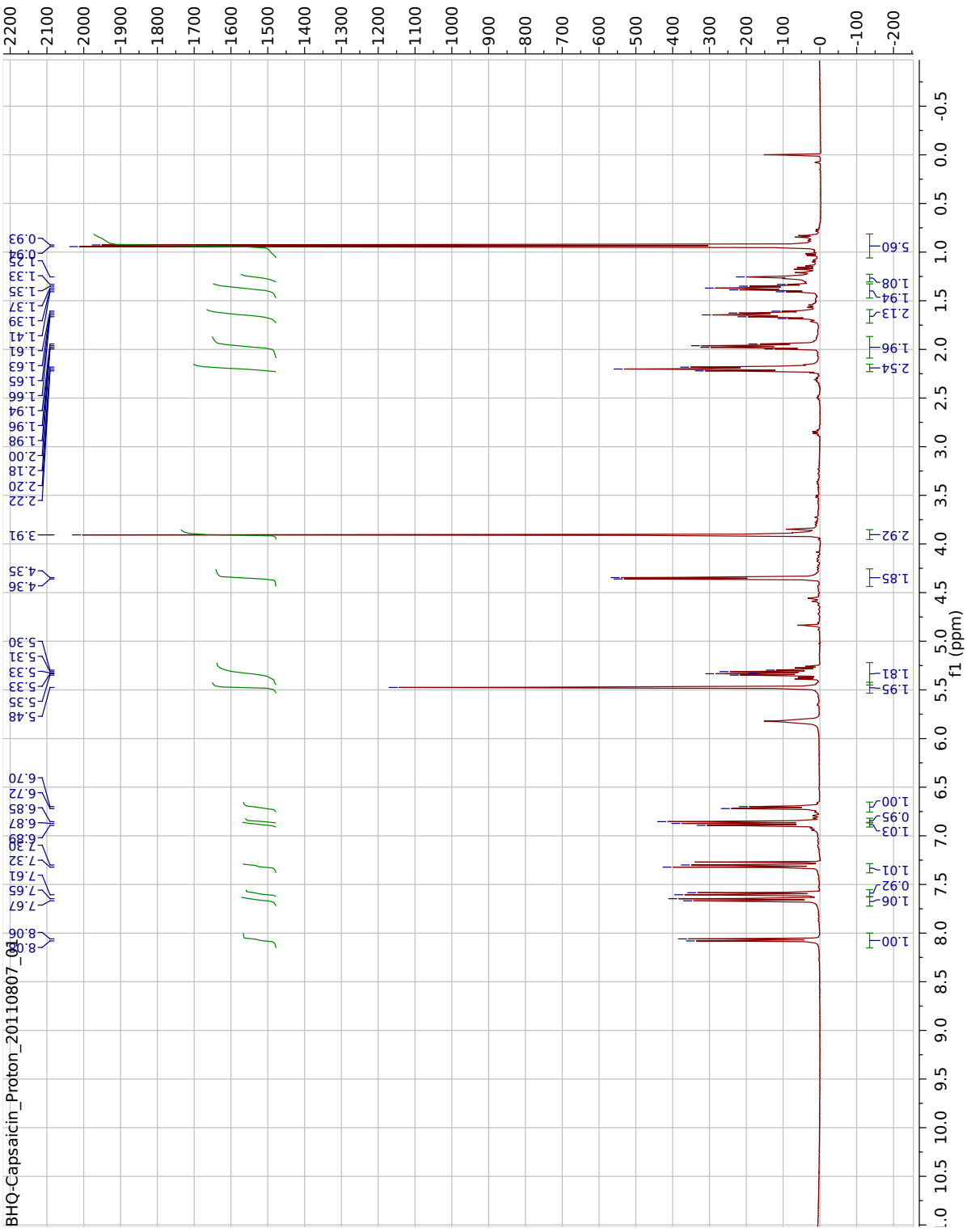
BHQ-Capsaicin_Proton_20110807_01.fid
f1 (ppm)

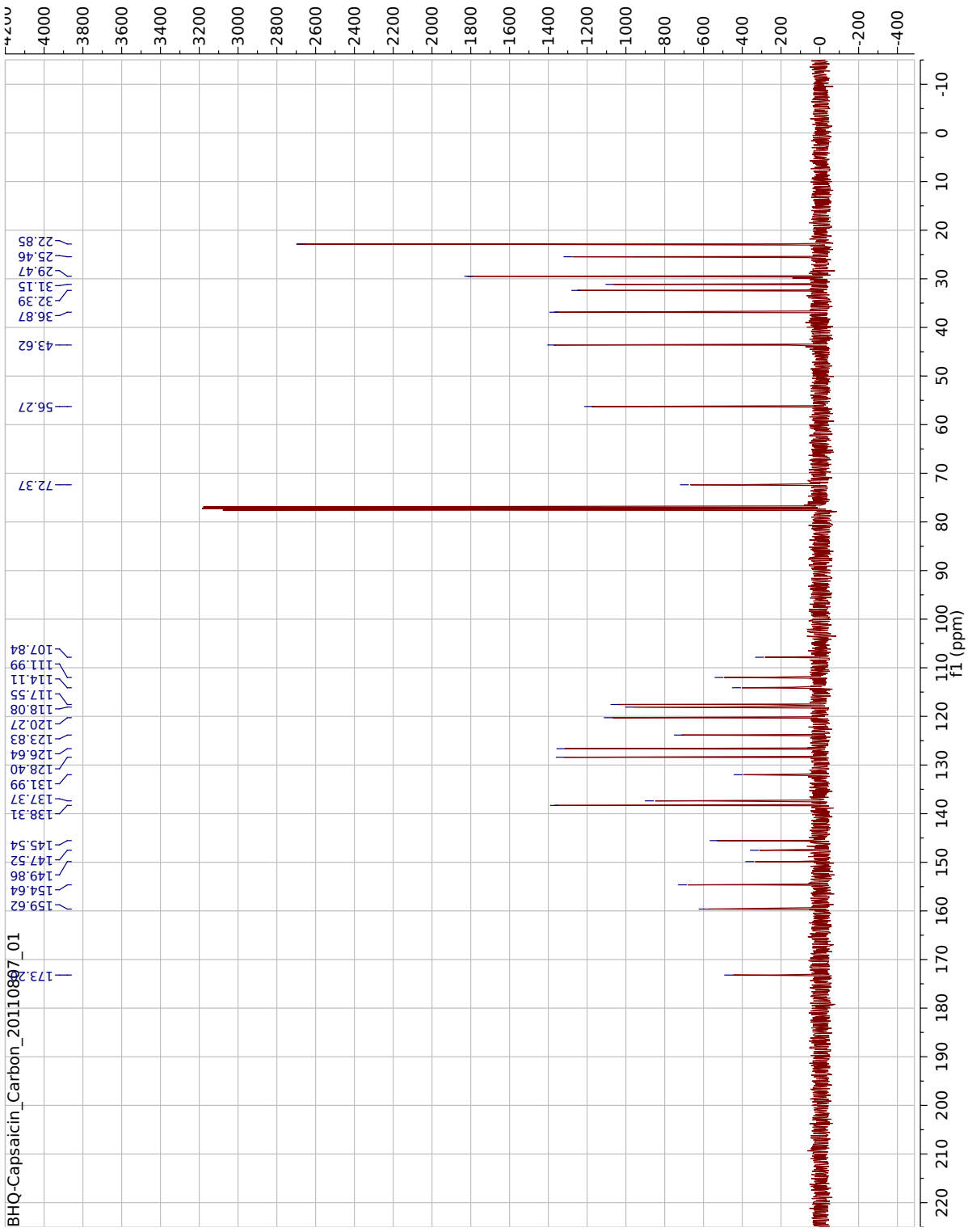
BHQ-Capsaicin_Carbon_20110807_01
f1 (ppm)
173.28
159.62
154.64
149.86
147.52
145.54
138.31
137.37
131.99
128.40
126.64
123.83
120.27
118.08
117.55
114.11
111.99
107.84
72.37
56.27
43.62
36.87
32.39
31.15
29.47
25.46
22.85

MOM-BHQ-VNA (50)

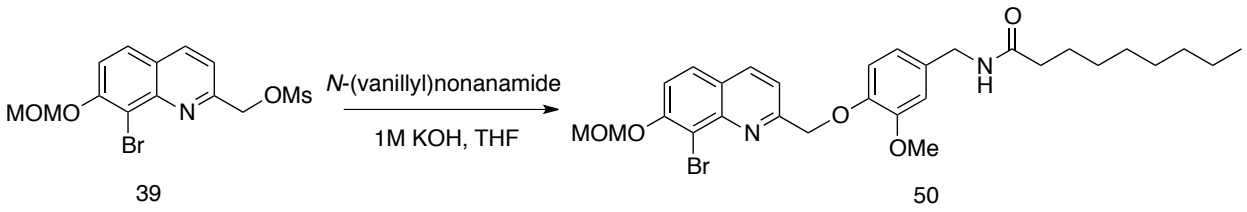

MOM-BHQ-OMs (107 mg, 0.30 mmol) was dissolved in THF. *N*-Vanillyl nonanamide (95 mg, 0.32 mmol) and 1 M NaOH (0.40 mL) were added and the reaction stirred overnight. The mixture was concentrated and the residue dissolved in $CHCl_3$. The solution washed with water and brine, dried over anhydrous $MgSO_4$, filtered, and concentrated in vacuo. The crude product was purified by column chromatography with a 2:3 mixture of EtOAc/Hex. The solvent was removed in vacuo (55 mg, 32 %).

^{1}H NMR (400 MHz, $CDCl_3$) δ 8.18 (d, *J* = 8.3 Hz,1H), 7.75 (d, *J* = 9.0 Hz, 1H), 7.63 (d, *J* = 8.3 Hz, 1H), 7.48 (d, *J* = 9.0 Hz, 1H), 6.88 (d, *J* = 8.2 Hz, 1H), 6.85 (s, 1H), 6.69 (d, *J* = 8.2 Hz, 1H), 5.78 (broad, 1H), 5.49 (s, 2H), 5.40 (s, 2H), 4.36 (s, 2H), 3.90 (s, 3H), 3.54 (s, 3H), 2.19 (t, *J* = 7.6 Hz, 2H), 1.60 (m, *J* = 7.6 Hz, 2H), 1.4 – 1.2 (m, 10 H), 0.84 (t, *J* = 6.7 Hz, 3H).

^{13}C NMR (101 MHz, $CDCl_3$) δ 173.06, 159.93, 155.43, 149.88, 147.53, 146.04, 137.31, 132.09, 128.09, 124.72, 120.30, 118.22, 117.44, 114.14, 112.02, 95.68, 72.46, 56.84, 56.28, 43.59, 37.06, 32.00, 29.52, 29.49, 29.33, 25.98, 22.82, 14.25.

HRMS (ESI) calcd for $[M+H]^+$ 573.1964, 575,1944; found 573.1972, 575.1952.

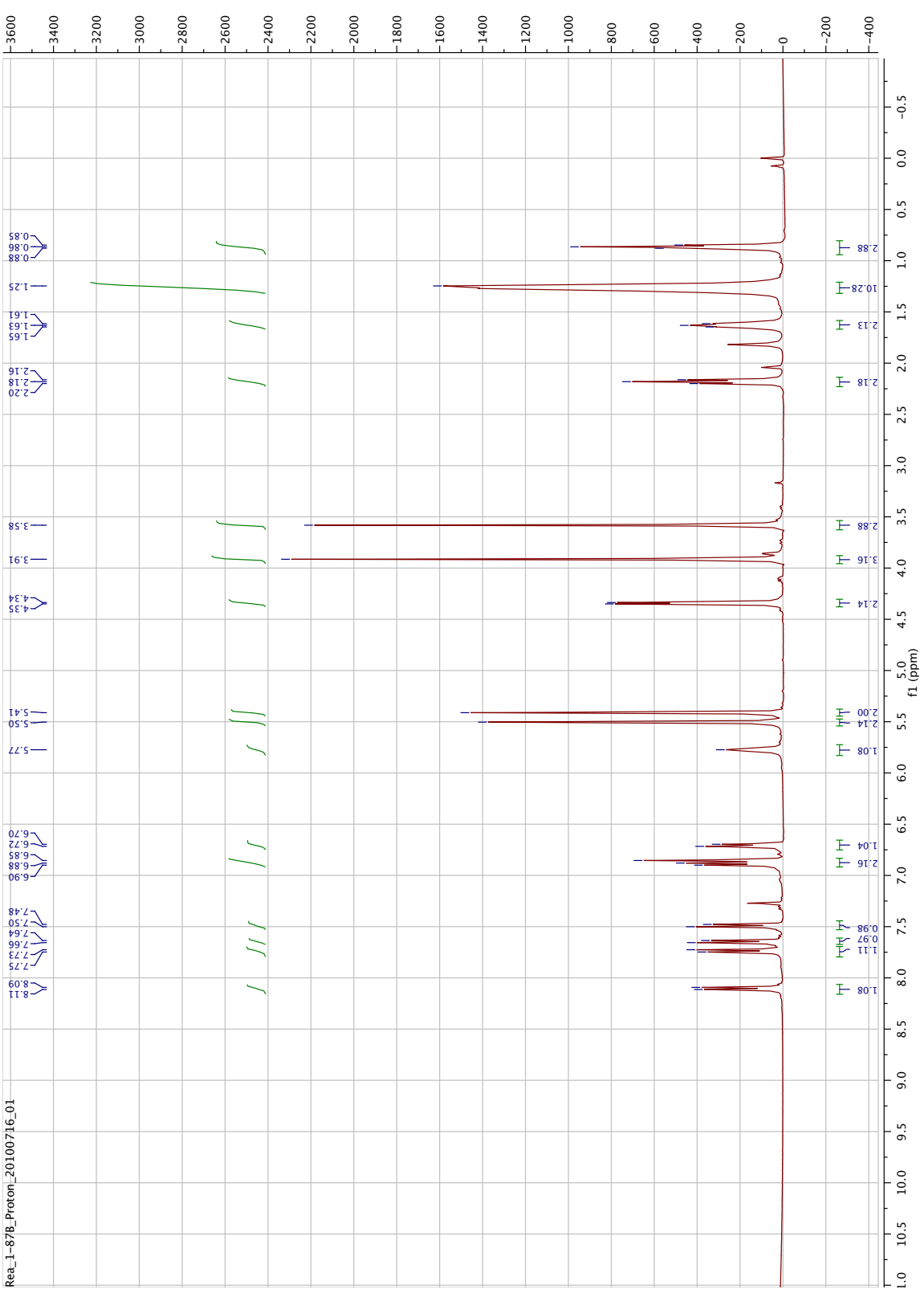
Rea_1-87B_Proton_20100716_01
f1 (ppm)

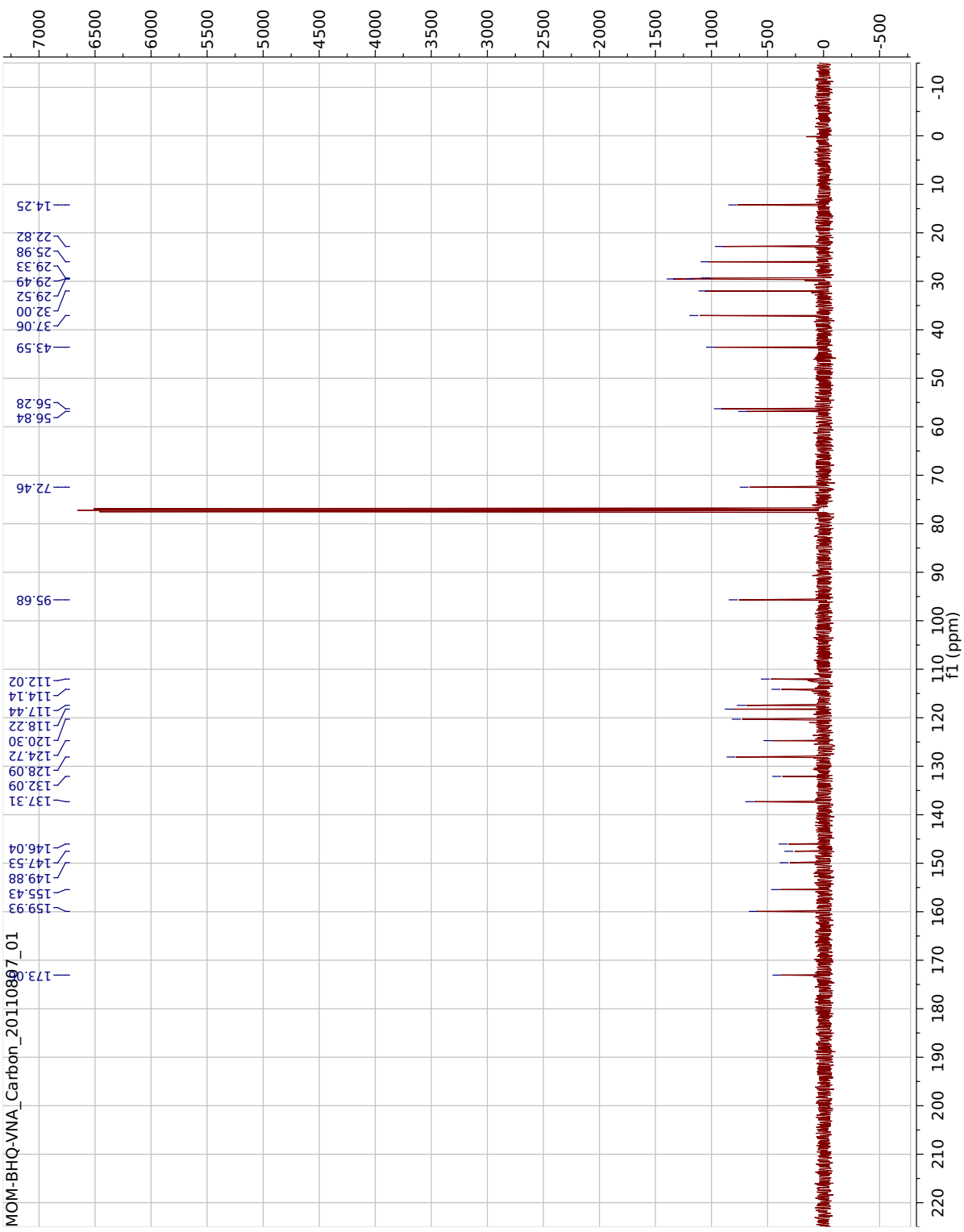
MOM-BHQ-VNA_Carbon_20110807_01
14.25
22.82
25.98
29.33
29.49
29.52
32.00
37.06
43.59
56.28
56.84
72.46
95.68
112.02
114.14
117.44
118.22
120.30
124.72
128.09
132.09
137.31
146.04
147.53
149.88
155.43
159.93
173.02
f1 (ppm)

BHQ-VNA (51)

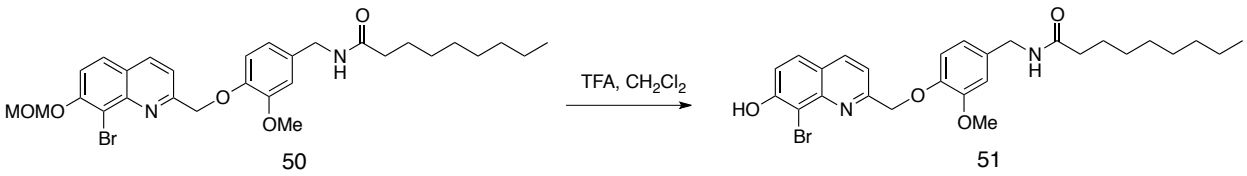

MOM-BHQ-VNA (55 mg, 0.096 mmol) was dissolved in methylene chloride. Trifluoroacetic acid was added and the reaction stirred at rt for 2 h. The solvent was removed in vacuo and the residue purified by HPLC with 50% CH_3CN/50% H_2O (w/ 0.1 % TFA). Fractions containing only one peak were combined and concentrated (29 mg, 57 %).

^{1}H NMR (400 MHz, $CDCl_3$) δ 8.10 (d, *J* = 8.4 Hz, 1H), 7.70 (d, *J* = 9.0 Hz, 1H), 7.62 (d, *J* = 8.4 Hz, 1H), 7.33 (d, *J* = 9.0 Hz, 1H), 6.90 (d, *J* = 8.2 Hz, 1H), 6.87 (s, 1H), 6.73 (d, *J* = 8.2 Hz, 1H), 5.78 (broad, 1H), 5.50 (s, 2H), 4.37 (s, 2H), 3.93 (s, 3H), 2.20 (t, *J* = 7.6 Hz, 2H), 1.64 (m, *J* = 7.6 Hz, 2H), 1.4 – 1.2 (m, 10 H), 0.87 (t, *J* = 6.7 Hz, 3H).

^{13}C NMR (101 MHz, $CDCl_3$) δ 173.23, 159.40, 154.41, 149.63, 147.25, 145.13, 137.39, 131.73, 128.33, 123.71, 120.09, 117.86, 117.35, 114.36, 113.84, 111.72, 72.03, 56.06, 43.46, 36.84, 31.80, 29.71, 29.30, 29.14, 25.79, 22.64, 14.09.

HRMS (ESI) calcd for $[M+H]^+$ 529.1702, 531.1681; found 529.1699, 531.1689.

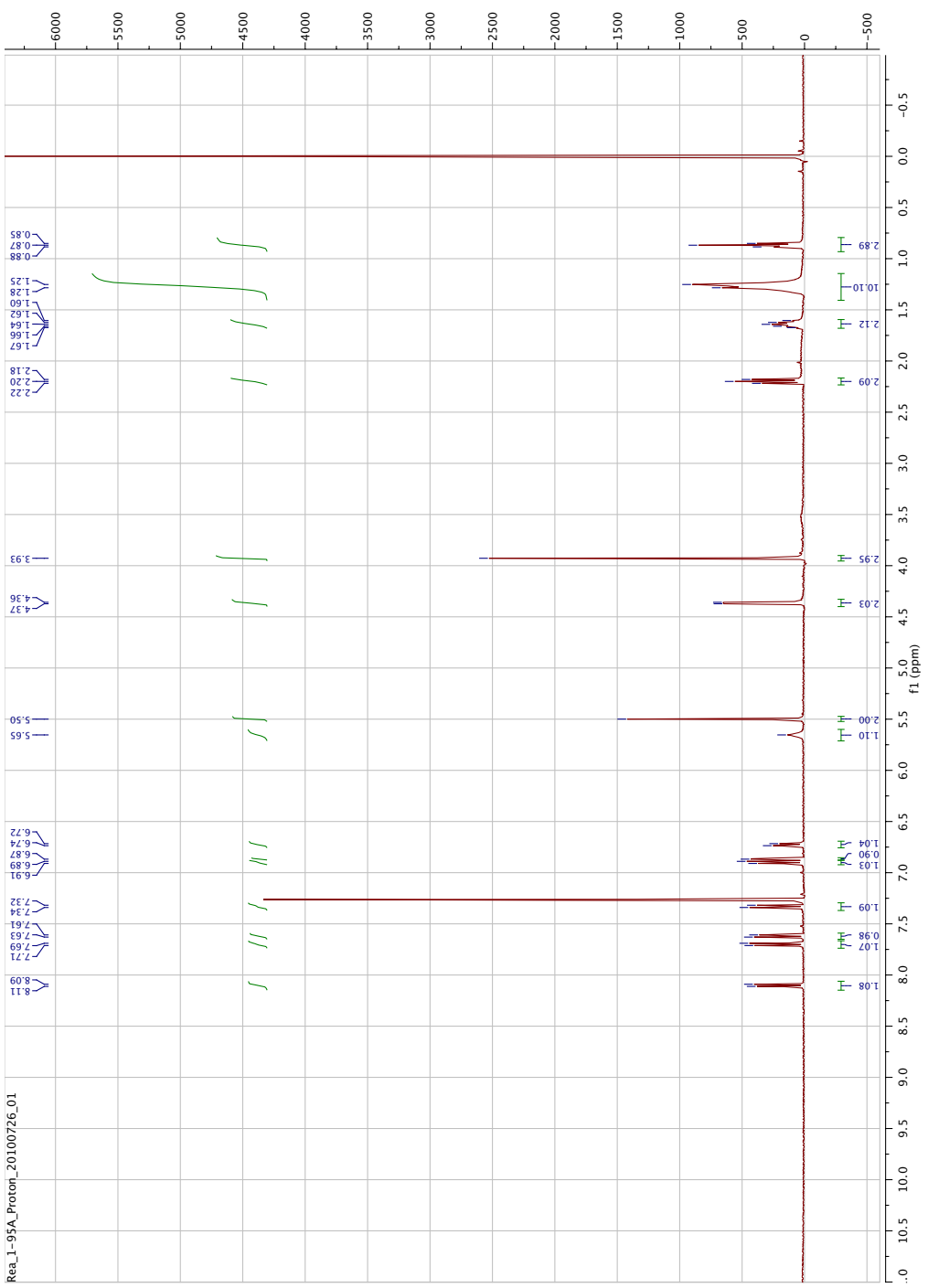
Rea_1-95A_Proton_20100726_01
f1 (ppm)

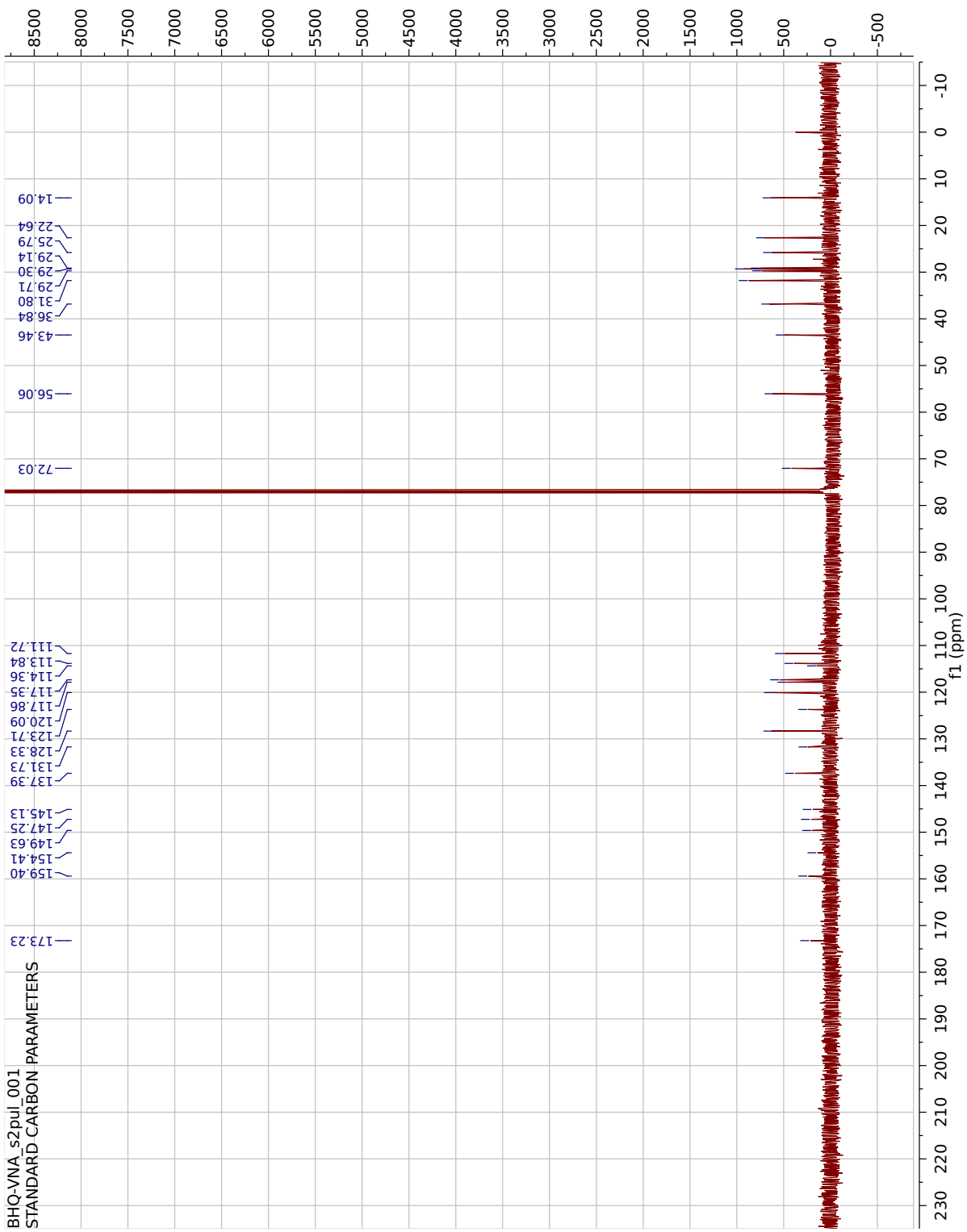
BHQ-VNA_s2pul_001
STANDARD CARBON PARAMETERS
173.23
159.40
154.41
149.63
147.25
145.13
137.39
131.73
128.33
123.71
120.09
117.86
117.35
114.36
113.84
111.72
72.03
56.06
43.46
36.84
31.80
29.71
29.30
29.14
25.79
22.64
14.09
f1 (ppm)

MOM-BHQ-VAA (46)

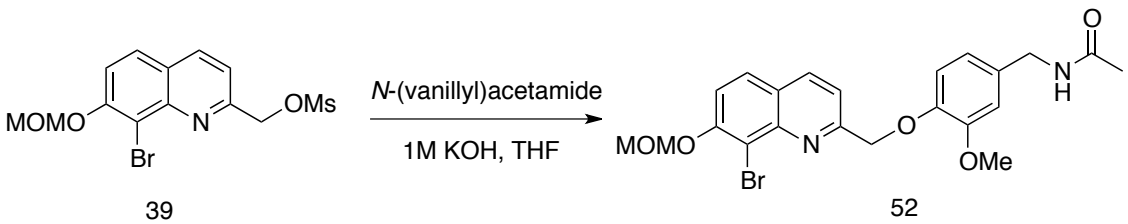

MOM-BHQ-OMs (73 mg, 0.195 mmol) was dissolved in THF. *N*-Vanillyl acetamide (38 mg, 0.195 mmol) and 1 M NaOH (0.3 mL) were added and the reaction stirred overnight. The mixture was concentrated and the residue dissolved in $CHCl_3$. The solution washed with water and brine, dried over anhydrous $MgSO_4$, filtered, and concentrated in vacuo. The crude product was purified by column chromatography with a 2:3 mixture of EtOAc/Hex. The solvent was removed in vacuo (31.2 mg, 33 %).

^{1}H NMR (400 MHz, $CDCl_3$) δ 8.11 (d, *J* = 8.4 Hz, 1H), 7.74 (d, *J* = 9.0 Hz, 1H), 7.65 (d, *J* = 8.4 Hz, 1H), 7.50 (d, *J* = 9.0 Hz, 1H), 6.90 (d, *J* = 8.2 Hz, 1H), 6.87 (s, 1H), 6.73 (d, *J* = 8.2 Hz, 1H), 5.52 (s, 2H), 5.42 (s, 2H), 4.34 (s, 2H), 3.93 (s, 3H), 3.59 (s, 3H), 2.01 (s, 3H).

^{13}C NMR (101 MHz, $CDCl_3$) δ 169.94, 159.91, 155.45, 149.90, 147.60, 146.05, 137.32, 131.86, 128.10, 125.70, 124.73, 120.40, 118.23, 117.46, 114.18, 112.13, 95.69, 72.47, 56.84, 56.32, 43.82, 30.55.

HRMS (ESI) calcd for $[M+H]^+$ 475.0869, 477.0848; found 475.0863, 477.0852.

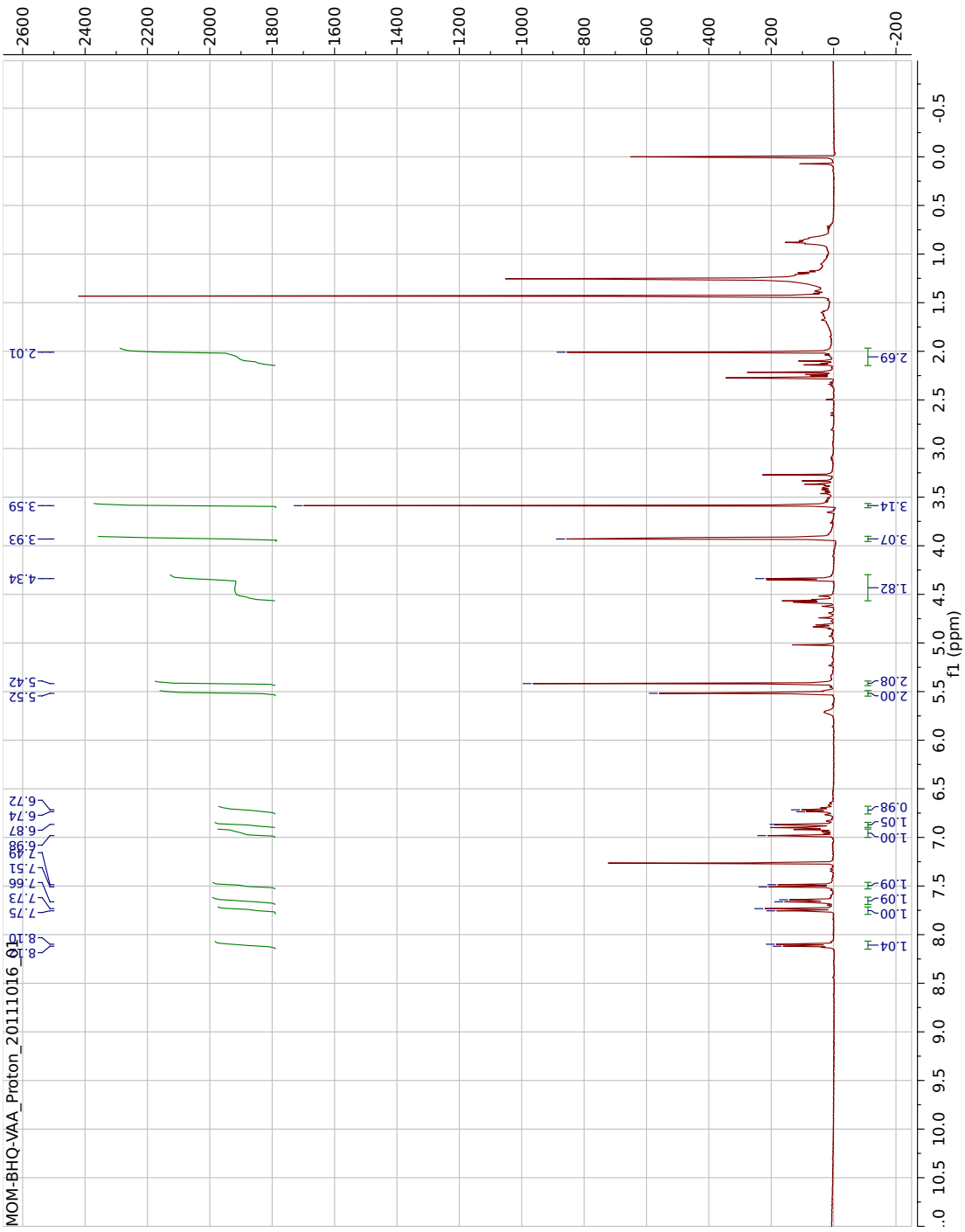
MOM-BHQ-VAA_Proton_20111016_01
f1 (ppm)
8.10
7.75
7.73
7.66
7.51
7.49
6.98
6.87
6.74
6.72
5.52
5.42
4.34
3.93
3.59
2.01
1.04
1.09
1.00
1.09
1.00
0.98
1.05
1.00
2.08
2.00
1.82
3.07
3.14
2.69

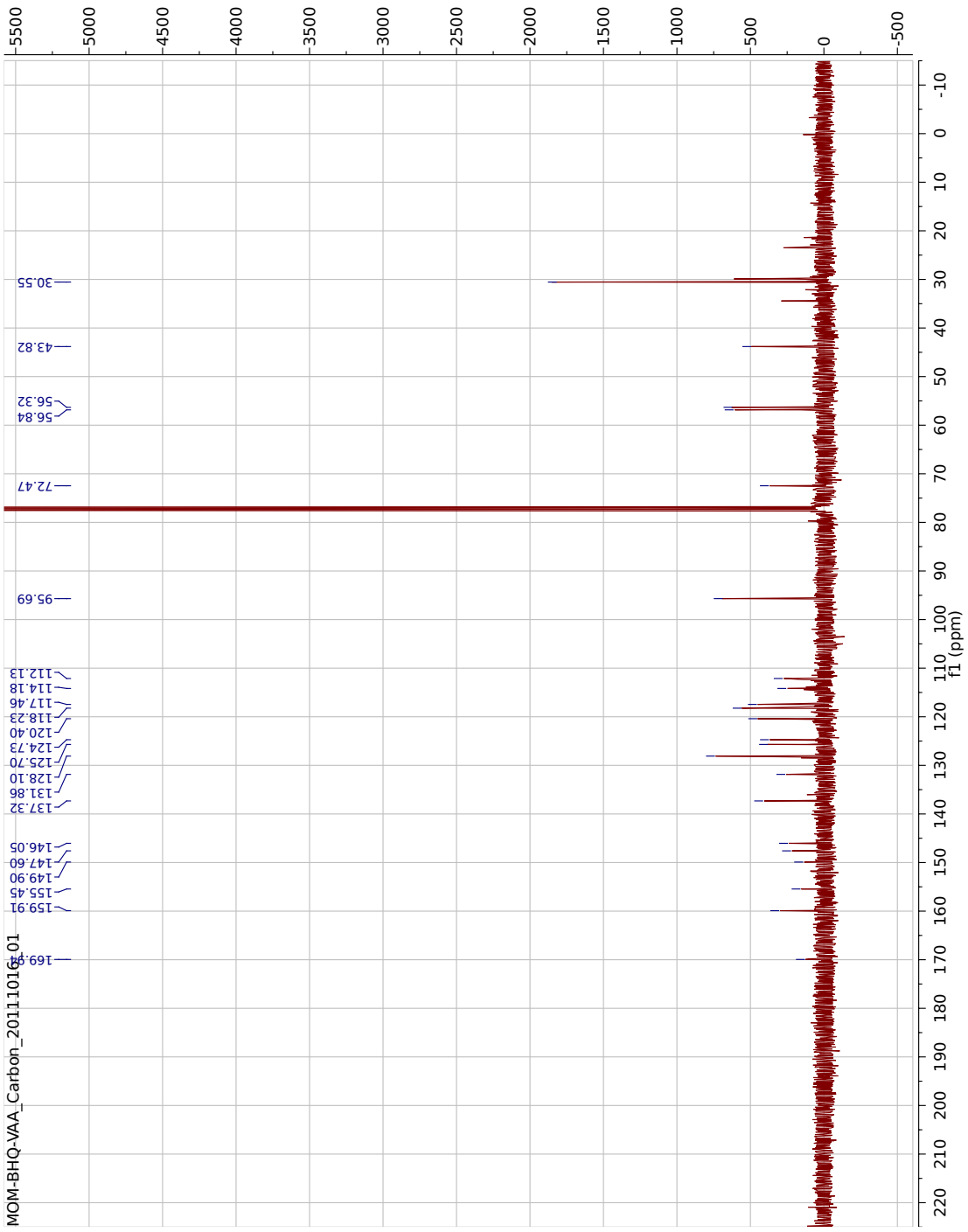
MOM-BHQ-VAA_Carbon_20111016_01
f1 (ppm)
30.55
43.82
56.84
56.32
72.47
95.69
112.13
114.18
117.46
118.23
120.40
124.73
125.70
128.10
131.86
137.32
146.05
147.60
149.90
155.45
159.91
169.93

BHQ-VAA (47)

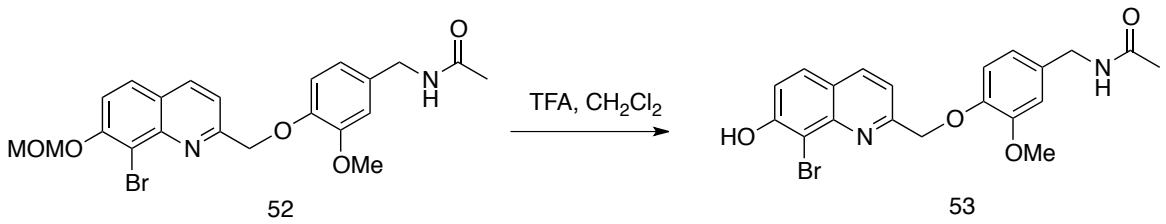

52 53

MOM-BHQ-VAA (31.2 mg, 0.066 mmol) was dissolved in methylene chloride. Trifluoroacetic acid was added and the reaction stirred at rt for 2 h. The solvent was removed in vacuo and the residue purified by HPLC with 50% CH_3CN/50% H_2O (w/ 0.1 % TFA). Fractions containing only one peak were combined and concentrated (20 mg, 70 %).

^{1}H NMR (400 MHz, CD_3OD) δ 8.38 (d, J = 8.4 Hz, 1H), 7.85 (d, J = 8.9 Hz, 1H), 7.67 (d, J = 8.4 Hz, 1H), 7.33 (d, J = 8.9 Hz, 1H), 7.02 (d, J = 8.2 Hz, 1H), 6.97 (s, 1H), 6.80 (d, J = 8.2 Hz, 1H), 5.49 (s, 2H), 4.27 (s, 2H), 3.88 (s, 3H), 1.96 (s, 3H).

^{13}C NMR (101 MHz, CD_3OD) δ 171.93, 165.58, 158.87, 150.10, 147.17, 136.42, 135.60, 133.06, 128.53, 123.69, 119.98, 119.13, 117.11, 117.08, 114.96, 112.13, 71.28, 55.39, 42.82, 21.35.

HRMS (ESI) calcd for $[M+H]^+$ 431.0606, 433.0586; found 431.0624, 433.0606.

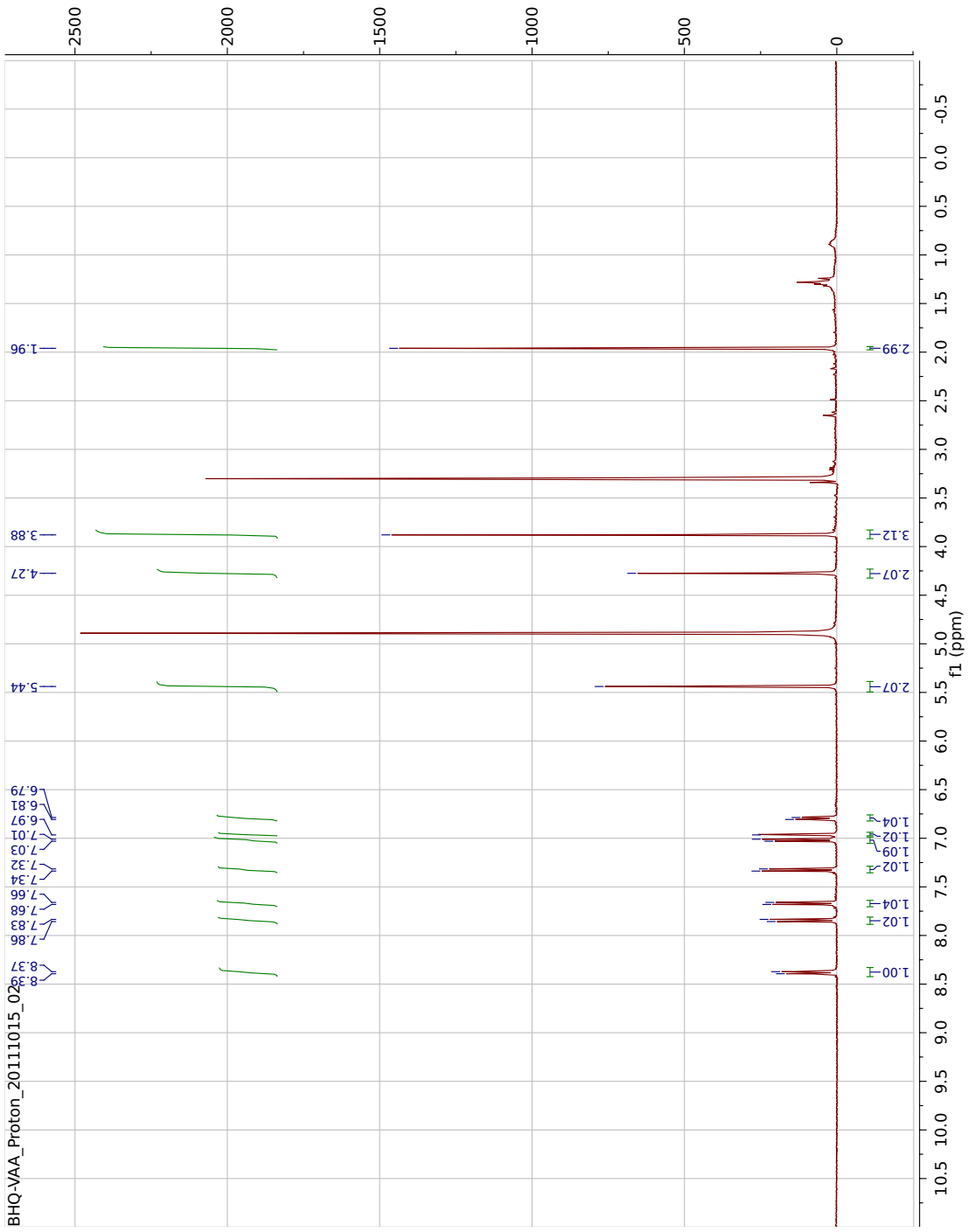
BHQ-VAA_Proton_20111015_02
f1 (ppm)
1.96
3.88
4.27
5.44
6.79
6.81
6.97
7.01
7.03
7.32
7.34
7.66
7.68
7.83
7.86
8.37
8.39
2.99
3.12
2.07
2.07
1.04
1.02
1.09
1.02
1.04
1.02
1.00

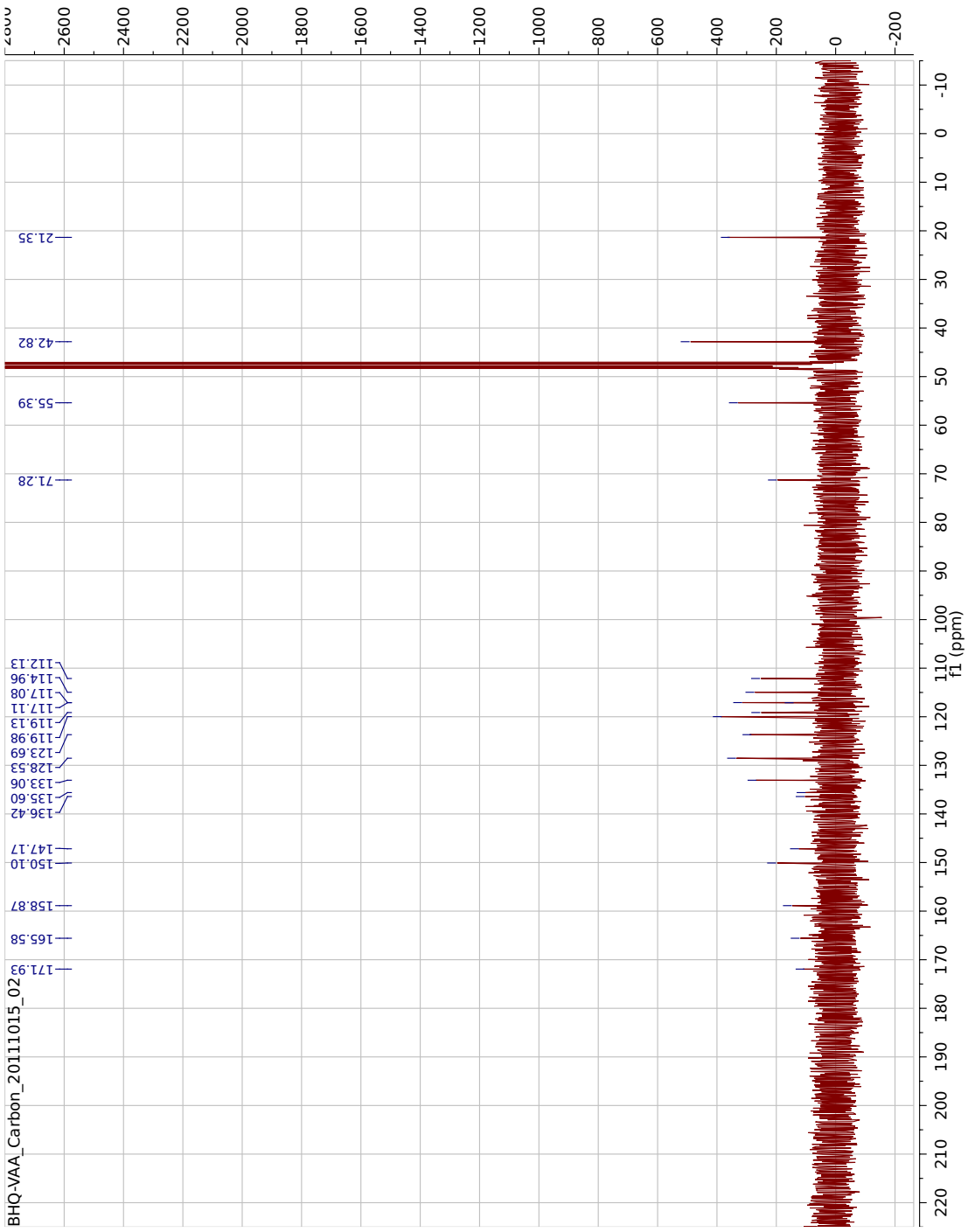
BHQ-VAA_Carbon_20111015_02
171.93
165.58
158.87
150.10
147.17
136.42
135.60
133.06
128.53
123.69
119.98
119.13
117.11
117.08
114.96
112.13
71.28
55.39
42.82
21.35
f1 (ppm)

Determination of the Molar Extinction Coefficient (ε)

A weighed portion of the compound was dissolved in an exact amount of methanol. A measured aliquot of this solution was withdrawn and placed in KMOPS buffer (3.0 mL) and mixed thoroughly to generate a 100 μM solution. The absorbance A of this solution at λ_{max} = 368 nm was measured. This method was repeated twice with different masses. The three absorbencies were averaged and the molar extinction coefficient (ε) at λ_{max} = 368 nm was calculated using the equation A = εlc, where A is the absorbance, l is the pathlength of the cuvette (1 cm), and c is the concentration of the solution (1 x 10^{-4} M).

HPLC Analysis of Photolysis Reactions

Reverse phase HPLC was used to monitor photolysis reactions of BHQ-*O*-Serotonin, BHQ-*N*-Serotonin, and BHQ-VAA for the purposes of calculating uncaging quantum efficiencies (Q_u) and two-photon action cross-sections (δ_u) for each compound. Briefly, an Agilent Technologies Microsorb-MV 100-5 C18 250 x 4.6 mm column was used for analysis. Standard curves for serotonin and *N*-vanillyl acetamide were created for quantitation of photolysis products. Mobile phase conditions and retention times are as follows:

Analysis of BHQ-*O*-Serotonin:

Method: 40% CH_3CN/60% H_2O (w/ 0.1 % TFA) isocratic, 1 mL/min flow rate

BHQ-*O*-Serotonin retention time: 5.47 min

Serotonin retention time: 3.79 min

BHQ-OH retention time: 4.19 min

Analysis of BHQ-*N*-Serotonin:

Method: 40% CH_3CN/60% H_2O (w/ 0.1 % TFA) isocratic, 1 mL/min flow rate

BHQ-*N*-Serotonin retention time: 4.95 min

Serotonin retention time: 3.79 min

BHQ-OH retention time: 4.19 min

Analysis of BHQ-VAA:

Method: 30% CH_3CN/70% H_2O (w/ 0.1 % TFA) isocratic, 1 mL/min flow rate

BHQ-VAA retention time: 8.92 min

VAA retention time: 3.11 min

BHQ-OH retention time: 4.32 min

Determination of the Uncaging Quantum Efficiency (*Q*u)

The quantum efficiency was calculated using the equation $Qu = (I \cdot \sigma t_{90\%})^{-1}$, where I is the irradiation intensity in ein·cm^{-2}, σ is the decadic extinction coefficient (1,000ε) and $t_{90\%}$ is the time in seconds required for the conversion of 90% of the starting material to product. To find $t_{90\%}$, a solution of the compound in KMOPS was prepared and placed in a cuvette along with a small stir bar. While stirring, the solution was irradiated with UV light from a mercury lamp (Spectroline SB-100P, Spectronics Corporation) equipped with two glass filters (CS0-52, CS7-60, Ace Glass) so that the wavelength was restricted to 365 ± 15 nm. Periodically, 20 µL aliquots were removed and analyzed by HPLC, and percent remaining was plotted verses time of photolysis. A simple single exponential decay curve provided the best fit for the data and was used to extrapolate $t_{90\%}$. The lamp's UV intensity I was measured using potassium ferrioxalate actinometry. Initially, 6 mM potassium ferrioxalate solution (3 mL) was irradiated with the mercury lamp for 60 s. A portion of this solution (2mL) was combined with aqueous buffer (3 mL), 0.1% phenanthroline solution (3 mL), and 2M KF solution (1 mL) in a 25 mL volumetric

flask. Deionized water was added to generate a 25 mL solution. A blank solution was also prepared using the same method, but the potassium ferrioxalate used in the blank was not irradiated. Both solutions were allowed to sit for one hour and the blank was then used as a baseline against which the absorbance of the irradiated solution was measured at 510 nm. The following equation was used to calculate lamp intensity:

$$I = \frac{V_3 \Delta D_{510}}{1000 \varepsilon_{510} V_2 \phi_{Fe} t}$$

where V_3 is the volume of dilution (25 mL), V_2 is the volume of irradiated potassium ferrioxalate solution taken for analysis (2 mL), ΔD_{510} is the absorption of the solution at 510 nm, ε_{510} is the actinometry extinction coefficient ($1.11 \cdot 10^4$), φ_{Fe} is the quantum yield for production of ferrous ions from potassium ferrioxalate at 365 nm (1.26), and t represents the time of irradiation (60 s). The ΔD_{510} value used for calculations is the average of two measurements taken before and after irradiation; specific values for each experiment are as follows: 0.610 for BHQ-*O*-Serotonin, 0.634 for BHQ-*N*-Serotonin, and 0.622 for BHQ-VAA. Calculation of lamp intensity yielded the following values for I: $9.09 \cdot 10^{-9}$ ein·cm^{-2} for BHQ-*O*-Serotonin, $9.44 \cdot 10^{-9}$ ein·cm^{-2} for BHQ-*N*-Serotonin, and $9.27 \cdot 10^{-9}$ ein·cm^{-2} for BHQ-VAA. Values for $t_{90\%}$ determined by HPLC analysis of each reaction were as follows: 183.4 s for BHQ-*O*-Serotonin, 504.4 s for BHQ-*N*-Serotonin, and 222.0 s for BHQ-VAA.

Determination of Two-photon Action Cross-Sections (δ_u)

A portion of the compound was dissolved in KMOPS buffer and the concentration of the solution was found using UV-Vis absorption in conjunction with Beer's law. 25 μL aliquots of this

solution were placed in a microcuvette (10×1×1 mm illuminated dimensions, 25 μL) and irradiated with a fs-pulsed and mode-locked Ti:Sapphire laser (Chameleon Ultra II, Coherent) with 740 nm light at an average power of 300 mW. Three samples were irradiated for various time periods. The samples were compiled and analyzed by HPLC. A solution of fluorescein at pH 9.0 was prepared to act as a standard because of its well-characterized 2PE cross-section (δ_{aF} = 30 GM at 740 nm) and quantum yield (Q_{F2} = 0.9). UV-Vis absorption spectroscopy was used to correlate absorption at 488 nm to precise concentration. 25 μL aliquots of fluorescein solution were placed in the microcuvette and irradiated by the laser under the same conditions used for the caged compound. The fluorescence output of the solution was measured with a radiometer before and after the caged compound samples were irradiated and the two values were averaged. The following equation was used to calculate the two-photon action cross-section for each compound:

$$\delta_u = \frac{N_p \phi Q_{F2} \delta_{aF} C_F}{< F(t) > C_s}$$

where N_p is the number of product molecules formed per second (determined by HPLC), φ is the collection efficiency of the detector ($8.77 \cdot 10^{-4}$; SED033 on an IL-1700, International Light) used to measure the fluorescence of fluorescein passing through the cuvette window and through a 535/545 nm bandpass filter at a right angle to the laser's beam, C_F is the concentration of fluorescein (M), $<F(t)>$ is the time averaged fluorescent photon flux (photons/s) of fluorescein and Cs is the initial concentration of the caged compound (M). Specific values for N_p are as follows: $8.87 \cdot 10^{15}$ for BHQ-*O*-Serotonin, $7.55 \cdot 10^{15}$ for BHQ-*N*-Serotonin, and $8.61 \cdot 10^{15}$ for

BHQ-VAA. Specific values for C_F are as follows: $21.22 \cdot 10^{-6}$ M for BHQ-*O*-Serotonin, $21.22 \cdot 10^{-6}$ M for BHQ-*N*-Serotonin, and $20.90 \cdot 10^{-6}$ for BHQ-VAA. Specific values for $\langle F(t) \rangle$ are as follows: $8.91 \cdot 10^{9}$ for BHQ-*O*-Serotonin, $9.03 \cdot 10^{9}$ for BHQ-*N*-Serotonin, and $6.99 \cdot 10^{9}$ for BHQ-VAA.

Determination of the Dark Hydrolysis Rate (τ)

Three 100 μM solutions of the compound in KMOPS were created and stored in the dark. 20 μL aliquots were removed periodically from each solution and analyzed by HPLC. The percent remaining for each compound for each time point for each solution were averaged and plotted versus time. A simple single exponential decay curve provided the best fit and yielded the time constant of dark hydrolysis (τ).

HPLC-MS Analysis of Photolyses of BHQ-OAc and CHQ-OAc

100 μm solutions of each caged compound were prepared in each of four solvent systems: dry CH_3CN, 40:60 CH_3CN/H_2O pH 4, 40:60 CH_3CN/H_2O pH 7, and KMOPS buffer at pH 7.2. Solutions were irradiated in a Rayonet photoreactor at 254 nm for 15 s in the case of BHQ-OAc and 30 s in the case of CHQ-OAc. HPLC analysis was conducted with an Agilent Technologies Microsorb-MV 100-5 C18 250 x 4.6 mm column with 40% CH_3CN/60% H_2O (w/ 0.1 % TFA) mobile phase composition and 1 mL/min flow rate. Eluate from the column was interfaced directly with a quadrupole mass spectrometer with electrospray ionization, or alternatively, eluate from peaks observed in the chromatogram was collected and immediately analyzed by ESI-MS. In the photolysis of BHQ-OAc (11.01 min retention time, *m*/*z* $[M+H]^+$ calcd 296.0, 298.0; found 296.0, 298.0), two photoproducts were identified, BHQ-OH (4.35 min retention time, *m*/*z* $[M+H]^+$ calcd 254.0, 256.0; found 254.0, 256.0) and HQ-OAc (4.83 min retention

time, *m*/*z* $[M+H]^+$ calcd 218.0, found 218.0). In the photolysis of CHQ-OAc (8.84 min retention time, *m*/*z* $[M+H]^+$ calcd 252.0, found 252.0), one photoproduct was identified, CHQ-OH (4.10 min retention time, *m*/*z* $[M+H]^+$ calcd 210.0, found 210.0).

References:

1. Adams, S. R.; Tsien, R. Y., Controlling cell chemistry with caged compounds. *Annu. Rev. Physiol.* **1993**, *55*, 755-84.
2. Pelliccioli, A. P.; Wirz, J., Photoremovable protecting groups: reaction mechanisms and applications. *Photochem. Photobiol. Sci.* **2002**, *1*, 441-58.
3. Kaplan, J. H.; Forbush, B., 3rd; Hoffman, J. F., Rapid photolytic release of adenosine 5'-triphosphate from a protected analogue: utilization by the Na:K pump of human red blood cell ghosts. *Biochemistry* **1978**, *17*, 1929-35.
4. Corrie, J. E., Photoremovable Protecting Groups Used for the Caging of Biomolecules. In *Dynamic Studies in Biology: Phototriggers, Photoswitches, and Caged Biomolecules*, Goeldner, M.; Givens, R. S., Eds. Wiley-VCH: Weinheim, Germany, 2005; pp 1-28.
5. Hagen, V.; Dzeja, C.; Frings, S.; Bendig, J.; Krause, E.; Kaupp, U. B., Caged compounds of hydrolysis-resistant analogues of cAMP and cGMP: synthesis and application to cyclic nucleotide-gated channels. *Biochemistry* **1996**, *35*, 7762-71.
6. Wang, L.; Corrie, J. E.; Wootton, J. F., Photolabile precursors of cyclic nucleotides with high aqueous solubility and stability. *J. Org. Chem.* **2002**, *67*, 3474-8.
7. Wieboldt, R.; Gee, K. R.; Niu, L.; Ramesh, D.; Carpenter, B. K.; Hess, G. P., Photolabile precursors of glutamate: synthesis, photochemical properties, and activation of glutamate receptors on a microsecond time scale. *Proc. Natl. Acad. Sci. U. S. A.* **1994**, *91*, 8752-6.

8. Dore, T. M., Multiphoton Phototriggers for Exploring Cell Physiology. In *Dynamic Studies in Biology: Phototriggers, Photoswitches, and Caged Biomolecules* Goeldner, M.; Givens, R. S., Eds. Wiley-VCH: Weinheim, Germany, 2005; pp 435-459.

9. Denk, W., Two-photon scanning photochemical microscopy: mapping ligand-gated ion channel distributions. *Proc. Natl. Acad. Sci. U. S. A.* **1994**, *91*, 6629-33.

10. Gug, S.; Bolze, F.; Specht, A.; Bourgogne, C.; Goeldner, M.; Nicoud, J. F., Molecular engineering of photoremovable protecting groups for two-photon uncaging. *Angew. Chem. Int. Ed. Engl.* **2008**, *47*, 9525-9.

11. Furuta, T.; Wang, S. S.; Dantzker, J. L.; Dore, T. M.; Bybee, W. J.; Callaway, E. M.; Denk, W.; Tsien, R. Y., Brominated 7-hydroxycoumarin-4-ylmethyls: photolabile protecting groups with biologically useful cross-sections for two photon photolysis. *Proc. Natl. Acad. Sci. U. S. A.* **1999**, *96*, 1193-200.

12. Fedoryak, O. D.; Dore, T. M., Brominated hydroxyquinoline as a photolabile protecting group with sensitivity to multiphoton excitation. *Org. Lett.* **2002**, *4*, 3419-22.

13. Zhu, Y.; Pavlos, C. M.; Toscano, J. P.; Dore, T. M., 8-Bromo-7-hydroxyquinoline as a photoremovable protecting group for physiological use: mechanism and scope. *J. Am. Chem. Soc.* **2006**, *128*, 4267-76.

14. Davis, M. J.; Kragor, C. H.; Reddie, K. G.; Wilson, H. C.; Zhu, Y.; Dore, T. M., Substituent effects on the sensitivity of a quinoline photoremovable protecting group to one- and two-photon excitation. *J. Org. Chem.* **2009**, *74*, 1721-9.

15. An, H. Y.; Ma, C.; Nganga, J. L.; Zhu, Y.; Dore, T. M.; Phillips, D. L., Resonance Raman characterization of different forms of ground-state 8-bromo-7-hydroxyquinoline caged acetate in aqueous solutions. *J. Phys. Chem. A.* **2009**, *113*, 2831-7.

16. Adayev, T.; Ranasinghe, B.; Banerjee, P., Transmembrane signaling in the brain by serotonin, a key regulator of physiology and emotion. *Biosci. Rep.* **2005**, *25*, 363-85.

17. Li, S.; Varga, V.; Sik, A.; Kocsis, B., GABAergic control of the ascending input from the median raphe nucleus to the limbic system. *J. Neurophysiol.* **2005**, *94*, 2561-74.

18. Millan, M. J.; Marin, P.; Bockaert, J.; Mannoury la Cour, C., Signaling at G-protein-coupled serotonin receptors: recent advances and future research directions. *Trends Pharmacol. Sci.* **2008**, *29*, 454-64.

19. Bagdy, E.; Kiraly, I.; Harsing, L. G., Jr., Reciprocal innervation between serotonergic and GABAergic neurons in raphe nuclei of the rat. *Neurochem. Res.* **2000**, *25*, 1465-73.

20. Liu, R.; Jolas, T.; Aghajanian, G., Serotonin 5-HT(2) receptors activate local GABA inhibitory inputs to serotonergic neurons of the dorsal raphe nucleus. *Brain. Res.* **2000**, *873*, 34-45.

21. Bagdy, G.; Kecskemeti, V.; Riba, P.; Jakus, R., Serotonin and epilepsy. *J. Neurochem.* **2007**, *100*, 857-73.

22. Richerson, G. B.; Buchanan, G. F., The serotonin axis: Shared mechanisms in seizures, depression, and SUDEP. *Epilepsia* **2011**, *52 Suppl 1*, 28-38.

23. Hortopan, G. A.; Dinday, M. T.; Baraban, S. C., Spontaneous seizures and altered gene expression in GABA signaling pathways in a mind bomb mutant zebrafish. *J. Neurosci.* **2010**, *30*, 13718-28.

24. Salgado, D.; Alkadhi, K. A., Inhibition of epileptiform activity by serotonin in rat CA1 neurons. *Brain. Res.* **1995**, *669*, 176-82.

25. Sarnyai, Z.; Sibille, E. L.; Pavlides, C.; Fenster, R. J.; McEwen, B. S.; Toth, M., Impaired hippocampal-dependent learning and functional abnormalities in the hippocampus in mice lacking serotonin(1A) receptors. *Proc. Natl. Acad. Sci. U. S. A.* **2000**, *97*, 14731-6.

26. Schmitz, D.; Empson, R. M.; Gloveli, T.; Heinemann, U., Serotonin blocks different patterns of low Mg2+-induced epileptiform activity in rat entorhinal cortex, but not hippocampus. *Neuroscience* **1997**, *76*, 449-58.

27. Schmitz, D.; Gloveli, T.; Empson, R. M.; Draguhn, A.; Heinemann, U., Serotonin reduces synaptic excitation in the superficial medial entorhinal cortex of the rat via a presynaptic mechanism. *J. Physiol.* **1998**, *508*, 119-29.

28. Tecott, L. H.; Sun, L. M.; Akana, S. F.; Strack, A. M.; Lowenstein, D. H.; Dallman, M. F.; Julius, D., Eating disorder and epilepsy in mice lacking 5-HT2c serotonin receptors. *Nature* **1995**, *374*, 542-6.

29. Upton, N.; Stean, T.; Middlemiss, D.; Blackburn, T.; Kennett, G., Studies on the role of 5-HT2C and 5-HT2B receptors in regulating generalised seizure threshold in rodents. *Eur. J. Pharmacol.* **1998**, *359*, 33-40.

30. Abi-Saab, W. M.; Bubser, M.; Roth, R. H.; Deutch, A. Y., 5-HT2 receptor regulation of extracellular GABA levels in the prefrontal cortex. *Neuropsychopharmacology* **1999,** *20*, 92-6.

31. Breitinger, H. G.; Wieboldt, R.; Ramesh, D.; Carpenter, B. K.; Hess, G. P., Synthesis and characterization of photolabile derivatives of serotonin for chemical kinetic investigations of the serotonin 5-HT(3) receptor. *Biochemistry* **2000**, *39*, 5500-8.

32. Boahen, Y. O.; MacDonald, G. M., A concise approach to caged serotonin for Fourier transform infrared (FT-IR) difference photolysis studies. *J. Ghana Sci. Assoc.* **2005**, *7*, 54-59.

33. Udgaonkar, J. B.; Hess, G. P., Chemical kinetic measurements of a mammalian acetylcholine receptor by a fast-reaction technique. *Proc. Natl. Acad. Sci. U. S. A.* **1987**, *84*, 8758-62.

34. Ouyang, X.; Shestopalov, I. A.; Sinha, S.; Zheng, G.; Pitt, C. L.; Li, W. H.; Olson, A. J.; Chen, J. K., Versatile synthesis and rational design of caged morpholinos. *J. Am. Chem. Soc.* **2009**, *131*, 13255-69.

35. Vining, E. P.; Mellitis, E. D.; Dorsen, M. M.; Cataldo, M. F.; Quaskey, S. A.; Spielberg, S. P.; Freeman, J. M., Psychologic and behavioral effects of antiepileptic drugs in children: a double-blind comparison between phenobarbital and valproic acid. *Pediatrics* **1987**, *80*, 165-74.

36. Loring, D. W.; Meador, K. J., Cognitive side effects of antiepileptic drugs in children. *Neurology* **2004**, *62*, 872-7.

37. Haffter, P.; Granato, M.; Brand, M.; Mullins, M. C.; Hammerschmidt, M.; Kane, D. A.; Odenthal, J.; van Eeden, F. J.; Jiang, Y. J.; Heisenberg, C. P.; Kelsh, R. N.; Furutani-Seiki, M.; Vogelsang, E.; Beuchle, D.; Schach, U.; Fabian, C.; Nusslein-Volhard, C., The

identification of genes with unique and essential functions in the development of the zebrafish, Danio rerio. *Development* **1996**, *123*, 1-36.

38. Chitnis, A. B.; Dawid, I. B., Neurogenesis in zebrafish embryos. *Methods Cell. Biol.* **1999**, *59*, 367-86.

39. Baraban, S. C.; Taylor, M. R.; Castro, P. A.; Baier, H., Pentylenetetrazole induced changes in zebrafish behavior, neural activity and c-fos expression. *Neuroscience* **2005**, *131*, 759-68.

40. Baraban, S. C.; Dinday, M. T.; Castro, P. A.; Chege, S.; Guyenet, S.; Taylor, M. R., A large-scale mutagenesis screen to identify seizure-resistant zebrafish. *Epilepsia* **2007**, *48*, 1151-7.

41. Hortopan, G. A.; Dinday, M. T.; Baraban, S. C., Zebrafish as a model for studying genetic aspects of epilepsy. *Dis. Model. Mech.* **2010**, *3*, 144-8.

42. McLean, D. L.; Fetcho, J. R., Ontogeny and innervation patterns of dopaminergic, noradrenergic, and serotonergic neurons in larval zebrafish. *J. Comp. Neurol.* **2004**, *480*, 38-56.

43. Clapham, D. E., TRP channels as cellular sensors. *Nature* **2003**, *426*, 517-24.

44. Caterina, M. J.; Schumacher, M. A.; Tominaga, M.; Rosen, T. A.; Levine, J. D.; Julius, D., The capsaicin receptor: a heat-activated ion channel in the pain pathway. *Nature* **1997**, *389*, 816-24.

45. Clapham, D. E.; Runnels, L. W.; Strubing, C., The TRP ion channel family. *Nat. Rev. Neurosci.* **2001**, *2*, 387-96.

46. Karai, L. J.; Russell, J. T.; Iadarola, M. J.; Olah, Z., Vanilloid receptor 1 regulates multiple calcium compartments and contributes to Ca2+-induced Ca2+ release in sensory neurons. *J. Biol. Chem.* **2004**, *279*, 16377-87.

47. Tsien, R. Y.; Bacskai, B. J.; Adams, S. R., FRET for studying intracellular signalling. *Trends Cell. Biol.* **1993**, *3*, 242-5.

48. Zhang, J.; Campbell, R. E.; Ting, A. Y.; Tsien, R. Y., Creating new fluorescent probes for cell biology. *Nat. Rev. Mol. Cell Biol.* **2002**, *3*, 906-18.

49. Mank, M.; Reiff, D. F.; Heim, N.; Friedrich, M. W.; Borst, A.; Griesbeck, O., A FRET-based calcium biosensor with fast signal kinetics and high fluorescence change. *Biophys. J.* **2006**, *90*, 1790-6.

50. Savidge, J. R.; Ranasinghe, S. P.; Rang, H. P., Comparison of intracellular calcium signals evoked by heat and capsaicin in cultured rat dorsal root ganglion neurons and in a cell line expressing the rat vanilloid receptor, VR1. *Neuroscience* **2001**, *102*, 177-84.

51. Zemelman, B. V.; Nesnas, N.; Lee, G. A.; Miesenbock, G., Photochemical gating of heterologous ion channels: remote control over genetically designated populations of neurons. *Proc. Natl. Acad. Sci. U. S. A.* **2003**, *100*, 1352-7.

52. Carr, J. L.; Wease, K. N.; Van Ryssen, M. P.; Paterson, S.; Agate, B.; Gallagher, K. A.; Brown, C. T.; Scott, R. H.; Conway, S. J., In vitro photo-release of a TRPV1 agonist. *Bioorg. Med. Chem. Lett.* **2006**, *16*, 208-12.

53. Zhao, J.; Gover, T. D.; Muralidharan, S.; Auston, D. A.; Weinreich, D.; Kao, J. P., Caged vanilloid ligands for activation of TRPV1 receptors by 1- and 2-photon excitation. *Biochemistry* **2006**, *45*, 4915-26.

54. Van Ryssen, M. P.; Avlonitis, N.; Giniatullin, R.; McDougall, C.; Carr, J. L.; Stanton-Humphreys, M. N.; Borgstrom, E. L.; Brown, C. T.; Fayuk, D.; Surin, A.; Niittykoski, M.; Khiroug, L.; Conway, S. J., Synthesis, photolysis studies and in vitro photorelease of caged TRPV1 agonists and antagonists. *Org. Biomol. Chem.* **2009**, *7*, 4695-707.

55. Gilbert, D.; Funk, K.; Dekowski, B.; Lechler, R.; Keller, S.; Mohrlen, F.; Frings, S.; Hagen, V., Caged capsaicins: New tools for the examination of TRPV1 channels in somatosensory neurons. *Chembiochem.* **2007**, *8*, 89-97.

56. Katritzky, A. R.; Xu, Y. J.; Vakulenko, A. V.; Wilcox, A. L.; Bley, K. R., Model compounds of caged capsaicin: design, synthesis, and photoreactivity. *J. Org. Chem.* **2003**, *68*, 9100-4.

57. Voets, T.; Talavera, K.; Owsianik, G.; Nilius, B., Sensing with TRP channels. *Nat. Chem. Biol.* **2005**, *1*, 85-92.